THE UNIVERSITY
of EDINBURGH

Mode of Action of Lymphostatin, a Key Virulence Factor of Attaching & Effacing *Escherichia coli*

Andrew Graham Bease

Master of Science by Research (M.Sc)

The University of Edinburgh

2015

Declaration

I, Andrew Graham Bease have read and understood the University of Edinburgh guidelines on plagiarism and hereby declare that this thesis is all of my own work except where indicated in the text. This work has also not been submitted for any other degree or professional qualification from any other University.

Signed……

Acknowledgements

I would like to thank Prof. Mark Stevens, Dr. Robin Cassady-Cain, Dr. Liz Blackburn, the Stevens and MMBP Laboratories and the Edinburgh Protein Production Facility for their help and support throughout the course of this study and preparation of this thesis.

Contents

List of Figures

List of Tables

List of commonly used abbreviations

A/E	Attaching and effacing
Amp	Ampicillin
BFP	Bundle-forming pili
BSA	Bovine serum albumin
CD	Circular dichroism
CFU	Colony forming unit
ConA	Concanavalin A
DLS	Dynamic light scattering
DMEM	Dulbecco's Modified Eagle's Medium
DNA	Deoxyribonucleic acid
Efa-1	EHEC factor for adherence-1
EHEC	Enterohaemorrhagic *Escherichia coli*
EPEC	Enteropathogenic *E. coli*
Esc	*E. coli* secretion components
Esp	*E. coli* secreted protein
FCS	Foetal calf serum
Glc	Glucose
GlcNAc	*N*-Acetylglucosamine
HEPES	4-(2-hydroxyethyl)-1-piperazineethanesulphonic acid
HRP	Horseradish peroxidase
HUS	Haemolytic uraemic syndrome
IL	Interleukin
IMAC	Ion metal affinity chromatography
Kan	Kanamycin
LB	Lysogeny broth
LCTs	Large clostridial toxins
LDH	Lactate dehydrogenase
LDS	Lithium dodecyl sulphate
LEE	Locus of enterocyte effacement
LifA	Lymphocyte inhibitory factor A (Lymphostatin)

MEM	Minimum Essential Medium Eagle
Nal	Nalidixic acid
OD	Optical density
PAGE	Polyacrylamide gel electrophoresis
PBMC	Peripheral blood mononuclear cell
PBS	Phosphate-buffered saline
PCR	Polymerase chain reaction
RPMI	Roswell Park Memorial Institute-1640 media
RPMI-CJ	RPMI complete media for Jurkat cells
RPMI-CT	RPMI complete media for bovine T lymphocytes
SDS	Sodium dodecyl sulphate
SEC	Size exclusion chromatography
Stx	Shiga toxin
T3S	Type III secretion
T3SS	Type III secretion system
TBS	Tris-buffered saline
TBS-T	Tris-buffered saline and Tween 20
Tir	Translocated intimin receptor
TRIS	Tris(hydroxymethyl)aminomethane
UDP	Uridine diphosphate

Abstract

Attaching and effacing *Escherichia coli* are significant diarrhoeal pathogens that can spread between humans or via animal reservoirs. One important virulence factor is a large multifunctional protein called lymphostatin (LifA), which has been reported to inhibit the mitogen-stimulated proliferation of lymphocytes and mediate adherence to epithelial cells. Mutants of Shiga toxin-producing *E. coli* lacking *lifA* are significantly impaired in their ability to colonise cattle. Little is known about the mode of action of LifA, however *in silico* analysis has identified a putative glycosyltransferase domain homologous to that of large clostridial toxins (LCTs). A shortened form of LifA has been shown to be Type III secreted, however it is not known if this is true for the full-length protein. Type III secretion assays using the prototype enteropathogenic *E. coli* strain E2348/69 and isogenic *lifA* and Type III secretion system mutants confirmed that LifA can be secreted through this transport system. Working in collaboration, I was also able to demonstrate that LifA can be purified in an active form that binds uridine diphosphate-*N*-Acetylglucosamine (UDP-GlcNAc) but not UDP-glucose. In order to probe the importance of a putative catalytic DXD motif within the glycosyltransferase domain, an in-frame DXD to AAA substitution mutant of full-length LifA was constructed. The ability of the purified wild-type and mutated protein to bind UDP sugars and inhibit bovine T cell proliferation were then examined. DXD-AAA substitution resulted in loss of binding of UDP-GlcNAc and the ability to inhibit mitogenic stimulation of bovine T cells, without obvious changes to the biophysical properties of the protein. Unlike LCTs, wild-type LifA did not appear to be directly cytotoxic to HeLa or Jurkat cells using a fluorescence-based assay for release of lactate dehydrogenase. Future studies will seek to define the cellular targets and consequences of GlcNAc modification by lymphostatin, as well as identifying other possible mechanisms of secretion and its ability to act as an adhesin.

Chapter 1: Introduction

1.1 *Escherichia coli*

Escherichia coli are Gram-negative facultative anaerobes that are commonly found living in the environment or as commensals in the gastrointestinal tract of animals and man (Winfield and Groisman, 2003). The survival of environmental *E. coli* populations is dependent on a number of factors including nutrient availability, temperature, the presence of toxic substances and predation (Carlucci and Pramer, 1959; Faust *et al*, 1975; Gerba and McLeod, 1976). The bacteria do not survive for long in temperate environments (Temple *et al*, 1980) and the population appears to be kept constant by the arrival of new bacteria from animal hosts (Savageau, 1983). However, several studies have shown that *E. coli* is capable of entering a viable but non-culturable state, meaning that the cells enter a state in which they are metabolically active but cannot be cultured by known laboratory methods, due to environmental stresses (Reissbrodt *et al*, 2002; Asakura *et al*, 2008; Li *et al*, 2014). Despite its poor survival in temperate climates, *E. coli* is capable of surviving in nutrient rich soil and fresh water in tropical environments where there is no obvious sign of faecal contamination (Solo-Gabriele *et al*, 2000; Rivera *et al*, 1988; Jiménez *et al*, 1989). Due to its prevalence in mammalian faeces and its relatively short survival time in the environment, *E. coli* is used as an indicator of faecal contamination of drinking water (Edberg *et al*, 2000). Its usefulness as an indicator in tropical countries, however, is limited due to the prevalence of the bacteria in the environment in such countries (Solo-Gabriele *et al*, 2000; Rivera *et al*, 1988; Jiménez *et al*, 1989).

E. coli primarily exist as a commensal in the lower intestines of warm blooded animals and reptiles, and make up a large component of the normal gut microflora (Leimbach *et al*, 2013). Its presence is usually beneficial to its host as *E. coli* is capable of synthesising vitamin K_2 (Bentley and Meganathan, 1982) and, along with the rest of the gut microflora, it exerts a protective effect against pathogenic bacteria (Hudault *et al*, 2001).

Although normally harmless to its host, *E. coli* is an opportunistic pathogen that, through the acquisition of mobile genetic elements, can become a serious pathogen (Croxen and Finlay, 2010). Pathogenic *E. coli* strains can be divided into two subgroups depending on the site of infection, with diarrhoeagenic *E. coli* infecting the intestines and extraintestinal *E. coli* (ExPEC) infecting sites beyond the intestines (Croxen and Finlay, 2010; Leimbach *et al*, 2013).

1.2 *E. coli* pathotypes

The diarrhoeagenic *E. coli* and ExPEC subgroups can be further divided into distinct pathotypes based on particular characteristics. ExPEC consists primarily of uropathogenic *E. coli*, which infects the urinary tract, and neonatal meningitis *E. coli*, which infects the brain (Croxen and Finlay, 2010; Leimbach *et al*, 2013). Other pathotypes of ExPEC exist such as septicaemia-associated *E. coli* and avian pathogenic *E. coli* although these are less well defined (Croxen and Finlay, 2010; Leimbach *et al*, 2013). The main diarrhoeagenic *E. coli* pathotypes are enterotoxigenic *E. coli* (ETEC), enteroaggregative *E. coli* (EAEC), enteroinvasive *E. coli* (EIEC), diffusely adherent *E. coli* (DAEC), enteropathogenic *E. coli* (EPEC) and enterohaemorrhagic *E. coli* (EHEC; Croxen and Finlay, 2010; Leimbach *et al*, 2013).

ETEC is the most common cause of traveller's diarrhoea and it is also important in the farming industry, particularly as a cause of acute enteritis and colibacillosis in young pigs and calves (Nataro and Kaper, 1998; Croxen and Finlay, 2010). It is characterised by its adherence to enterocytes via colonisation factors and the secretion of heat-labile and heat-stable toxins, which cause diarrhoea (Nataro and Kaper, 1998; Croxen and Finlay, 2010). EAEC is the second most common cause of traveller's diarrhoea and is characterised by forming biofilms on enterocytes using aggregative adherence fimbriae (Croxen and Finlay, 2010). EIEC, which include bacteria of the genus *Shigella*, is characterised by its facultative intracellular lifestyle. It achieves this by passing through microfold cells via transcytosis, replicating inside macrophages in the intestinal submucosa, then invading enterocytes from their basolateral side (Croxen and Finlay, 2010). DAEC is

characterised by forming diffuse attachments to enterocytes using fimbrial and afimbrial adhesins (Croxen and Finlay, 2010).

EPEC and EHEC are collectively known as attaching and effacing (A/E) *E. coli* (Croxen and Finlay, 2010; Stevens and Frankel, 2014) and are described in greater detail below.

1.3 Attaching and effacing *E. coli*

A/E lesions are characterised by intimate bacterial attachment to the surface of enterocytes on actin-rich 'pedestals' and the destruction of microvilli, thereby disrupting the absorption of nutrients by the gut, contributing to diarrhoea (Figure 1.1; Croxen and Finlay, 2010; Stevens and Frankel, 2014). The pedestals are also assembled with other cytoskeletal proteins besides actin, such as α-actinin, talin, ezrin and myosin light-chain (Finlay *et al*, 1992; Manjarrez-Hernandez *et al*, 1992). Recently, Law *et al* (2015) identified more than 90 proteins present in the pedestals formed by EPEC, 17 of which were in a significantly higher abundance than in uninfected cells. Actin-associated proteins such as cyclophilin A may only be present due to their interactions with actin, but non-actin-associated proteins such as transgelin may have other as yet undefined roles (Law *et al*, 2015). A/E lesion formation in *E. coli* is mediated by various virulence factors, which are only produced by A/E pathogens (Nataro and Kaper, 1998).

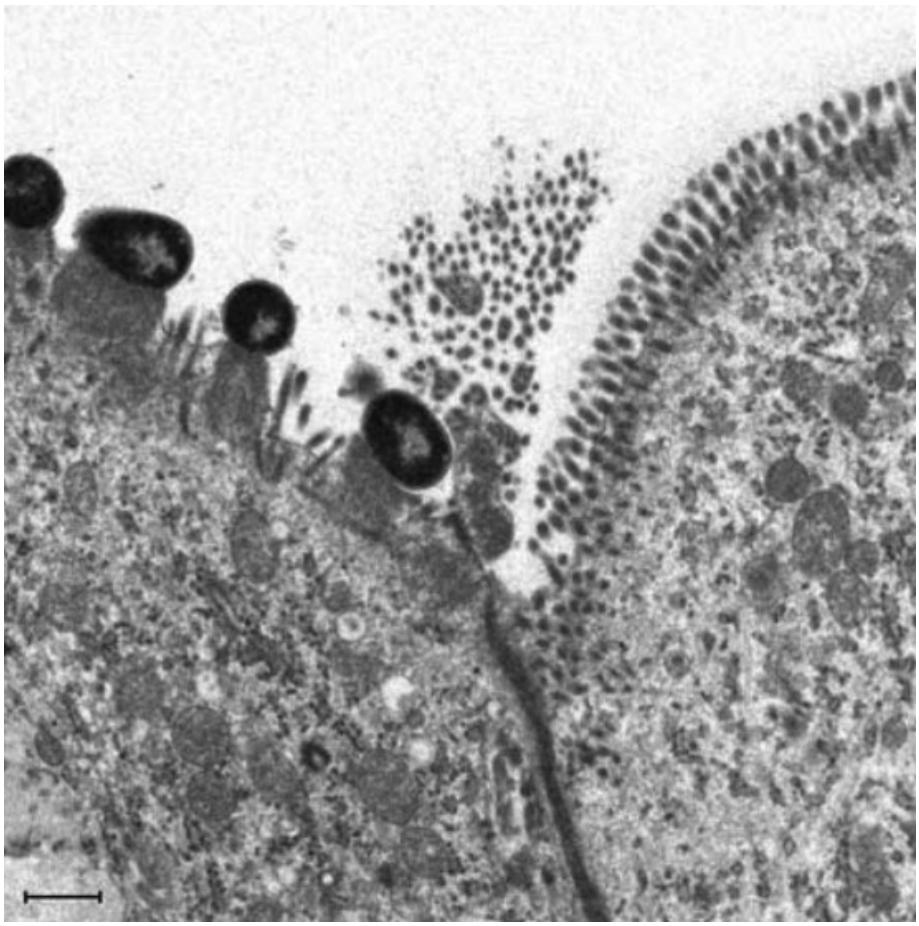

Figure 1.1. Transmission electron micrograph of EHEC O111:H- E45035N forming attaching and effacing lesions on a bovine calf colonocyte. Actin rich pedestals can be seen as electron dense regions beneath the EHEC cells. An uninfected cell to the right gives a comparison of a healthy cell surface and microvilli. Scale bar = 1μm (taken from Stevens *et al*, 2002).

EPEC is a major cause of infantile diarrhoea in the developing world and causes both acute and chronic diarrhoea (Ochoa and Contreras, 2011). Once attached to an enterocyte, EPEC disrupts ion balance and water absorption resulting in diarrhoea (Croxen and Finlay, 2010). Sanger *et al* (1996) also found that EPEC are able to use A/E pedestals as a form of motility to travel across the surface of host cells at speeds of up to 0.07μm/second. EPEC strains can be further divided into typical EPEC, which possess bundle-forming pili (BFP), and atypical EPEC, which do not (Trabulsi *et al*, 2002). Prevalent EPEC serotypes include O55:H6, O127:H6, O128:H2 and O142:34 among others (Gomes *et al*, 1989; Trabulsi *et al*, 2002). The

genome of the prototypic EPEC strain E2348/69 consists of an ~5Mb circular chromosome, an ~97kb EPEC adherence factor (EAF) plasmid and a small ~6kb drug-resistant plasmid (Iguchi *et al*, 2008). The core genome is highly conserved with lab strains, commensal *E. coli* and other pathotypes of *E. coli*, but is broken up by 13 prophages and eight integrative elements (Iguchi *et al*, 2008). Iguchi *et al*, (2008) also identified 424 genes that were specific to EPEC E2348/69.

EHEC causes a zoonotic infection and ruminants are a key reservoir (Croxen and Finlay, 2010). Outbreaks in both the developing and developed world have been caused by cattle, due to faecally contaminated food or water (Ho *et al*, 2013). EHEC is responsible for haemorrhagic colitis and haemolytic uraemic syndrome in humans (HUS; Ho *et al*, 2013), which it causes by the production of one or more Shiga toxins (Stx; Croxen and Finlay, 2010). The pathogenesis of EHEC is similar to that of EPEC with the exception of the production of Stx, which acts as a cytotoxin (Croxen and Finlay, 2010). The most prevalent EHEC serogroups are O26, O45, O103, O111, O121, O145 and O157:H7 (Brooks *et al*, 2005). The chromosome of the prototypic EHEC O157:H7 strain EDL933 has a similar backbone sequence to *E. coli* K-12 except for a 422kb inversion, which spans the replication terminus (Perna *et al*, 2001). This backbone sequence is interrupted by 177 O-islands found in *E. coli* O157:H7 but not laboratory-adapted *E. coli* K-12, many of which encode known virulence proteins (Perna *et al*, 2001). There are also 18 prophages throughout the chromosome and various single nucleotide polymorphisms create proteins that are identical in size and function to *E. coli* K-12 homologues but overall only 25% of proteins are identical (Perna *et al*, 2001). EHEC O157:H7 also contains the pO157 plasmid, which encodes various virulence factors (Burland *et al*, 1998).

1.4 Major virulence factors in A/E *E. coli*

EPEC and EHEC produce several key virulence factors that aid their colonisation of human and animal hosts, many of which are required for the formation of A/E lesions.

1.4.1 The locus of enterocyte effacement (LEE)

The LEE is a pathogenicity island comprising over 40 contiguous genes, which encode virulence factors that aid colonisation of a host, some of which are required for attachment and effacement (Stevens and Frankel, 2014). It is a ≥ 35kb locus that is conserved amongst EPEC and EHEC as well as other A/E pathogens including certain strains of rabbit diarrhoeagenic *E. coli* (RDEC), *Hafnia alvei* and the mouse pathogen *Citrobacter rodentium* (McDaniel *et al*, 1995; Deng *et al*, 2001). The GC content of the LEE is only 38.36% (Elliot *et al*, 1998) compared with 50.8% across the whole *E. coli* genome (Blattner *et al*, 1997), which is typical of pathogenicity islands (Hacker *et al*, 1997). The LEE consists of 41 open reading frames arranged into five polycistronic operons (Figure 1.2; Elliot *et al*, 1998), three of which are involved in the production of proteins required for the assembly of a Type III secretion system (T3SS; Mellies *et al*, 2007).

The LEE contains the *E. coli* secretion (*esc*)/secretion of *E. coli* proteins (*sep*) genes and genes that encode initimin, *E. coli* secreted proteins (Esps) including translocated intimin receptor (Tir) as well as chaperones and regulatory genes (Elliot *et al*, 1998). The 3′ end of the LEE in EPEC is homologous to genes from *Shigella sonnei* (Donnenberg *et al*, 1997), however, the DNA sequences surrounding the LEE vary since it is inserted into different positions depending on the serotype and strain of bacteria (Ogura *et al*, 2009). These variable end sequences along with the low GC content suggests that *E. coli* and other A/E pathogens have acquired this DNA from another species, or that it once existed as a mobile genetic element (Donnenberg *et al*, 1997).

The regulation of the LEE is complex, with different regulatory systems specific to different operons (Mellies and Lorenzen, 2014). The production of LEE proteins is tightly regulated by temperature and growth phase, with the most protein synthesis occurring at 37°C in the early logarithmic phase of growth (Rosenshine *et al*, 1996). Regulatory systems of the LEE include silencing by histone-like nucleoid-structuring protein, the LEE-encoded regulatory cascade, post-transcriptional regulation and control by phage- or plasmid-encoded regulators (Mellies and Lorenzen, 2014).

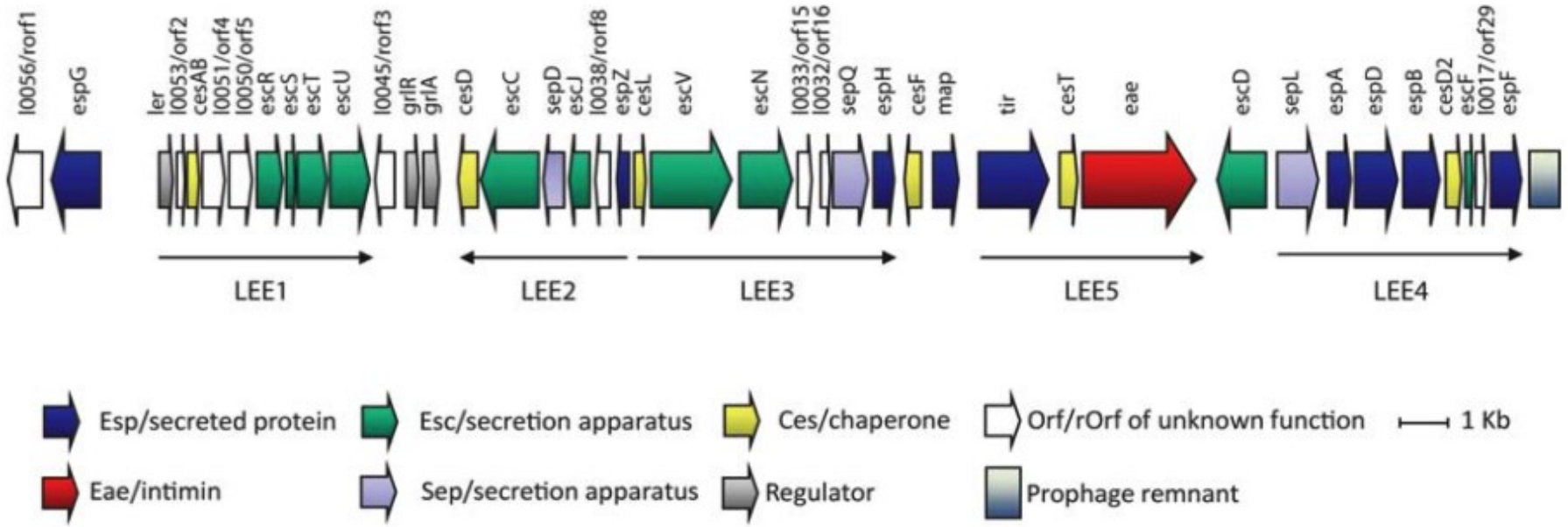

Figure 1.2. Schematic of the locus of enterocyte effacement from EHEC O157:H7 showing the five polycistronic operons and the genes encoded within them (taken from Stevens and Frankel, 2014).

1.4.2 The Type III secretion system

T3SSs are widely used by a range of Gram-negative pathogens of animals and plants (Büttner, 2012). There are at least five other well characterised secretion systems in Gram-negative bacteria (Costa *et al*, 2015) but the T3SS is particularly important for the purpose of this study. The T3SS in A/E *E. coli* is encoded by the LEE and is composed of Esc/Sep proteins as well as EspA, B and D (Elliot 1998; Stevens and Frankel, 2014). It was discovered by Jarvis *et al* (1995), who found that certain LEE-encoded proteins exhibited homology to proteins encoding T3SSs in other bacteria. T3SSs include flagella (Büttner, 2012) but for the purpose of this study, it is the translocation-associated T3SS that is being referred to. This T3SS is akin to a molecular syringe that can inject effector proteins directly into a host cell (Figures 1.3 and 1.4; Büttner, 2012; Stevens and Frankel, 2014). It consists of a region that spans both membranes of the bacterial cell, which is connected via EscF to the EspA filament and the translocon, which is composed of EspB and D (Büttner, 2012; Stevens and Frankel, 2014; Warawa *et al*, 1999).

The proteins SepL and SepD regulate the order that effector proteins are secreted in with mutations leading to hypersecretion of effector proteins rather than translocon components (Kresse *et al*, 2000; O'Connell *et al*, 2004; Wang *et al*, 2008). EspZ halts effector translocation from inside the host cell, possibly by interacting with EspD (Berger *et al*, 2012; Creasey *et al*, 2003). The secretion of effector proteins via the T3SS is contact-dependent in some bacteria such as *Yersinia* (Rosqvist *et al*, 1994) but contact between the T3SS and host cells is not required for the secretion of effector proteins in *E. coli* (Kenny *et al*, 1997b). Various inhibitors of the T3SS have been identified, many of which are part of a family of salicylidene acylhydrazides that inhibit the transcription of T3SS encoding genes (Gauthier *et al*, 2005; Rasko *et al*, 2008; Tree *et al*, 2009). This is in contrast to T3SS inhibitors that work against *Shigella* by interfering with T3SS protein assembly (Veenendaal *et al*, 2009). Vaccines including the LEE-encoded proteins EspA, intimin and Tir as well as the H7 flagellin have been shown to significantly reduce the shedding of EHEC O157:H7 in cattle faeces (McNeilly *et al*, 2010), consistent with a key role for this

system in intestinal colonisation of cattle (Dziva *et al*, 2004; Naylor *et al*, 2005; Vlisidou *et al*, 2006).

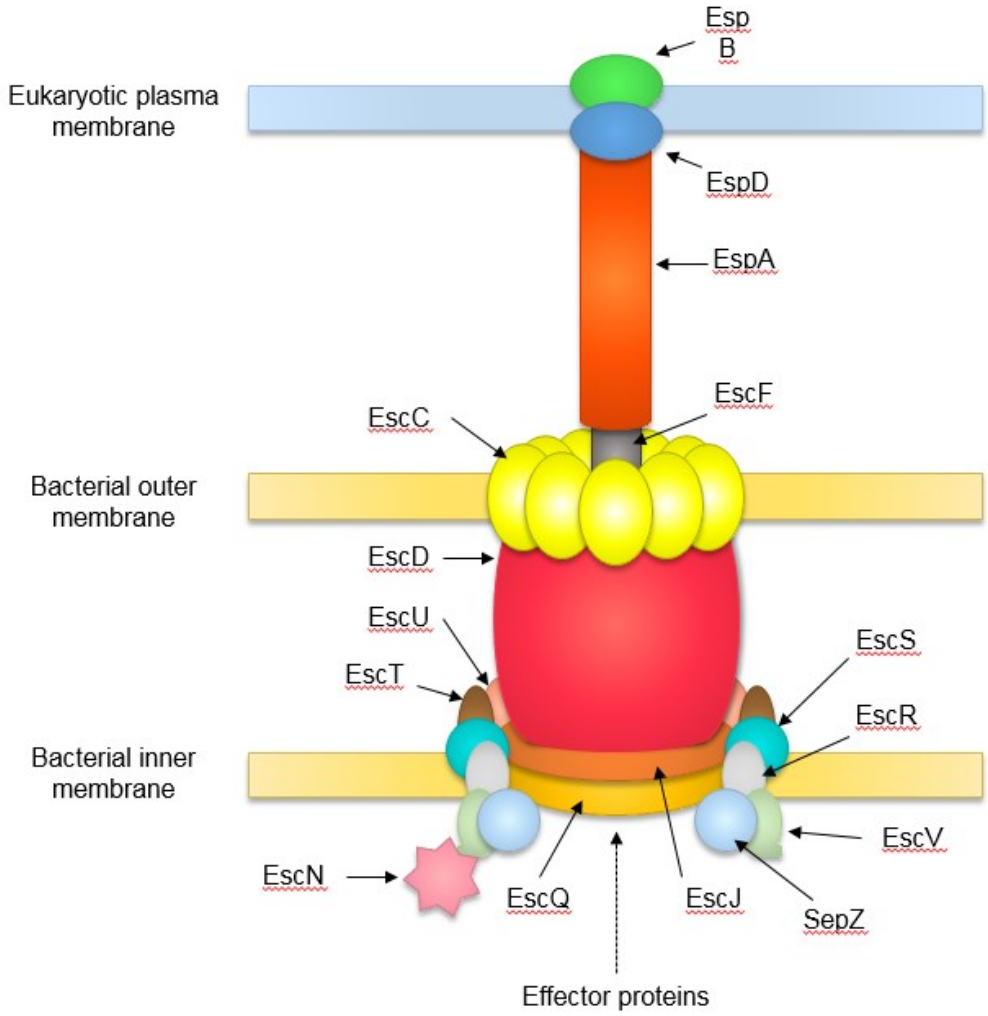

Figure 1.3. Schematic of the Type III secretion system showing the proteins required for its formation in attaching and effacing *E. coli*. Effector proteins are translocated through the needle complex spanning the inner and outer membranes, then the EspA filament and the transolcon composed of EspD and B into the host cell cytoplasm (adapted from Stevens and Frankel, 2014).

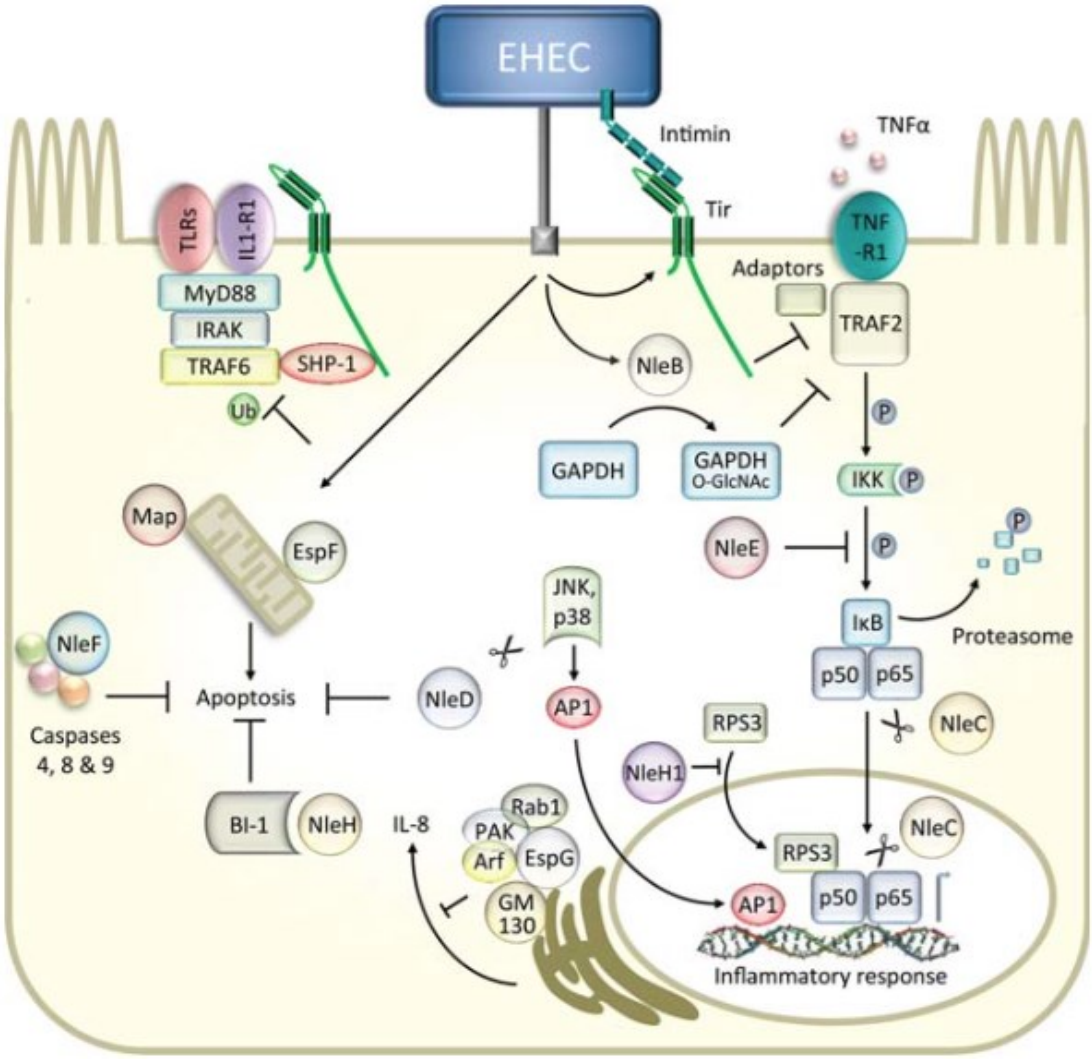

Figure 1.4. Schematic of EHEC adhering to an enterocyte and injecting various effector proteins into it via the Type III secretion system (taken from Stevens and Frankel, 2014).

1.4.3 *E. coli* secretion/secretion of *E. coli* proteins

The Esc and Sep proteins are part of the same family but some Seps were renamed as Escs after Elliot *et al* (1998) sequenced the LEE in order to conform with the naming convention of homologous *Yersinia* proteins. Esc/Sep proteins comprise the *E. coli* T3SS and are essential for the translocation of effector proteins (Jarvis *et al*, 1995; Stevens and Frankel, 2014). EscN is the most relevant of these proteins in terms of this study as an EPEC strain lacking the *escN* gene (Garmendia *et al*, 2004)

is used as a T3SS deficient control. EscN is an ATPase that provides the energy for the secretion of effector proteins and the energy output of the protein increases when it oligomerises (Jarvis *et al*, 1995; Andrade *et al*, 2007). Two other proteins in this family that are important for the formation of A/E lesions are SepL and SepD, which act as gatekeeper proteins (Wang *et al*, 2008). These proteins form a complex in the bacterial inner membrane and SepL binds to Tir to prevent effector proteins from being secreted before translocator proteins such as EspA (Kresse *et al*, 2000; O'Connell *et al*, 2004; Wang *et al*, 2008).

1.4.4 *E. coli* secreted proteins

The Esp series of proteins consists of a large number of proteins, the functions of some of which have been extensively studied (Stevens and Frankel, 2014). EspA forms a hollow filamentous extension of the T3SS needle complex (Ebel *et al*, 1998; Knutton *et al*, 1998) that bridges the bacterial and host cells and allows the translocation of effector proteins such as Tir and EspB into the host cell (Kenny *et al*, 1997a; Wolff *et al*, 1998). EspA polymerises in a helical manner to form a channel that effector proteins can be secreted through (Daniell *et al*, 2003; Crepin *et al*, 2005). A/E *E. coli* lack these EspA filaments during intimate adhesion but the mechanism behind this is unknown (Steven and Frankel, 2014). EspB functions as both a component of the T3SS and an effector protein (Warawa *et al*, 1999; Taylor *et al*, 1998). It associates with EspD to form a pore in the host cell plasma membrane at the end of the EspA filament (Warawa *et al*, 1999) but is also injected into host cells by the T3SS (Wolff *et al*, 1998). As an effector protein it binds to myosin and inhibits the interaction of myosin with actin, resulting in microvillus effacement and the inhibition of phagocytosis (Iizumi *et al*, 2007). EspB also suppresses NF-κB activation, which results in the inhibition of proinflammatory cytokine production (Hauf and Chakraborty, 2003), although it is unclear if this reflects a direct role or the requirement for EspB in injection of other effectors.

EspD is another Type III secreted (T3S) protein (Lai *et al*, 1997) that is translocated into host cells before forming pore complexes with EspB in host cell plasma membranes (Kresse *et al*, 1999; Warawa *et al*, 1999; Wachter *et al*, 1999).

$EspF_U$, also known as Tir-cytoskeleton coupling protein (TccP), is a secreted effector protein of EHEC O157:H7 that is particularly important in EHEC because it binds to the insulin receptor tyrosine kinase substrate (IRTKS)/insulin receptor substrate p53 (IRSp53) complex and neural Wiskott-Aldrich syndrome protein (N-WASP), resulting in the formation of A/E lesions (Garmendia *et al*, 2004; Brady *et al*, 2007; Stevens and Frankel, 2014). The homologous protein EspF has a wide range of functions including the disruption of mitochondrial function, cytoskeletal manipulation and the induction of apoptosis (Holmes *et al*, 2010; Stevens and Frankel, 2014). There are many other proteins in the Esp family but those described above are the major proteins, with the exception of EspF, that are required for A/E lesion formation.

1.4.5 Non-LEE-encoded (Nle) proteins

In addition to the LEE-encoded effector proteins, the Nle proteins are also secreted effector proteins but are encoded outwith the LEE (Stevens and Frankel, 2014). NleA disrupts tight junction integrity between enterocytes by inhibiting protein trafficking via COPII-dependent pathways, resulting in a breakdown of the intestinal epithelial barrier and causing diarrhoea (Thanabalasuriar *et al*, 2010). NleB is an immunomodulatory protein that disrupts tumour necrosis factor signalling in infected cells including NF-κB signalling, which in turn prevents the expression of pro-inflammatory cytokines, and apoptosis (Li *et al*, 2013). NleC, E and H also interfere with NF-κB signalling in different ways (Stevens and Frankel, 2014). NleC is a zinc metalloprotease that degrades NF-κB (Pearson *et al*, 2011) and NleE prevents the degradation of the NF-κB inhibitor IκB (Nadler *et al*, 2010). NleH interferes with NF-κB by both preventing the phosphorylation and translocation of NF-κB transcriptional complexes and by suppressing IκB degradation (Stevens and Frankel, 2014) as well as inhibiting apoptosis by binding the protein Bax inhibitor-1 (Hemrajani *et al*, 2009). NleD is another zinc metalloprotease that cleaves the host proteins JNK and MAPK to inhibit both apoptosis and pro-inflammatory cytokine expression via AP-1 activation (Baruch *et al*, 2011). NleF prevents apoptosis of infected cells by binding to caspases (Blasche *et al*, 2013) and the NleG acts in a

similar manner to RING-like E3 ubiquitin ligases from eukaryotic cells (Wu *et al*, 2010).

1.4.6 Intimin

Intimin is a 94kDa protein (Yu and Kaper, 1992) that is encoded by the *E. coli* attaching and effacing (*eae*) gene (Jerse *et al*, 1990) and has an 83% amino acid homology between EPEC and EHEC strains (Yu and Kaper, 1992). The protein also has sequence homology with the invasin proteins in *Yersinia pseudotuberculosis* and *Y. enterocolitica* with the lowest homology at the N- and C-terminal ends (Jerse *et al*, 1990; Yu and Kaper, 1992). The C-terminal end of intimin has been shown to bind to the surface of HEp-2 and HeLa cells (Frankel *et al*, 1994; Deibel *et al*, 2001) and it has been suggested the N-terminal end masks the C-terminus to prevent non-specific binding to host cells (Deibel *et al*, 2001).

Initmin is a membrane-bound protein that primarily targets Tir, which is translocated into host cells and expressed on their surface (Kenny *et al*, 1997a; Rosenshine *et al*, 1992; DeVinnney *et al*, 1999). Intimin is able to bind to the surface of epithelial cells independently of Tir by binding to host cell β_1-integrins and the growth regulation protein nucleolin (Frankel *et al*, 1996; Sinclair and O'Brien, 2004). Intimin binds Tir preferentially but it is possible that nucleolin acts as a target for adhesion before Tir is translocated into host cells (Sinclair and O'Brien, 2004).

1.4.7 Translocated intimin receptor

As mentioned above, Tir is required for intimin binding to host cells and the formation of A/E lesions (Kenny *et al*, 1997a; Rosenshine *et al*, 1992; DeVinnney *et al*, 1999). It was independently described as EspE and is translocated into host cells via the T3SS (Deibel *et al*, 1998; Kenny *et al*, 1997a). In EPEC O127:H6, actin assembly requires phosphorylation of tyrosine 474 in Tir (Kenny, 1999), which results in the recruitment of the host cell proteins Nck, N-WASP and actin-related protein 2/ actin-related protein 3 (Arp2/3; Guenheid *et al*, 2001). The proteins CrkII

and Grb2 are recruited in EPEC infection but not in EHEC infection (Goosney *et al*, 2001).

In EHEC O157:H7 and O55:H7 strains, the phosphorylation of Tir is not required because these strains lack tyrosine 474 (DeVinney *et al*, 1999; DeVinney *et al*, 2001). Instead these strains utilise a 12 amino acid motif containing an asparagine-proline-tyrosine sequence that recruits the proteins IRTKS, IRSp53, $EspF_U$, N-WASP and Arp2/3 in a manner independent of Nck (Brady *et al*, 2007; Stevens and Frankel, 2014). The tyrosine in the amino acid motif can be phosphorylated in EPEC strains to initiate Nck-independent pedestal formation but at a much lower efficiency than in EHEC (Campellone and Leong, 2005).

1.5 Differences in virulence factor expression by EPEC and EHEC

While most of the virulence factors mentioned above are produced by both EPEC and EHEC, each pathotype has unique virulence factors that differentiate them.

1.5.1 Type IV bundle-forming pili

Bundle-forming pili (BFP) are produced by EPEC and are part of the Type IV pili family, which are expressed by several bacterial pathogens (Girón *et al*, 1991; Strom and Lory, 1993). They are encoded on an ~97kb EAF plasmid (Girón *et al*, 1991; Nataro *et al*, 1987) by a cluster of 14 *bfp* genes, several of which are homologous to genes required for Type IV pilus production in other Gram-negative bacteria (Sohel *et al*, 1996; Stone *et al*, 1996). BfpA is the major subunit of BFP (Donnenberg *et al*, 1992) and is produced as a preprotein before being cleaved into a functional form by BfpP (Zhang *et al*, 1994). The proteins BfpD and BfpF bind nucleotides and act as ATPases to control pilin export and assembly (Sohel *et al*, 1996; Stone *et al*, 1996).

BFP expression is controlled by the EAF plasmid-encoded regulatory proteins BfpT, V and W as well as the chromosome-encoded protein DsbA (Tobe *et al*, 1996; Zhang and Donnenberg, 1996). DsbA stabilises BFP by catalysing the

formation of disulphide bonds (Zhan and Donnenberg, 1996). Environmental signals also control BFP expression, with expression occurring optimally between 35°C and 37°C during the exponential growth phase, in the presence of calcium (Puente *et al*, 1996). Puente *et al* (1996) also found that ammonium suppresses the expression of BFP.

BFP are important virulence factors for the colonisation of hosts, including humans, by EPEC (Bieber *et al*, 1998) and are required for the formation of microcolonies and adhesion to epithelial cells (Girón *et al*, 1991). BFP bind to *N*-Acetyllactosamine on the surface of host enterocytes (Hyland *et al*, 2008) and also act in conjunction with *E. coli* common pili to form microcolonies (Saldaña *et al*, 2009). They are important for initial adhesion of EPEC to host cells and are also involved in the dispersal of bacteria from microcolonies (Cleary *et al*, 2004; Knutton *et al*, 1999).

1.5.2 Shiga toxin

The Stx family of cytotoxins is composed of two major groups, Stx1 and Stx2, which are produced in various combinations by EHEC (Nataro and Kaper, 1998). Stx2, however, is more common in cases of haemorrhagic colitis and HUS (Croxen and Finlay, 2010). Stx1 is identical to Stx from *Shigella dysenteriae* serotype I and is highly conserved whereas Stx2 exhibits sequence variation and is separated into a series of subtypes (Nataro and Kaper, 1998). The *stx* genes are encoded by lysogenic lambdoid bacteriophages, which are integrated into the bacterial chromosome (O'Brien *et al*, 1984; Johansen *et al*, 2001) and Stx production is induced by activation of the phage lytic cycle (Nelly and Friedman, 1998). The regulation of Stx production is complex, with many different regulatory cues affecting gene expression including phage replication cycle, antibiotics, reactive oxygen species, iron concentration, temperature, growth phase and quorum sensing (Pacheco and Sperandio, 2012).

Stx is an AB_5 toxin consisting of an A subunit, which in turn is made from an A_1 and A_2 peptide, that is non-covalently bound to a pentameric ring of B subunits (Stein *et al*, 1992; Fraser *et al*, 1994). The Stx toxins are not secreted but are released

as a result of phage-mediated lysis of the bacterial cell in response to DNA damage and the SOS response (Toshima *et al*, 2007), meaning that certain antibiotics can induce the phage lytic cycle and Stx production (Zhang *et al*, 2000). The B subunit pentamer binds to the Gb_3 variant of the glycolipid receptor globotriaosylceramide that is present on the surface of Paneth cells in the intestine and kidney epithelial cells (Jacewicz *et al*, 1987; Lindberg *et al*, 1987). Stx2e, which is typically associated with porcine oedema disease, uses the Gb_4 variant of this receptor (Pierard *et al*, 1991). Cattle lack the vascular Gb_3 receptor meaning that EHEC infection in cattle is asymptomatic (Pruimboom-Brees *et al*, 2000). There is evidence to suggest that Gb_3 can be found on crypt epithelial cells in cattle, however, Stx does not appear to be cytotoxic in these cells as it is localised in lysosomes (Hoey *et al*, 2003).

Once Stx binds to its receptor, it is endocytosed by both clathrin-dependent and independent mechanisms (Sandvig *et al*, 1989; Römer *et al*, 2007), and a protease sensitive loop connecting the A_1 and A_2 subunits is cleaved by the enzyme furin (Garred *et al*, 1995; Lea *et al*, 1999). The A subunits remain connected by a disulphide bond (Lea *et al*, 1999). Stx bypasses the late endocytic pathway to undergo retrograde transportation to the trans-Golgi network and then to the endoplasmic reticulum (ER; Sandvig *et al*, 1992; Mallerd *et al*, 1998). The remaining disulphide bond is reduced in the ER and the A_1 subunit is translocated into the cytoplasm of the host cell (Johannes and Römer, 2010; Tam and Lingwood, 2007). Once in the cytoplasm, the A_1 subunit exhibits *N*-glycosidase activity and removes an adenine nucleotide from the 28S rRNA of the host cell's ribosomes, resulting in the inhibition of proteins synthesis and cell death (Endo *et al*, 1988).

Stx enters Gb_3-negative intestinal cells via macropinocytosis (Malyukova *et al*, 2008) and is translocated through the cells into the bloodstream in order to reach the kidneys (Acheson *et al*, 1996). Stx is also capable of retrograde transportation in these cells but does not inhibit protein synthesis (Schüller *et al*, 2004). Instead it modulates NF-κB activation and suppresses the host's immune response (Gobert *et al*, 2007).

1.6 The discovery of lymphostatin

In 1995 Klapproth *et al* discovered that cell lysates of certain EPEC strains were capable of dose-dependent inhibition of cytokine expression by human peripheral blood mononuclear cells (PBMCs), but that lab strains, other *E. coli* pathotypes and whole bacteria lacked this ability. Lysates of EHEC O157:H7 strain EDL933 were found to inhibit cytokine expression but were not tested in a dose-dependent manner. Only one EPEC strain tested, O119:H6 0659-79, did not have inhibitory activity against PBMCs, which may be due to known variation in EPEC strains (Levine and Edelman, 1984). Klapproth *et al* (1995) were able to determine that inhibitory activity was caused by a protein or proteins encoded on the bacterial chromosome. They also found, using lysates of an *E. coli* lab strain transformed with an EPEC cosmid (pIV-8-A), that these lysates inhibited cytokine expression in human peripheral blood lymphocytes irrespective of the mechanism of lymphocyte activation. These cosmid clone lysates could also inhibit the mitogen-stimulated proliferation of lymphocytes. The inhibition observed in these experiments was not due to cellular toxicity.

In 1996, further experiments by Klapproth *et al* found that lysates of *E. coli* K-12 containing the EPEC pIV-8-A cosmid clone exhibited dose-dependent inhibition of interleukin-2 (IL-2) against lamina propria mononuclear cells (LPMCs). The inhibition of cytokine synthesis was non-selective and the inhibition of lymphocyte proliferation was not caused by the inhibition of IL-2 receptor expression. CD25 expression was not inhibited in CD45R0 cells by cosmid clone lysates. It was found that the inhibitory effect of EPEC O127:H6 strain E2348/69 lysates was similar in mitogen-stimulated PBMCs and LPMCs. The culture supernatants of EPEC were also found to inhibit IL-2 and IL-5 expression in mitogen-stimulated PBMCs. Lastly, Klapproth *et al* (1996) found that EPEC and cosmid clone lysates could inhibit cytokine expression in lymphocytes activated by non-pathogenic *E. coli* bacterial products.

Malstrom and James (1998) observed that EPEC O127:H6 strain E2348/69 lysates inhibited IL-2 expression in murine splenic cells stimulated with 12-myristate 13-acetate and phytohaemagglutinin without causing apoptosis. EPEC lysates

inhibited multiple cytokines but increased the production of IL-10, which itself inhibits inflammatory cytokine expression. However, the inhibitory activity of EPEC lysates was independent of IL-10 and the regulatory cytokine TGF- β. Macrophages were also not required for the increased production of IL-10. IL-2 expression was inhibited by EPEC lysates in mitogen-stimulated Jurkat cells as well as small intestinal intraepithelial and Peyer's patches lymphocytes. Pre-exposure of murine splenic cells to EPEC lysates resulted in decreased IL-2 and increased IL-10 expression when the cells were both mitogen- and antigen-stimulated. Malstrom and James (1998) also found that lysates of EHEC O157:H7 strain ED933, RDEC-1 and *C. rodentium* had inhibitory activity against murine splenic lymphocytes and that this activity was not related to EspB, which was examined due its requirement for signal transduction in host cells and the activation of NF-κB transcription factors (Foubister *et al*, 1994; Savkovic *et al*, 1997)

In 2000 Klapproth *et al* discovered the protein responsible for the inhibitory activity, which they named lymphosatin or lymphocyte inhibitory factor A (LifA) due its ability to specifically inhibit lymphocyte proliferation and cytokine expression. DNA sequencing of the pIV-8-A cosmid determining inhibitory activity revealed the *lifA* gene to be 9,669bp encoding a predicted 365,950Da protein – the largest protein produced by *E. coli*. The deletion of the *lifA* gene from EPEC O127:H6 strain E2348/69 abolished the inhibitory activity of bacterial lysates but did not affect the A/E ability of intact cells. LifA homologues were found in non-O157 EHEC, RDEC, and *C. rodentium*. Sequence homology was also found with proteins from *Chlamydia trachomatis* and the large clostridial toxin (LCT) family, including a predicted conserved N-terminal glycosyltransferase domain. However, unlike LCTs, EPEC lysates did not disrupt actin distribution in HEp-2 cells, suggesting that LifA does not function in the same manner as LCTs.

1.7 Homologous proteins and sequences to lymphostatin

Nicholls *et al* (2000) discovered a protein in EHEC O111:H- strain E45035 that increased the adhesion of bacteria to Chinese hamster ovary (CHO) cells *in vitro* and named it EHEC factor for adherence (Efa-1). Efa-1 was identical in size to LifA

and was predicted to be 99.9% identical to LifA at a nucleotide level and 97.4% identical at an amino acid level (Nicholls *et al*, 2000). As such, LifA and Efa-1 are thought of as the same protein and their names are used interchangeably in the literature.

LifA and homologous proteins have been found in EPEC, EHEC, RDEC, *C. rodentium*, *H. alvei*, and various *Chlamydia* species (Klapproth, 2010). EHEC O157:H7 does not produce LifA but rather encodes two homologous proteins. The first is LifA′, which is a truncated version of LifA that is encoded on open reading frames *z4332* and *z4333* on O-island 122 of the chromosome (Hayashi *et al*, 2001; Perna *et al*, 2001). LifA′ is identical to amino acids 1 – 433 and 435 – 710 of LifA (Hayashi *et al*, 2001; Perna *et al*, 2001). It is unclear if only the 433 amino acid protein is made or if a 710 amino acid protein can be made via ribosome frameshifting. The second is ToxB, which is of a similar predicted size to LifA and is encoded on the EHEC O157:H7 large plasmid pO157 (Burland *et al*, 1998; Makino *et al*, 1998). ToxB is overall 47% homologous at the nucleotide level and 28% homologous at the amino acid level to LifA (Burland *et al*, 1998; Makino *et al*, 1998). ToxB sequences have also been found in non-O157 EHEC strains and EPEC but the function of the encoded protein remains unclear (Badea *et al*, 2003; Tozzoli *et al*, 2005). In *Chlamydia*, *C. psittaci* contains a single *lifA* homologue, *C. muridarum* possesses three copies and *C. trachomatis* contains a pseudogene with frameshift mutations (Xie *et al*, 2003). Belland *et al*, 2001 have shown that these LifA homologues act as cytotoxins and suggested that it is possible that the immunomodulatory ability of LifA homologues may allow *Chlamydia* species to cause persistent infections.

1.8 Secretion of lymphostatin

Little work has been carried out towards understanding the mechanism of secretion of LifA. Recently, Deng *et al* (2012) reported that LifA appeared to be secreted by the T3SS based on quantitative proteomic (SILAC) analysis of proteins secreted by EPEC O127:H6 strain E2348/69 in a T3SS-dependent manner. This involved mapping peptides across the protein and detecting them using mass

spectrometry. Reporter assays using the N-terminal 50 – 100 amino acids of LifA fused to TEM-1/β-lactamase showed that this sequence of LifA was capable of being injected into HeLa cells and reacting with a β-lactamase substrate to cause a colour change in fluorescence. Due to the limitations of the cloning vector that was used, the N-terminal 50 – 100 amino acids were used instead of the full-length protein. This was suitable for examining Type III secretion as Charpentier and Oswald (2004) found that as little as 20 amino acids from the N-terminus of various T3S proteins is sufficient to mediate translocation through the T3SS. However, without examining the full-length protein it is not possible to determine if Type III secretion is the normal mechanism of LifA secretion, or whether the protein is secreted in its entirety or in processed forms. It is possible that LifA may be secreted via different secretion systems.

The mechanism of LifA secretion is important for understanding how it acts as both a lymphostatin and an adhesin. Studies by Klapproth *et al* (1995, 1996 and 2000), Malstrom and James (1998) and Stevens *et al* (2002) have all shown that bacterial lysates containing LifA have inhibitory activity against lymphocytes and mononuclear cells, indicating that injection is unlikely to be needed for lymphostatin activity. Moreover, activity can be transferred to laboratory-adapted *E. coli* K-12 containing cloned LifA even though it lacks the T3SS. Purified recombinant LifA has also been found to inhibit the mitogen-stimulated proliferation of lymphocytes (Stevens Laboratory unpublished data). This suggests that even if LifA is Type III secreted, it does not absolutely require T3SS-mediated injection into host cells in order to function.

Exactly how LifA acts as an adhesin is unclear but there are multiple possible methods of how it may achieve this. It may gain access to host cells via the T3SS or other means, where like Tir, it becomes a receptor for another bacterial protein or recruits other proteins to act a receptor. An alternative method is that LifA is secreted and then re-associates with the bacterial cell surface before binding to a receptor. This mechanism has been observed with the giant fibronectin-binding adhesin SiiE in *Salmonella enterica* serovar Typhimurium (Morgan *et al*, 2007; Gerlach *et al*, 2007).

1.9 Importance of lymphostatin as a virulence factor

LifA has been shown to be an important virulence factor in A/E pathogens (Stevens *et al*, 2002; Badea *et al*, 2003; Klapproth *et al*, 2005; Deacon *et al*, 2010). Stevens *et al* (2002) found that deleting the *lifA* gene in EHEC O5:H- strain S102-9 caused a 19-fold reduction in adherence to HeLa cells. A reduction in adherence was not observed in the EPEC strain O127:H6 strain E2348/69 but this may have been due to the expression of BFP. Lysates of both EPEC O127:H6 strain E2348/69 and EHEC O5:H- strain S102-9 were found to inhibit the mitogen-stimulated proliferation of PBMCs, although the inhibition caused by EHEC may have been due to other toxins such as Stx. Stx is capable of inhibiting the proliferation of lymphocytes (Menge *et al*, 1999) and deleting the *lifA* gene did not relieve the inhibitory effect of the EHEC lysate. Deleting the *lifA* gene in EHEC O5:H- and O111:H- strain E45035N was found to reduce the adherence of bacteria to the intestinal epithelium of cattle, reduce the overall ability of the bacteria to colonise cattle and reduce pathology. It was also found that EHEC O5:H- Δ*lifA* mutants were reduced in their ability to produce and secrete EspA and Tir, but were still able to form A/E lesions. This suggests that the loss of LifA could have indirectly affected gut colonisation via indirect effects on Type III secretion, which is known to be vital for colonisation of the bovine gut by EHEC O157:H7 (Dziva *et al*, 2004; Naylor *et al*, 2005).

Badea *et al* (2003) reported that LifA was necessary for the *in vitro* adherence of rabbit EPEC to epithelial cells. The rabbit EPEC strain used lacked BFP, which would otherwise have likely masked the effects of LifA. Rabbit EPEC with mutated LifA had reduced adherence to CHO and HeLa cells and polyclonal antibodies against LifA also reduced adherence. The mutation of the *lifA* gene did not disrupt EspA secretion and therefore the decrease in adherence could not be attributed such a disruption.

Klapproth *et al* (2005) found that mutating the *lifA* gene in *C. rodentium* did not reduce the ability of the bacteria to colonise the colon of mice but did result in reduced pathology and accelerated clearance of the bacteria. In these experiments Klapproth *et al* (2005) mutated the putative glycosyltransferase and cysteine protease

domains as well as a domain between these two that does not encode any known activity. However, later it was discovered that the mutations created stop codons, which resulted in the truncation of the LifA protein (Deacon *et al*, 2010). This means that the results were invalid in relation to the effects of the specific domains but still proved that the protein as a whole is required for pathology in mice.

Deacon *et al* (2010) also investigated the importance of the putative glycosyltransferase and cysteine protease domains by substituting specific motifs within these domains in EHEC O26:H- strain 193 nal^R. This strain was incapable of producing Stx1 in order to prevent it from masking the effects of LifA. It was found that LifA null mutants had a reduced ability to colonise cattle but mutants of the putative glycosyltransferase and cysteine protease domains did not. No effect of the *lifA* mutation on expression of EspA was observed in EHEC O26:H-. In contrast to Stevens *et al* (2002), this shows that LifA has a direct role in gut colonisation independently of EspA. LifA was not necessary to induce enteritis in bovine ileal loops. In contrast to previous experiments, LifA null and motif mutants did not have significantly reduced adherence to HeLa cells or ability to inhibit the mitogen-stimulated proliferation of lymphocytes. However, when the motif substitutions were transferred to the chromosome of EPEC O127:H6 E2348/69 it was observed that the ability to inhibit mitogen-stimulated proliferation of lymphocytes was significantly reduced in the motif mutants compared with parental EPEC E2348/69.

Stevens *et al* (2004) reported that the LifA homologues LifA′ and ToxB influenced the adherence of EHEC O157:H7 to HeLa cells but were not required for the colonisation of cattle or sheep. They also reported that mutations in the *lifA′* and *toxB* genes reduced the production and secretion of proteins encoded by the LEE4 operon but did not affect the activity of the LEE1, 4 and 5 operon promoters. This is consistent with observations by Tatsuno *et al* (2001) that suggest that ToxB affects expression and secretion of LEE-encoded proteins at a post-transcriptional level. Abu-Median *et al* (2006) also performed experiments with *lifA′* and *toxB* mutants and found that these proteins did not appear to confer lymphostatin-like activity against mitogen-stimulated peripheral blood lymphocytes, however, the assay relied on crude bacterial lysates and is relatively insensitive.

1.10 Structural motifs of lymphostatin

The N-terminal portion of LifA is ~40% homologous to the LCT family which includes TcdA and B from *Clostridium difficile*, the lethal and haemorrhagic toxins from *C. sordellii* and α-toxin from *C. novyi* (Klapproth *et al*, 2000; Nicholls *et al*, 2000; Busch *et al*, 1998). This homologous region in LifA encompasses a catalytic DXD motif that is necessary for sugar binding in LCTs (Klapproth *et al*, 2000; Nicholls *et al*, 2000; Busch *et al*, 1998). The LCTs are known glycosyltransferases (Triadafilopoulos *et al*, 1987), most of which bind uridine diphosphate (UDP)-Glucose (Glc; Just *et al*, 1995; Schirmer and Aktories, 2004). *C. novyi* α-toxin can bind UDP-Glc but its primary substrate is UDP-*N*-Acetylglucosamine (GlcNAc; Selzer *et al*, 1996; Schrimer and Aktories, 2004). LCTs are known to act as cytotoxins by hydrolysing UDP-sugars and transferring the sugar onto Rho GTPases, thereby inhibiting RhoGTPase activity and causing the collapse of the actin cytoskeleton (Just *et al*, 1995; Selzer *et al*, 1996). Early experiments by Klapproth *et al* (1995 and 2000) and Stevens *et al* (2002) did not show LifA to act in this manner, however, recent experiments by Babbin *et al* (2009) suggest that LifA from *C. rodentium* targets Rho GTPases in mice. It is unknown whether this is true for LifA produced by EPEC and EHEC. Deacon *et al* (2010) were not able to replicate these results as they did not detect any activation of RhoA in cells infected with EPEC, and so the possible cytotoxic effects of LifA remain unclear.

LifA also contains a cysteine protease domain that is homologous to the YopT protein family in *Yersinia* (Shao *et al*, 2002). YopT proteins cleave Rho GTPases near their C-terminal end, releasing them from the host cell membrane and disrupting the actin cytoskeleton (Shao *et al*, 2002). The function of the cysteine protease domain in LifA is unknown. LCTs are autoproteolytic (Reinke *et al*, 2007), using this domain to release the catalytic N-terminal portion into the cytoplasm after insertion of the LCT across endosome membranes. It is therefore possible that if LifA acts in the same manner as LCTs, that the target of the cysteine protease domain is LifA itself. It appears that these glycosyltransferase and cysteine protease domains are dispensable during intestinal colonisation of calves by EHEC O26:H-,

however, they influence LifA activity, at least when assayed using crude bacterial lysates (Deacon *et al*, 2010).

1.11 Recent advances in understanding the mode of action of lymphostatin

LifA clones are unstable and under-represented in cosmid libraries (Klapproth *et al*, 2000; Janka *et al*, 2002). Nicholls *et al* (2000) reported that they were unable to assemble the full-length *lifA/efa-1* gene from cloned N- and C-terminal fragments and that the protein may be toxic to the *E. coli* cell. Recent work by the Stevens Laboratory has enabled the further study of LifA. Through the use of tightly inducible expression vectors, it has been possible to create a stable plasmid encoding recombinant LifA with a 6x-histidine (6xHis) tag. This recombinant LifA has been purified and biophysically characterised by our collaborators at the Edinburgh Protein Production Facility. It has been observed to bind UDP-GlcNAc but not UDP-Glc, suggesting it may act to some degree as a glycosyltransferase, and it is also capable of inhibiting the mitogen-stimulated proliferation of bovine T lymphocytes in a dose-dependent manner. Lastly, a rabbit polyclonal antibody has been produced against this recombinant LifA, allowing for the sensitive detection of the protein by western blotting.

1.12 Aims and objectives

Given that very little is understood about the molecular mechanisms of LifA activity, this study sought to determine a possible secretion mechanism for the full-length protein, to investigate the role of LifA as a putative glycoyltransferase and to examine the possible cytotoxic effects of LifA on mammalian cells. The overall objectives of this study were to:

1. Determine if full-length LifA can be secreted via the T3SS by examining the secretion of LifA by EPEC wild-type (WT) and mutant strains under T3S-inducing conditions.

2. Probe the role of a predicted DXD catalytic motif within the putative glycosyltransferase domain in LifA by:
   a) Creating a DXD-AAA substitution mutant and purifying the mutant protein.
   b) Comparing the sugar binding ability of the DXD-AAA mutant LifA protein with the WT protein.
   c) Comparing the ability of the DXD-AAA mutant LifA protein to inhibit the Concanavalin A (ConA)-stimulated proliferation of bovine T lymphocytes with the WT protein.

3. Determine if purified WT LifA has any direct cytotoxic effects against mammalian cells.

Chapter 2: Materials and Methods

2.1 Bacterial growth media and chemicals

Bacterial strains were cultured in suspension using lysogeny broth (LB) or on LB agar plates (Sigma Aldrich) and supplemented with antibiotics as indicated. Antibiotics were used at the following final concentrations: Nalidixic acid (Nal), 20µg/mL; Kanamycin (Kan), 30µg/mL; Ampicillin (Amp), 25µg/mL. Where indicated, cultures were supplemented with 0.5% (w/v) D-glucose. Glycerol stocks for bacteria were prepared from fresh liquid cultures and supplemented with glycerol at a final concentration of 15% (v/v). For Type III secretion assays, bacteria were cultured in Eagle's Minimum Essential Medium (Sigma Aldrich) supplemented with 4-(2-hydroxyethyl)-1-piperazineethanesulphonic acid (MEM-HEPES, Sigma Aldrich), 1g/L D-glucose and antibiotics as indicated (MEM-C; Kenny *et al*, 1997b).

2.2 Bacterial strains, plasmids and oligonucleotides

The strains and plasmids used in this study are listed in Table 2.1. The pRham-LifA-6xHis plasmid encodes the *lifA* gene, which is controlled by a rhamnose-inducible promoter. The pRham empty plasmid was a re-ligated pRham vector backbone and was used as a negative control. The oligonucleotides used for site-directed mutagenesis and double stranded sequencing are shown in Table 2.2.

Table 2.1. Strains and plasmids used in this study. Properties of strains and plasmids used are shown with references.

Strain	Description	Antibiotic resistance	Reference/source
E. coli E2348/69	WT EPEC O127:H6 strain.	Nal^R	Taylor, 1970; Levine *et al*, 1978; Levine *et al*, 1985
E. coli E2348/69 Δ*lifA*	Lacks *lifA*.	Nal^R	Stevens *et al*, 2002
E. coli E2348/69 Δ*escN*::Kan^R	Defective T3SS.	Kan^R	Garmendia *et al*, 2004
E. cloni® 10G	Chemically competent cells for transformation. F¯ *mcr*A Δ(*mrr-hsd*RMS-*mcr*BC) *end*A1 *rec*A1 Φ80d*lac*ZΔM15 Δ*lac*X74 *ara*D139 Δ(*ara,leu*)7697 *gal*U *gal*K *rps*L (Str^R) *nup*G λ– *ton*A	Str^R	Lucigen
XL 10-Gold Ultracompetent cells	Chemically competent cells for transformation. Tet^R Δ(*mcrA*)*183* Δ(*mcrCB-hsdSMR-mrr*)*173* *endA1 supE44 thi-1 recA1 gyrA96 relA1 lac* Hte [F′ *proAB laclqZΔM15 Tn10* (Tet^R) Amy Cam^R]	Tet^R, Cam^R	Agilent Technologies
Plasmid	**Description**	**Antibiotic resistance**	**Reference/source**
pRham-LifA-6xHis	Encodes 6xHis tagged LifA with rhamnose inducible promoter.	Kan^R	Courtesy of Dr. Robin Cassady-Cain, Roslin Institute
pRham empty	Re-ligated pRham vector backbone.	Kan^R	Courtesy of Dr. Robin Cassady-Cain, Roslin Institute
pRham-LifA 6xHis DXD-AAA	Encodes 6xHis tagged LifA with rhamnose inducible promoter and DXD motif substituted with AAA.	Kan^R	Made in this study
pWhitescript	Mutagenesis control. Allows for colour screening.	Amp^R	Agilent Technologies
pUC18	Transformation control. Allows for colour screening.	Amp^R	Agilent Technologies

Table 2.2. Oligonucleotides used in this study.

Primer	Sequence (5' to 3')	Purpose	Source
LifA-DXD-1	GGATGTATATCCTTAAAGAGCATGGT GGTATTTATACAGCGGCCGCGATGAT GCCTGCATACTCTAAACAAGTAATTT TTAAAA	DXD-AAA substitution using QuikChange mutagenesis	Sigma Aldrich
LifA-DXD-2	TTTTAAAAATTACTTGTTTAGAGTAT GCAGGCATCATCGCGGCCGCTGTATA AATACCACCATGCTCTTTAAGGATAT ACATCC	As LifA-DXD-1	Sigma Aldrich
pRham forward	GAAGGAGATATACATATGAGACTGC CAGAGAAAGTTCTT	Replication and sequencing of the pRham vector backbone	Lucigen
pETite reverse	GTGATGGTGGTGATGATGGTTAAAA AGGTTGTCACCATT	Replication of the pRham vector backbone	Lucigen
LifA FL For1	GCAGGAAAGATAGCTGGTAAC	Sequencing of the DXD-AAA *lifA* gene from 5' to 3'	Sigma Aldrich
Lifa FL For2	GTTCCCCACCTGAAAGCATT	As LifA FL For1	Sigma Aldrich
LifA FL For3	GGTGAAAACCGCATTTCAAT	As LifA FL For1	Sigma Aldrich
LifA FL For4	CGTGGGCTCAATGGATTCATG	As LifA FL For1	Sigma Aldrich
LifA FL For5	CCTGTTCAAAGATGTTTCAAC	As LifA FL For1	Sigma Aldrich
LifA FL For6	GACTCCTGAAAACTGGGAAG	As LifA FL For1	Sigma Aldrich
LifA FL For7	CGGACTAGGAATAACTGGTG	As LifA FL For1	Sigma Aldrich
LifA FL For8	GGATTACCAACTATTGCCG	As LifA FL For1	Sigma Aldrich
LifA FL For9	CCAACGAATCGCTACTACA	As LifA FL For1	Sigma Aldrich
LifA FL For10	CTGTCCCGCACAGTTCTGAC	As LifA FL For1	Sigma Aldrich
LifA FL For11	CCGAAGCAACTCTCGGCAGC	As LifA FL For1	Sigma Aldrich
LifA FL For12	CAGTCTCCTCCTCTCTTGC	As LifA FL For1	Sigma Aldrich
LifA FL For13	CCGGAAGAGTTTCCGCTCACC	As LifA FL For1	Sigma Aldrich
LifA FL For14	CAGGCTGTTTATCCGGAAG	As LifA FL For1	Sigma Aldrich
LifA FL For15	GGTCATACACCAACGGTAAAC	As LifA FL For1	Sigma Aldrich
LifA FL For16	GAACAGCCAGGTATCGGCAG	As LifA FL For1	Sigma Aldrich
LifA FL For17	CTTATCCGAAATCCCTCAG	As LifA FL For1	Sigma Aldrich

Primer (cont.)	Sequence (5' to 3')	Purpose	Source
LifA FL For18	GCGGCTACCAAGTGTATTATC	As LifA FL For1	Sigma Aldrich
LifA FL Rev15	CCATCAGATATTGCACGACG	Sequencing of the DXD-AAA *lifA* gene from 3' to 5'	Sigma Aldrich
LifA FL Rev16	GTAGCATAAAGCTCTCTGAG	As LifA FL Rev 15	Sigma Aldrich

2.3 Culture of mammalian cell lines

HeLa cells were cultured at 37ºC, 5% CO_2 in Dulbecco's Modified Eagle's Medium (DMEM, Gibco and Sigma Aldrich) with 10% (v/v) heat-inactivated foetal calf serum (FCS, Gibco) and 20mM L-glutamine (Gibco; DMEM-C). The cells were grown to a confluence of 80 – 90% then passaged into fresh medium as follows. The cell monolayer was washed with 10mL Hank's balanced salt solution (HBSS, Gibco) and cells lifted by incubation with 2mL trypsin (1x; 0.05% (w/v) trypsin; 0.02% (w/v) EDTA in HBSS, Sigma Aldrich) at 37ºC for ~2 – 3 minutes. The cells were dislodged from the flask by rinsing with 10 volumes (V) DMEM-C. The cells were then centrifuged at 1200g for 10 minutes at room temperature. The cells were resuspended in fresh medium, counted by trypan blue exclusion (0.4% (w/v) trypan blue, HyClone) using disposable haemocytometer grids (Kova International) and re-seeded at a density of $0.5x10^6$ cells/mL in a T175 filter cap flask (Fisher Scientific). TIB-152 (Jurkat) cells were cultured in suspension at 37ºC, 5% CO_2 in RPMI-1640 medium (Gibco) with 10% (v/v) FCS (Gibco) and 20mM L-glutamine (Gibco; RPMI-CJ) to a density of $3x10^6$ – $7x10^6$ cells/mL. The cells were centrifuged as above and the pellet was resuspended in fresh RPMI. Jurkat cells were counted as above and re-seeded at a density of $0.5x10^6$ cells/mL. For long-term storage at -150ºC, cells were spun down and resuspended in Recovery™ Cell Culture Freezing Medium (10% (v/v) DMEM with 10% (w/v) dimethylsulphoxide, Invitrogen) at a density of $1x10^6$ cells/mL, frozen in a cell freezer at -80ºC overnight, followed by transfer to -150ºC.

2.4 Plasmid DNA purification

Plasmid DNA was prepared from small-scale stationary phase bacterial cultures (5 – 10mL, Miniprep) or larger-scale cultures (50 – 100mL, Midiprep). To perform a Miniprep, 3mL from overnight cultures were each added to two 1.5mL microcentrifuge tubes and centrifuged at 17,949g for 10 minutes. DNA from the pellets was purified using a QIAprep Spin Miniprep Kit (Qiagen) following the manufacturer's instructions. One QIAprep spin column was used for each 3mL culture and columns were left to dry for 10 minutes. The DNA was eluted in 30µL of nuclease free distilled water (nH_2O), which was left to stand for 5 minutes before being centrifuged for 1 minute.

To perform a Midiprep, 50mL overnight cultures were centrifuged at 6000g, 4°C for 15 minutes. Plasmid DNA from the pellets was purified using a QIAprep Spin Midiprep Kit with filter cartridges (Qiagen) following the manufacturer's instructions and the final DNA pellet was dissolved in 50µL of nH_2O.

The DNA concentrations were measured in ng/µL using a NanoDrop (ND-1000) Spectrophotometer (Thermo Scientific).

2.5 Preparation of secreted proteins

Duplicate mid-logarithmic phase cultures of the EPEC E2348/69 (WT), E2348/69 Δ*lifA* (Δ*lifA*) and E2348/69 Δ*escN*::Kan^R (Δ*escN*) strains were grown from 1.5mL of overnight LB cultures in 25mL of MEM with appropriate antibiotics. They were incubated at 37ºC for 5 hours so that the OD_{600} of the cultures was between 0.3 and 0.6. Each set of cultures was pooled and 100µL was taken from each to enumerate viable bacteria by plating of serial dilutions onto LB agar plates with appropriate antibiotics with incubation at 37ºC overnight. The number of colonies on plates with 30 – 300 colonies were counted and multiplied by the dilution factor, and this value was divided by the volume plated in mL to give the number of colony forming units (CFUs).

The pooled cultures were centrifuged at 3220g, 4ºC for 10 minutes, before the supernatants were decanted and filtered through a 0.2µm filter (Ministart

Sartorius) to remove any residual bacteria. Proteins were precipitated by the addition of trichloroacetic acid (Sigma Aldrich) to a final concentration of 10% (v/v) with incubation at 4ºC overnight. The samples were centrifuged at 3220g, 4ºC for 1 hour, the supernatant was decanted, and the pellets were left to air dry before being resuspended in 200µL of 1.5M Tris(hydroxymethyl)aminomethane (TRIS) buffer (pH 8.8). Protein samples were denatured by the addition of an appropriate volume of sample reducing agent (Novex) and 1x lithium dodecyl sulphate (LDS) sample buffer (Novex) and heated at 70ºC for 10 minutes. Samples were stored at -20ºC until analysis.

The bacterial pellets were resuspended in 50mL of phosphate-buffered saline (PBS) and 1mL was processed to make whole cell lysates. The samples were washed by centrifugation at 17,949g, 4ºC for 10 minutes, washed in PBS and centrifuged again. The pellets were lysed using 100µL of BugBuster MasterMix (Novagen) and mixed for 10 minutes at room temperature. Protein concentration was quantified using the Direct Detect system (Merck Millipore) according to the manufacturer's instructions using BugBuster as the buffer control. The samples were then denatured in sample reducing agent and LDS sample buffer as above. Samples were stored at -20ºC until analysis.

2.6 Sodium dodecyl sulphate-polyacrylamide gel electrophoresis (SDS-PAGE)

Proteins were analysed by SDS-PAGE using the Novex (Life Technologies) gel system. Where the detection of LifA was required, 3 – 8% Tris-Acetate gels (Novex) were used. For analysis of proteins <100kDa, 4 – 12% Tris-Glycine gels (Novex) were used. The Tris-Acetate and Tris-Glycine gels were run with 1x Tris-Acetate SDS running buffer (Novex), with 0.25% (v/v) antioxidant (Invitrogen) in the buffer that was in contact with the anode of the gel tank, and 1x Tris-Glycine SDS running buffer (Novex) respectively. HiMark pre-stained protein standards (Invitrogen) and Precision Plus Protein pre-stained standards (Bio-Rad) were used with the Tris-Acetate and Tris-Glycine gels respectively. The gels were run at 150V until the dye front had left the bottom of the gel. Gels were analysed by staining with Coomassie stain (Bio-Rad), according to the manufacturer's instructions, or by

western blot detection. Where the gels were stained, the images were captured using a Gel Doc EZ system (Bio-Rad).

2.7 Western blotting

Proteins were transferred to polyvinylidene fluoride (PVDF) membranes (Amersham Hybond) for western blotting. The gels were soaked in 2x transfer buffer (Novex) with 0.04% (w/v) SDS for 15 minutes while PVDF membranes were washed in methanol then distilled water before being soaked and gently rocked in 2x transfer buffer with 10% (v/v) methanol and 0.1% (v/v) antioxidant for 15 minutes. To get efficient transfer of large proteins (>100kDa), the Tris-Acetate gels were transferred using a wet transfer at 30V for 75 minutes, using an XCell II Blot Module (Thermo Scientific). The Tris-Glycine gels were transferred using the semi-dry method at 15V for 60 minutes in a Trans-Blot Turbo Transfer System (Bio-Rad). Membranes were blocked in Tris-buffered saline/0.1% (v/v) Tween 20 (TBS-T, VWR International) and 5% (w/v) bovine serum albumin (BSA, Merck Millipore) for 1 hour on a rocker, then rinsed briefly with TBS-T and washed for 15 minutes, followed by an additional two washes of 5 minutes. Each membrane was treated with either rabbit polyclonal anti-LifA (Stevens Laboratory, Clone 45), mouse monoclonal anti-RecA (LifeSpan Biosciences) or mouse monoclonal anti-EspD (Ebel *et al*, 1998) antibody at dilutions of 1/25,000, 1/10,000 and 1/5000 respectively in TBS-T/5% (w/v) skimmed milk powder (Chem Cruz). All of the membranes were incubated at 4ºC overnight.

Blots were washed with TBS-T as above. Horseradish peroxidase (HRP)-conjugated secondary antibodies were applied at the following concentrations in TBS-T/2% (w/v) skimmed milk powder: goat anti-rabbit HRP (Bio-Rad), 1/10,000; goat anti-mouse HRP (AbD Serotec), 1/10,000. The membranes were incubated at room temperature for 1 hour and the blots washed TBS-T as above. The membranes were dried and developed using SuperSignal West Pico Chemiluminescent Substrate (Thermo Scientific) following the manufacturer's instructions and exposed to Amersham Hyperfilm for various times to achieve clear images. Films were developed using an SRX-101A film processor (Konica Minolta).

2.8 Site-directed mutagenesis of the DXD motif of lymphostatin

Mutagenesis of the DXD motif was performed using a QuikChange II XL Site-Directed Mutagenesis Kit (Figure 2.1, Agilent Technologies) following the manufacturer's instructions with some modifications. The primers LifA-DXD-1 (forward) and LifA-DXD-2 (reverse; see Table 2.2) were designed using the QuikChange Primer Design Program (www.agilent.com/genomics/qcpd), with the aim of replacing DXD at amino acid positions 557 – 559 of E2348/69 *lifA* with 3 alanine residues using codons that simultaneously create a *Not* I restriction site. Polymerase chain reaction (PCR) was performed using 10ng of the pRham-LifA-6xHis plasmid as a template, 1x reaction buffer, 125ng of each of the forward and reverse primers, 2% (v/v) dNTP mix, 6% (v/v) QuikSolution reagent and nH_2O to make up to 50µl reaction volume. *PfuUltra* HF DNA polymerase was added to the reaction mixture at 2.5U/µL. PCR was used to introduce the AAA sequence by complete replication of the plasmid, followed by digestion of the parent plasmid using 10U/µL *Dpn* I, which digests methylated template DNA but not DNA generated in the PCR reaction. A commercial pWhitescript plasmid was used as a positive mutagenesis control, using primers (sequence not disclosed by manufacturer) that repair a mutation in the β-galactosidase gene, which can be detected by blue-white screening using a chromogenic β-galactosidase substrate. The PCR parameters are listed in Table 2.3.

XL 10-Gold Ultracompetent cells were thawed on ice and prepared according to the manufacturer's instructions. The *Dpn* I-treated DNA samples were added to separate aliquots of cells. A quantity of 0.01ng of pUC18 plasmid was added to an aliquot of cells for use as a transformation control. The transformation reactions were gently swirled and incubated on ice for 30 minutes. The cells were transformed by heat shock at 42ºC for 30 seconds and incubated on ice for 2 minutes. The cells were suspended in NZY^+ broth (see Appendix 1), which was used as a recovery medium before plating, and incubated at 37ºC for 1 hour with shaking at 225 – 250rpm. The cells transformed with the mutant plasmid were spread onto LB/Kan agar with 0.5% (w/v) glucose and cells transformed with the pWhitescript and pUC18 plasmids were spread onto LB/Amp agar. The LB/Amp plates also had 250µL of 80µg/mL X-gal

(Promega) and 250µL of 20mM IPTG (Sigma Aldrich) spread onto the agar before the cells were added to allow for blue-white screening. The plates were incubated at 37°C for >16 hours.

Table 2.3. PCR programme used for site-directed mutagenesis of the pRham-LifA-6xHis plasmid.

Segment	No. of cycles	Temperature (°C)	Time
1	1	95	1 minute
2	18	95	50 seconds
		68	50 seconds
		68	13 minutes (1 minute/kb of plasmid)
3	1	68	7 minutes
4	1	15	∞

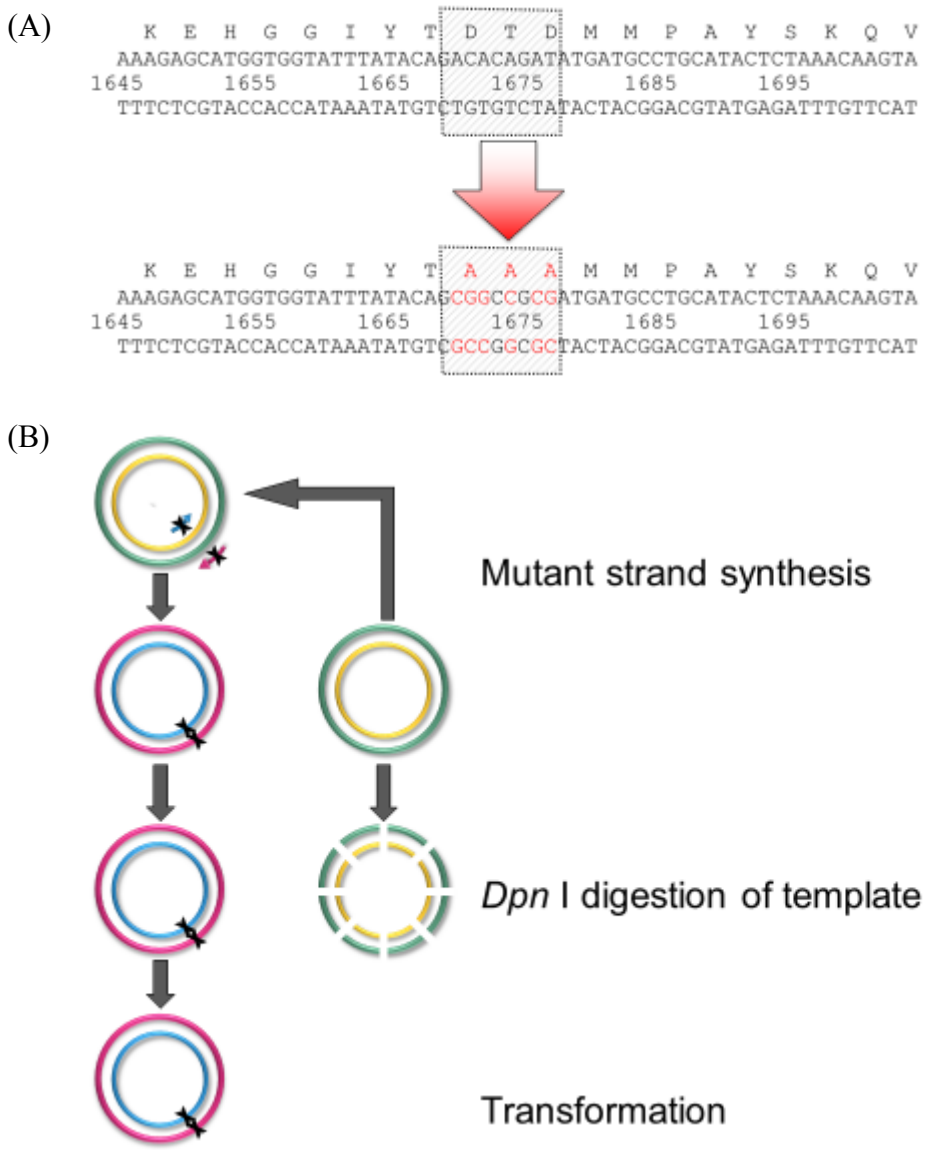

Figure 2.1. The process of creating the DXD-AAA substitution mutant of LifA. (A) Nucleotide and amino acid sequence of the part of the catalytic DXD motif within the putative glycosyltransferase domain of LifA, highlighting the codons that were targeted for site-directed mutagenesis in order to create an AAA substitution mutant. It was also possible to incorporate a new *Not* I restriction site (GCGGCCGC) at this location. (B) Schematic of the procedure for QuikChange Mutagenesis. Mutant strand synthesis is carried out using the mutagenic primers to replicate the entire plasmid using PCR. This is followed by *Dpn* I digestion of methylated and hemimethylated template DNA to remove the parental plasmid DNA. Finally, the mutated plasmid is transformed into chemically competent cells (adapted from Aligent Technologies, 2015).

2.8.1 PCR screening of putative mutant constructs

Putative clones of pRham-LifA-6xHis with the DXD-AAA change were initially screened by PCR to verify that they contained plasmid harbouring the *lifA* gene. Glycerol stocks were made from each of the cultures, which were stored at -80°C for further use and 2µL of each culture was lysed in 198µL of nH_2O. The lysed cells were mixed with 1x PCR master mix, which contained 1x HF buffer (Thermo Scientific), 10µM pRham forward primer, 10µM pETite reverse primer (see Table 2.2), 10mM dNTPs and 2U/µL Phusion polymerase (Thermo Scientific) to make up 20µL reaction volume. A no-template negative control and a parent plasmid DNA pRham-LifA-6xHis positive control were included. The PCR parameters are listed in Table 2.4. The PCR products were analysed on a 0.8% (w/v) agarose (Invitrogen) gel against a 1kb DNA ladder (Promega). Gels stained with SYBRsafe (Invitrogen) were run at 120V for 20 minutes.

Table 2.4. PCR programme used for screening transformants.

Segment	No. of cycles	Temperature (°C)	Time
1	1	98	10 seconds
2	25	98	10 seconds
		55	15 seconds
		72	10 minutes
3	1	72	10 minutes
4	1	4	∞

2.8.2 *Not* I digests of plasmids

Not I was used to distinguish between mutated *lifA*, which contains a *Not* I restriction site at the location of the DXD-AAA substitution (see Figure 2.1), and false positives. Miniprep DNA from the colonies that tested positive for the presence of *lifA* were mixed with 1x *Not* I master mix, which contained 1x buffer D, 10mg/mL BSA, 10U/µL *Not* I (all from Promega) and nH_2O. A negative and positive control of nH_2O and pRham-LifA-6xHis plasmid were also treated with *Not* I. The DNA was

digested at 37°C for 1 hour and the digestion products were analysed on a 0.8% (w/v) agarose gel against a 1kb DNA ladder. Gels were run as previously described.

2.8.3 Sanger sequencing of mutated plasmids

Mutant plasmids were verified by conventional Sanger sequencing by GATC Biotech. The LifA forward primers FL For1 – 18, the reverse primers FL Rev15 and 16 and the pRham forward primer (see Table 2.2) were used to sequence the entire *lifA* gene.

The sequences were assembled using Lasergene SeqMan Pro (DNASTAR). Briefly, the sequence was clipped using SeqMan Pro to remove any areas of low sequence quality. The complete sequence was constructed by creating a contig of overlapping sequences in SeqMan Pro and differences in the original sequences were resolved by comparison of overlapping sequences with reference to sequencing chromatograms if needed. The complete sequence was compared with the WT *E. coli* E2348/69 genome using NCBI Blast (Iguchi, 2009; Madden, 2003) to identify any undesirable mutations that may have been introduced to the sequence (see Appendix 2).

2.9 Pilot protein expression assays

Protein was overexpressed in *E. cloni*® 10G and XL 10-Gold Ultracompetent cells transformed with the pRham-LifA-6xHis and pRham-LifA-6xHis DXD-AAA plasmids respectively. *E. cloni*® 10G with the pRham empty plasmid was used as a negative control. Fresh 50mL LB subcultures were made from overnight cultures inoculated with single colonies. The subcultures were incubated at 30°C until they reached an OD_{600} between 0.5 and 0.6. Uninduced samples were collected and 0.2% (w/v) L-rhamnose was added to induce LifA production. At 2 hours post-induction, the induced and uninduced samples were centrifuged at 3220g, 4°C for 20 minutes and the pellets were collected, washed in PBS and centrifuged again. Protease inhibitors (Roche) were added to the cell suspension, which was then lysed by cell disruption (20kpsi, Constant Cell Disruption Systems). The lysates were centrifuged

at 3220g, 4°C for 20 minutes, the supernatant was decanted, and pellets were further lysed in 1mL BugBuster for analysis by SDS-PAGE.

Protein concentrations of the soluble lysates were measured and the samples were denatured as previously described. The samples were centrifuged at 17,949g for 10 minutes to separate the large cell debris and analyzed by western blotting as described above.

2.10 Optimisation of DXD-AAA LifA protein production

Overnight cultures of *E. cloni*® 10G transformed with the pRham-LifA-6xHis DXD-AAA plasmid, grown in LB/Kan broth were diluted 10-fold in Enpresso B media (BioSilta) and grown at 37°C to an OD_{600} of 0.5. Cultures were cooled to the appropriate induction temperature and induced with the addition of 0.2% (w/v) L-rhamnose when the OD_{600} reached 0.6. The cultures were incubated at either 20 or 30°C and OD_{600} measurements were taken 30 minutes, 1, 2, 3 and 4 hours after induction. Aliquots of 1mL of culture were taken at each time point. The aliquots were centrifuged at 12,500g in a benchtop centrifuge for 10 minutes, the supernatant was discarded and the pellets were stored at -20°C until ready for further processing. The pellets were dissolved in 6µL of BugBuster for every 0.01 OD_{600} unit measured and sonicated with 3 x 10 second bursts using a Soniprep 150 Ultrasonic disintegrator (MSE). The pellets were kept on ice in between sonication bursts. A volume of 5µL from each lysate was mixed with 5µL of 10x sample reducing agent and 5µL of 4x LDS sample buffer then boiled at 100°C for 2 minutes and run on a 4 – 12% Tris-Glycine gel (Bio-Rad) at 250V for 22 minutes.

Large-scale protein production was carried out by first inoculating 2 x 25mL LB/Kan overnight cultures with a single colony each. From these overnight cultures, 5mL was added to each of 10 x 500mL LB and grown at 30°C for 3 hours with 0.2% (w/v) L-rhamnose. The cultures were centrifuged at 6000g, 4°C for 20 minutes, the supernatant was discarded, and the pellets were flash frozen in liquid nitrogen and stored at -80°C until required for protein purification.

2.11 Purification of DXD-AAA LifA

The DXD-AAA LifA protein was purified using a five-step process using ion metal affinity chromatography (IMAC), size exclusion chromatography (SEC), ion exchange chromatography and two desalt columns on a fast protein liquid chromatography (FPLC) unit (ÄKTA Explorer 10 UV900 LC system, GE Healthcare Life Sciences ÄKTA). All buffers used throughout the purification process were filtered and degassed to remove particulate matter (see Appendix 1 for their compositions). The presence of the DXD-AAA LifA protein in the filtrates throughout the purification was monitored using SDS-PAGE and UV absorbance at 280nm. The operation of the FPLC unit was carried out by Dr Liz Blackburn throughout the purification process at The Edinburgh Protein Production Facility.

Initially, the protein lysate was subjected to HiTrap nickel-Sepharose IMAC column chromatography (GE Healthcare Life Sciences). Cell pellets were thawed, lysed with IMAC lysis buffer (IMAC buffer A (see Appendix 1) with 500mM non-detergent sulphobetaine 201, 1 protease inhibitor tablet/1L of cell culture, 0.1mg/mL benzamidine and 0.1% (v/v) phenylmethanesulphonylfluoride to prevent protein degradation) and lysed further by cell disruption (30kpsi, Constant Cell Disruption Systems). The lysed pellet lysate was centrifuged at 50,000g, 4°C for 1 hour then run over the column at a flow rate of 2mL/minute, followed by a wash of 22 column volumes (CV) of 4% IMAC buffer B (see Appendix 1), equivalent to 20mM imidazole. The DXD-AAA LifA protein was eluted with 3 CV of 100% IMAC buffer B containing 500mM imidazole and collected in 1mL fractions.

The fractions of the IMAC filtrate that contained DXD-AAA LifA were pooled and applied to a Superose-6pg XK16/60 SEC column (GE Healthcare Life Sciences), for size exclusion, using SEC buffer. The most pure IMAC fractions, determined by SDS-PAGE, were run through the column first, followed by the less pure fractions.

The fractions of the SEC filtrates that contained DXD-AAA LifA, determined by SDS-PAGE, were run through a HiPrep 26/10 desalt column (GE Healthcare Life Sciences) in a 50mM NaCl low salt buffer to remove excess salt that may interfere with binding to the ion exchange chromatography column.

The desalt fractions containing DXD-AAA LifA, determined by SDS-PAGE, were applied to a Mono Q strong anion exchange column (GE Healthcare Life Sciences) to separate proteins based on their net charge. The percentage of 1M NaCl buffer in the column was increased gradually from 0% to 50%, then sharply to 100%. The fractions of the ion exchange filtrates that contained LifA were then run through another desalt column to remove excess salt. The most pure fractions were pooled into a single aliquot, which was used in all further experiments involving DXD-AAA LifA. Protein concentration was quantified using a NanoDrop Lite Spectrophotometer (Thermo Scientific). Two batches of DXD-AAA LifA were desalted into either assay buffer or CD buffer (see Appendix 1) before use in the biophysical charaterisation and sugar binding experiments.

2.12 Dynamic light scattering (DLS)

Assay buffer with 1.1µM DXD-AAA LifA was passed through a 0.22µm Ultrafree-MC filter (Merck Millipore) and centrifuged at 12,000g, 4°C for 15 minutes. The mean hydrodynamic radius of DXD-AAA LifA was measured using a Zetasizer Automated Plate Sampler (Malvern Instruments, UK) equipped with a 50mW laser light source, with a wavelength of 830nm. DLS data were collected at a scattering angle of 90° for 10 seconds. This was repeated 12 times in triplicate and the values were averaged. Autocorrelation data were fit to a model of a multiple-exponential form suitable for polydisperse solutions using the protein-specific software supplied with the instrument. This generated a distribution of particles by size (Maslon *et al*, 2010). Assay buffer was used as a background control. Experimental data collection and analysis was carried out by Liz Blackburn, observed and supported by the candidate.

2.13 Circular dichroism (CD)

Samples of 0.11µM WT and DXD-AAA LifA in CD buffer were centrifuged at 12,000g, 4°C for 15 minutes. The samples were first checked for aggregation in CD buffer by DLS as described above. The mean residue ellipticity ([θ]) for each

protein was measured using a J-810 Spectropolarimeter (Jasco; Kelly *et al*, 2005) between wavelengths of 190 and 260nm. The [θ] for each protein was plotted against wavelength using Microsoft Excel 2013. The percentage of different secondary structure motifs were determined using DichroWeb (http://dichroweb.cryst.bbk.ac.uk/html/home.shtml; Lobley *et al*, 2002).
Experimental data collection and analysis was carried out by Liz Blackburn.

2.14 Thermal shift assays

WT and DXD-AAA LifA proteins at a concentration of 0.1µM in assay buffer, along with a buffer control were mixed with 5x SYPRO orange and put into a 96 well plate. The plate was sealed and centrifuged at 3220g for 2 minutes to remove air bubbles then put into an IQ5 Multicolor Real-Time PCR Detection System (Bio-Rad). The temperature was increased from 15 to 70°C in 0.5°C increments every 30 seconds and the fluorescence was recorded at each increment. A second thermal shift assay was performed with the addition 0.2µM DXD-AAA LifA to determine whether the concentration of protein would affect the unfolding temperature of the protein. Normalised relative fluorescence units (RFU) for each sample were plotted against temperature using Microsoft Excel 2013. The unfolding transition temperature (T_m) of each protein was calculated from the steepest part of the melting curve. To find the steepest part of the melting curve, the curves were differentiated with respect to temperature (T; -dRFU/dT), therefore the T_m of each protein was the average of the lowest -dRFU/dT values.

2.15 Determination of sugar-binding ability of WT and DXD-AAA LifA

Samples were excited at 295nm and fluorescent emission was collected from 310 to 400nm in 1nm increments every second. The temperature of all samples was held at 20°C in the temperature controlled cuvette holder of the spectrophotometer (Fluoromax 3 Spectrophotometer, HORIBA Jobin Yvon). Assay buffer was put in a quartz cuvette to measure the background fluorescence. Protein was added at a concentration of 0.05µM and the fluorescence was measured again. Titrations of

increasing UDP-sugar concentrations were carried out, the fluorescence of each titration point was measured and background fluorescence subtracted. The fluorescence of the solutions was recorded in triplicate and the values were averaged. UDP-sugar was added between each triplicate of scans. UDP-GlcNAc and UDP-Glc (both Sigma Aldrich; both >98% pure) were titrated against buffer as a negative control. The experiment in which UDP-GlcNAc was titrated against WT LifA was performed by Liz Blackburn while all others were performed by myself. The results were analysed by Liz Blackburn using the law of mass action and the Stern-Volmer relationship.

2.16 Preparation of bovine lymphocytes and T cell enrichment

Peripheral blood was collected into heparinised bags from 3 different 12 – 18 month old Holstein-Friesian calves. Blood was centrifuged at 1200g for 15 minutes with no brake and the lymphocyte interfaces were removed, pooled into two centrifuge tubes, and made up to 30mL with PBS. Each 30mL was overlaid onto 20mL Ficoll-Paque Plus density medium (GE Healthcare Life Sciences) and centrifuged at 1200g for 25 minutes with no brake. The lymphocyte cells at the interface were removed and pooled for each donor and made up to 50mL with PBS and centrifuged at 1200g for 10 minutes. Where the cells were contaminated with erythrocytes, the pellet was resuspended in 1mL of red blood cell lysis buffer (see Appendix 1) and then made up to 50mL with RPMI-1640 medium (Gibco) with 10% (v/v) FCS (Gibco), 20mM HEPES (Sigma Aldrich), 1mM sodium pyruvate (Gibco), 20mM L-glutamine (Gibco) and 100µg/mL penicillin/streptomycin (Sigma Aldrich; RPMI-CT). The cells were washed twice in RPMI-CT and resuspended in 2mL RPMI-CT. The cells were then counted as described above.

To enrich for T cells, a nylon wool fiber column (Polyscience Inc.) was conditioned by adding 10mL RPMI-CT, tapping to remove air bubbles, and draining the media. The column was washed twice with RPMI-CT, filled with 5mL RPMI-CT, sealed and incubated at 37°C, 5% CO_2 for 1 hour. The media was drained from the column, cells were applied at a density of $1x10^8$ cells/mL and run into the column. The column was sealed and incubated at 37°C, 5% CO_2 for 1 hour. The cells

were eluted from the column, which was then washed twice with RPMI-CT to remove any cells residual cells. The cells were counted as described above and the concentration was adjusted to be $4x10^6$ cells/mL.

2.16.1 T lymphocyte proliferation assays

Wells of a 96 well plate were seeded in triplicate with $2x10^5$ cells in 50µL RPMI-C. Serial dilutions were made for the WT and DXD-AAA LifA at concentrations of 400 – 0.004ng/mL and 40µg/mL – 0.4ng/mL respectively. The buffer that the mutant protein was dissolved in (see Appendix 1) was diluted using the same volumes as the DXD-AAA LifA dilution series as a control. Titrations of protein and buffer were added in triplicate to the appropriate wells at the following concentrations in 25µL: WT LifA, 100 – 0.001ng/mL; DXD-AAA LifA, 10µg/mL – 0.1ng/mL; dilutions of buffer representing 10µg/mL, 100ng/mL and 0.1ng/mL of mutant LifA. Concanavalin A (ConA) at a concentration of 50µg/mL was added to the cells in a volume of 25µL RPMI-CT. A background control was set up using 100µL RPMI-CT. Cells alone and cells with ConA, made up to 100µL with RPMI-CT, were used as negative and positive controls respectively. Empty wells were filled with PBS to prevent evaporation of the media.

The plates were incubated at 37°C, 5% CO_2 for 3 days and at 16 hours before the end of the assay 20µL CellTitre 96 AQ_{ueous} One Solution (Promega) was added to each well. The absorbance was read at 492nm using a Multiskan Ascent Spectrophotometer (Thermo Scientific). Ratios of the absorbance value for each titration against the positive control were calculated using averaged experimental (E), maximum proliferation (Mp) and background (B) absorbance values with the following formula:

$$\text{Ratio of cells+LifA/cells+ConA alone} = (E - B)/(Mp - B)$$

The ratios were plotted against the concentration of WT or DXD-AAA LifA protein added with standard deviations using Microsoft Excel 2013. The ED_{50} for the WT and DXD-AAA LifA was calculated using R with the drc package (R Core

Team, 2015). The standard error of the mean was calculated for each ED_{50} using Minitab 17.

2.17 Cytotoxicity assays

HeLa and Jurkat cells were seeded in triplicate at a density of $25x10^3$ cells/50µL in opaque sided 96 well plates (Costar). Cells alone were used as a positive control. Media alone and buffer only were included as background and negative controls respectively. WT LifA titrations of 10µg/mL – 1ng/mL were applied in 50µL DMEM-C or RPMI-CJ to the appropriate cells, which were incubated at 37°C, 5% CO_2. Two identical plates were set up for each assay and one was incubated for 24 hours and the other for 48 hours. Empty wells were filled with PBS to prevent evaporation of the media.

At 24 and 48 hours, a cytotoxicity assay was performed on the cells using a CytoTox-ONE Homogeneous Membrane Integrity Assay Kit (Promega) following the manufacturer's instructions. The cells were equilibrated to 22°C and maximum signal was determined by total cell lysis of the positive control cells with Triton X-100. A volume of CytoTox-ONE Reagent equal to the volume present in each well (100µL) was added to each well and incubated at 22°C for 10 minutes. A volume of Stop Solution equal to half the volume of CytoTox-ONE Reagent used was added to each well and shaken for 10 seconds. The fluorescence was measured with an excitation wavelength of 560nm and an emission wavelength of 590nm using a Glomax Multi Detection System (Promega). The percent cytotoxicity of LifA was calculated using averaged experimental (E), maximum signal (Ms) and background (B) fluorescence values with the following formula:

$$\text{Percent cytotoxicity} = (E - B)/(Ms - B) \times 100$$

The percent cytotoxicity values for the HeLa and Jurkat cells were plotted against the concentration of LifA protein added with standard deviations using Microsoft Excel 2013.

2.18 Statistical analysis

The *P* value was generated for the T cell proliferation assay ED_{50}s using a Two-Sample T-Test created in Minitab 17. A *P* value ≤ 0.05 was taken to be significant.

Chapter 3: Results

3.1 LifA can be secreted via Type III secretion in EPEC

Very little is known about the processing and production of LifA. Although Deng *et al* (2012) reported LifA could be secreted via the T3SS in a hypersecreting strain by SILAC anlysis, secretion of the full-length LifA protein has not been demonstrated in WT *E. coli*. Recently, a polyclonal rabbit antibody against highly purified 6xHis-tagged LifA was produced, allowing the investigation of whether full-length LifA protein can be secreted and the role of the LEE-encoded T3SS in this process.

The WT EPEC E2348/69 strain was used to identify whether or not LifA is a T3S effector protein while the E2348/69 Δ*lifA* strain, which lacks the ability to produce LifA, served as a negative control. An additional strain, E2348/69 Δ*escN*, which cannot produce the T3S-associated ATPase EscN (Garmendia *et al*, 2004), was used to examine any T3S-dependent secretion of LifA. Equal quantities of protein in culture supernatants were loaded based on protein concentration in whole cell lysates. Full-length LifA was successfully detected by western blotting in the culture supernatant of WT *E. coli* E2348/69 under T3S-inducing conditions but not in the supernatant from the Δ*lifA* and Δ*escN* strains (Figure 3.1).

In order to be sure that the LifA detected in the culture supernatants was derived solely from secretion, the proteins RecA and EspD were also probed for as controls. RecA is an intracellular protein (Clark and Margulies, 1965), and so should not be found in supernatants derived from culture of intact bacterial cells. In contrast, EspD is a known Type III secreted protein (Lai *et al*, 1997) that should not be present in the supernatant of the Δ*escN* strain, which is deficient in T3S (Garmendia *et al*, 2004). All controls worked as expected. There was no secretion of LifA detected in supernatants derived from the culture of the Δ*escN* strain even though it was produced in whole cell lysates of this strain, indicating that secretion of lymphostatin occurs via the T3SS.

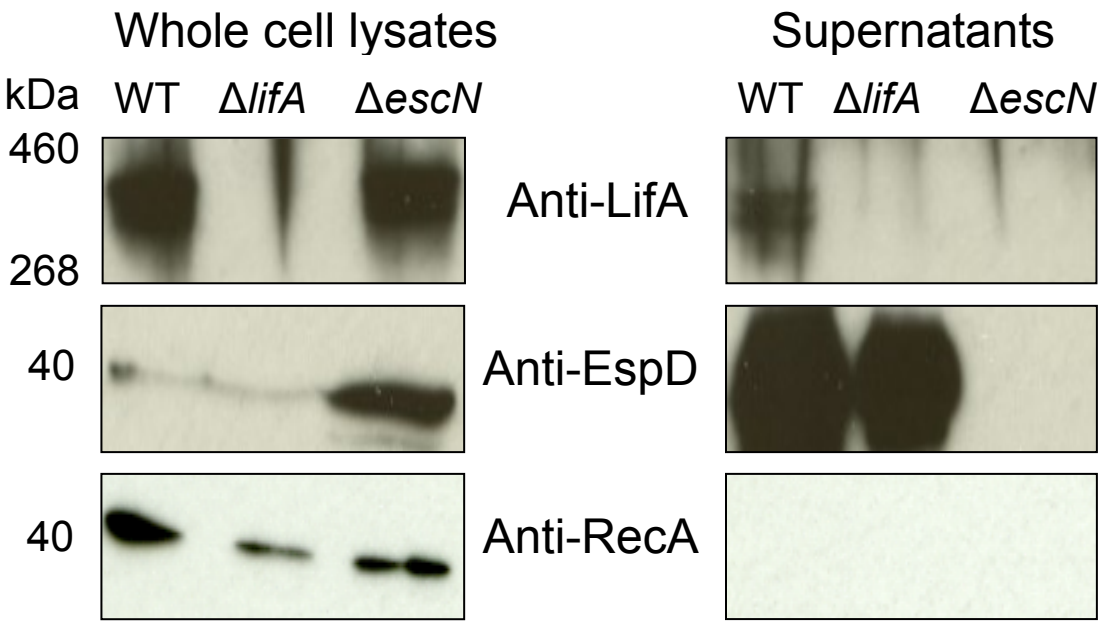

Figure 3.1. Lymphostatin is secreted via the LEE-encoded T3SS in EPEC E2348/69. Western blot of whole cell lysates and culture supernatants for EPEC strains E2348/69 (WT), E2348/69 Δ*lifA* (Δ*lifA*) and E2348/69 Δ*escN*::Kan^R (Δ*escN*). Equal quantities of protein were loaded based on the protein concentration of the whole cell lysates. Samples were probed for LifA to analyse production and secretion, EspD to show that the Δ*escN* strain is defective in T3S, and RecA to show that no lysis of bacteria had occurred during the assay. Three independent assays were carried out and a representative blot is shown.

The average viable counts of cultures and protein concentration of the whole cell lysates for the WT and Δ*lifA* strains were similar, while the viable count and protein concentration for the Δ*escN* strain was lower (Table 3.1).

Table 3.1. Average viable count of cultures and total protein concentration for each strain used in Figure 3.1.

Strain	Average viable count (CFU/mL)	Total protein concentration (mg/mL)
WT	6.75×10^8	2.752
Δ*lifA*	5.89×10^8	2.273
Δ*escN*	1.39×10^8	1.634

Finally, it is noteworthy that there are protein species reactive to anti-LifA antibody that were present in the whole cell lysates of the WT and Δ*escN* strains but not present in the Δ*lifA* strain (Figure 3.2). It is possible that these may be processed or truncated forms of LifA but investigation of the nature of these bands was beyond the scope of the present study.

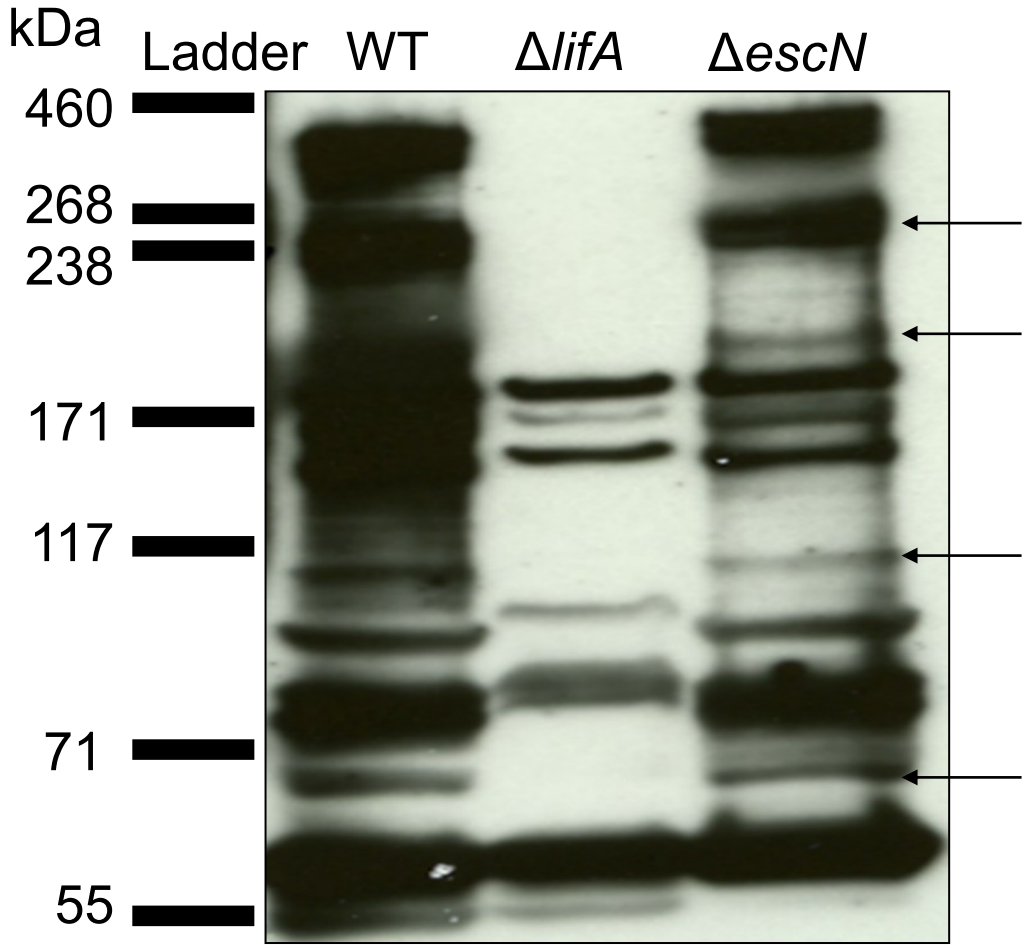

Figure 3.2. Western blot of whole cell lysates of EPEC strains using anti-LifA antibody. Protein species marked with arrows are not present in the Δ*lifA* strain, suggesting that these protein species may be processed or truncated forms of LifA. However, their function within the cell and possible secretion mechanisms remain unknown. Some species in the Δ*lifA* strain appear not to be in the WT or Δ*escN* strain but these likely correspond to the nearby bands at a slightly lower molecular weight. This gel was run using the same samples as Figure 3.1 but at a higher protein concentration.

3.2 Generation of the pRham-LifA-6xHis DXD-AAA clone

The N-terminal portion of LifA is homologous to large clostridial toxins (LCTs) and contains a putative glycosyltransferase domain homologous to that in *C. difficile* toxins TcdA and B (Busch *et al*, 1998). LCTs contain a catalytic DXD motif that Busch *et al* (1998) reported was essential for catalysis as substitution of the amino acids in this motif caused an ~5000 fold decrease in enzyme activity. Given this homology it was hypothesized that LifA may act as a glycosyltransferase and that substituting the DXD motif in LifA for other residues may result in a decrease in the activity of LifA. In order to test this hypothesis, site-directed mutagenesis was used to substitute the DTD amino acid sequence that forms the DXD motif in LifA for an AAA sequence. AAA was chosen because alanine residues are small, non-polar and unreactive, which should allow the protein to fold correctly in the same manner as WT LifA.

QuikChange mutagenesis was performed using the existing pRham-LifA-6xHis plasmid as a template to create the AAA substitution in the *lifA* gene, which also created a new *Not* I restriction site in the plasmid. Different concentrations of template plasmid were used in separate reactions to optimise the yield of putative mutants. The process was controlled using a negative control consisting of template plasmid but no primers. The pWhitescript plasmid and oligonucleotide control primers were used as a positive mutagenesis control. The oligonucleotide control primers repair a mutation in the β-galactosidase gene, which can be detected by blue-white screening using a chromogenic β-galactosidase substrate. The pUC18 plasmid was used as a positive transformation control because it contains part of the *E.coli lac* operon, which complements the host cell's defective $lac^{q}Z\Delta M15$ gene, which can be detected by blue-white screening using a chromogenic β-galactosidase substrate.

Thirty of the largest colonies from across the plates with cells transformed with *Dpn* I digested DNA derived from 100 and 200ng of the original pRham-LifA-6xHis plasmid were cultured overnight, with only one failing to grow. The expected yield of colonies was 10 to 1000 colonies per plate. No colonies grew on the plates with cells transformed with 500ng of the original plasmid digested with

Dpn I or the negative control. The pWhitescript control had a mutagenesis efficiency of >80% and the pUC18 control had a transformation efficiency of $>10^9$ CFU/μg.

The 29 colonies that had grown overnight were screened by colony PCR, using primers to amplify the full-length *lifA* gene and vector, and analysed by agarose gel electrophoresis to test whether the cells has been transformed with the plasmid. Out of the 29 colonies that were screened, 25 tested positive for the presence of the full-length plasmid (Figure 3.3). The colonies were screened against purified parental plasmid as a positive control and a no template negative control. To test whether these transformed colonies actually contained the mutant insert and were not simply false positives, 10 clones that tested positive for the presence of the plasmid were selected to be screened by *Not* I digestion.

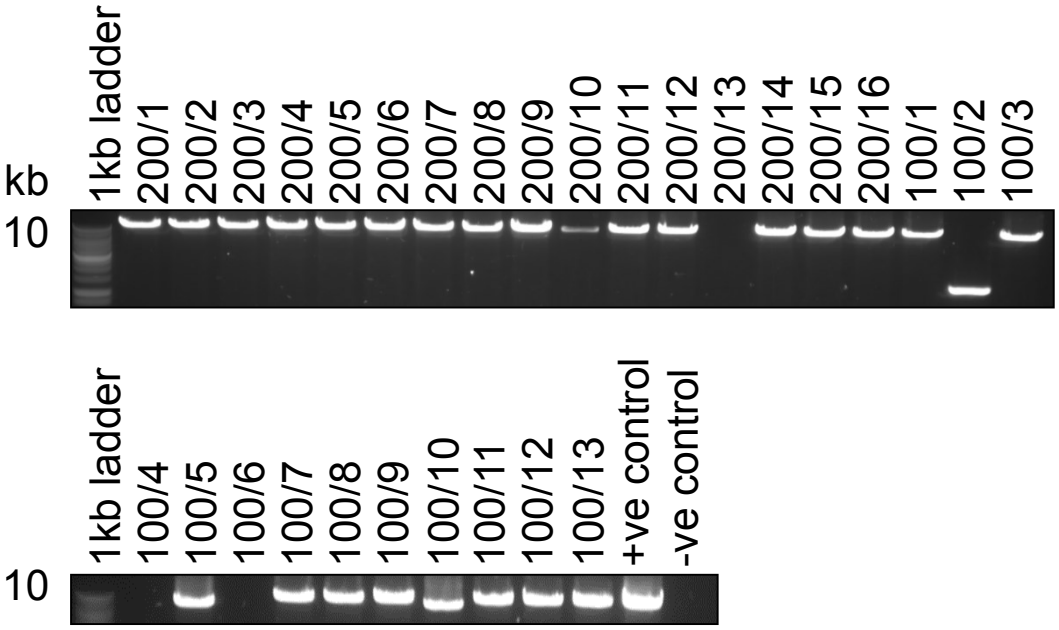

Figure 3.3. Initial screening for putative pRham-LifA-6xHis DXD-AAA mutants with *Dpn* I digested DNA from the QuikChange mutagenesis reaction. 29 transformants of XL 10-Gold Ultracompetent cells were screened by colony PCR using primers that amplified the full plasmid and examined by gel electrophoresis. A positive control of purified pRham-LifA-6xHis plasmid was used and a no template sample was included as a negative control. A product of ~12kb is expected in positive reactions. 25 colonies were positive, 2 gave a reduced amplicon size (200/10 and 100/2), and 3 were negative.

In designing the primers for DXD mutagenesis, it was possible to use alanine codons to introduce a new *Not* I restriction site. As there is only one other *Not* I restriction site in the parent plasmid (Figure 3.4), this makes a useful diagnostic tool to quickly identify putative mutant clones. Digestion of the putative mutant plasmid DNA was expected to give fragments of ~4 and 8kb on a gel if the plasmid was mutated successfully (Figure 3.4). If the mutant insert was not present, a linear single band of ~12kb would be expected. Five of the 10 clones tested were found to contain the mutant insert. The clones were screened against *Not* I digested and undigested purified template plasmid, undigested clone DNA and a no template negative control. It is possible that three other plasmids contained the mutation but were not digested by *Not* I to completion (200/6, 200/10 and 200/11).

From the putative mutant clones identified, three clones were verified by sequencing, initially at the site of mutation to confirm that the expected sequence was present. Once this was confirmed, the entire *lifA* gene was sequenced in all three clones to verify that no additional mutations were introduced during the mutagenesis process. Although all three clones were verified to contain the appropriate mutation, two of the clones sequenced were found to contain additional mutations in the *lifA* gene outside the site of mutation. Only one clone was found to contain the expected sequence of the mutated E2348/69 *lifA* gene and was carried forward for further characterisation (see Appendix 2 for full sequence).

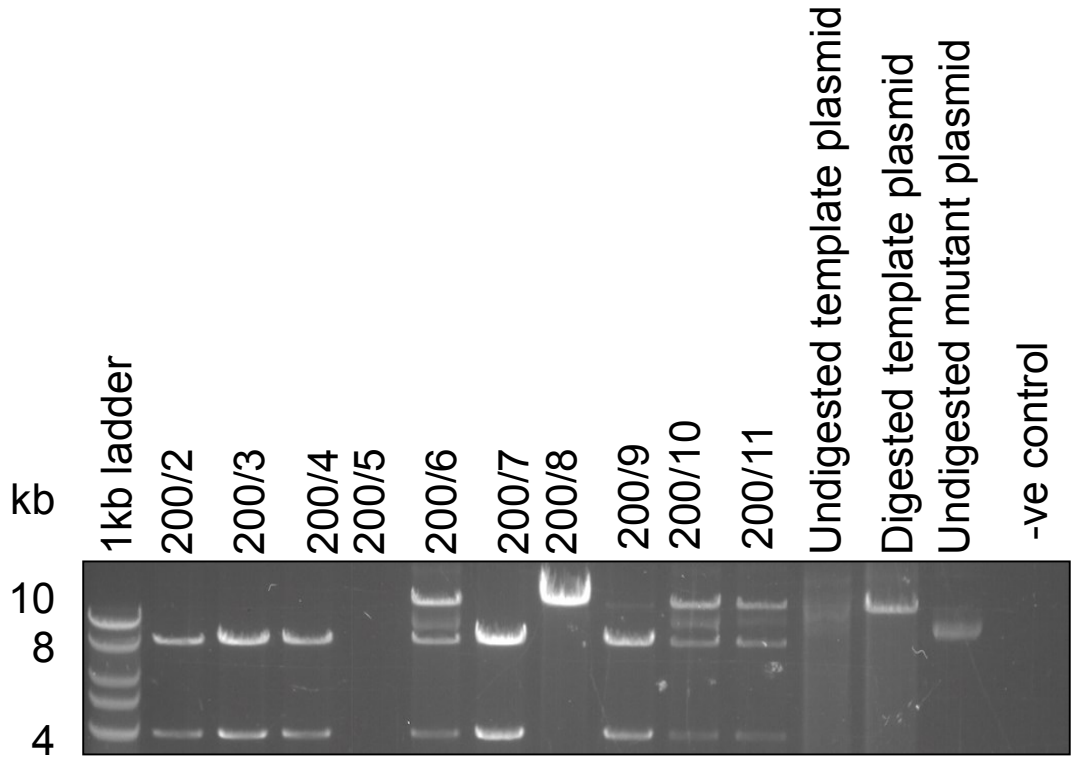

Figure 3.4. *Not* I digestion products of purified pRham-LifA-6xHis DXD-AAA plasmid clones. Of the 25 colonies that tested positive for the presence of the pRham-LifA-6xHis DXD-AAA plasmid, 10 were selected to be screened by *Not* I digestion. Purified plasmid DNA from putative clones was digested with *Not* I and analysed by gel electrophoresis. Each sampled analysed on the gel contained 2µg of plasmid DNA. Undigested plasmid DNA was included as a control and digested parent plasmid DNA was included as a negative control. Positive clones show bands at ~4 and 8kb. Plasmids without the insert show a single band at ~12kb. Out of the 10 colonies selected only 5 tested positive for the presence of the DXD-AAA insert. The three plasmids 200/6, 200/10 and 200/11 may have contained the DXD-AAA insert but were not digested completely by *Not* I.

3.3 Production of the LifA-6xHis DXD-AAA protein

Initially, the pRham-LifA-6xHis DXD-AAA plasmid was examined for its ability to produce full-length DXD-AAA LifA when induced by rhamnose. Production of DXD-AAA LifA was compared to protein produced from the parental

pRham-LifA-6xHis plasmid. Cells transformed with the pRham empty plasmid were used to show that LifA is only produced by cells containing the *lifA* gene. An uninduced sample from the mutant plasmid-containing cells was used to ensure that the DXD-AAA LifA was not being produced without being induced by rhamnose.

LifA was detected by western blotting of crude lysates of the different strains. In pilot experiments, cells transformed with the mutant plasmid were capable of producing full-length DXD-AAA LifA when induced by the addition of rhamnose to the culture and the DXD-AAA LifA protein can be found in the soluble and insoluble fractions (data not shown). LifA was not present in the pRham empty plasmid-containing cells or the uninduced mutant plasmid-containing cells.

Once it had been verified that the clone could produce soluble DXD-AAA LifA, optimization of protein production was carried out. The optimal growth conditions for the production of WT LifA were previously determined to be growth in LB media incubated at 30°C for 3 hours with 0.2% (w/v) rhamnose. To determine the optimal growth conditions for the production of the DXD-AAA LifA protein, time courses were conducted using different media, temperatures and rhamnose concentrations. A time course using Enpresso B media, which allows cells to achieve a higher density than in normal media, was performed at temperatures of 20°C and 30°C with a final rhamnose concentration of 0.2% (w/v). Samples were taken for SDS-PAGE at 30 minutes, 1, 2, 3 and 4 hours (Figure 3.5). This was based on the optimal conditions for WT LifA production. Production of DXD-LifA could be detected at 30°C optimally after 3 hours (Figure 3.5). Two protein species were observed under these conditions in Enpresso B media. Time courses using LB and 2xTY media were also run with additional temperatures, final rhamnose concentrations and sample collection time points (carried out by Liz Blackburn). The optimal conditions for large-scale production of the DXD-AAA LifA protein was ultimately determined to be the same as for the WT protein (Figure 3.6). A single species was detected but appeared to only be 250kDa instead of the expected ~366kDa, however, this was actually the result of running the whole cell lysates on a small Tris-Glycine gel rather than the Tris-Acetate gel used for western blotting.

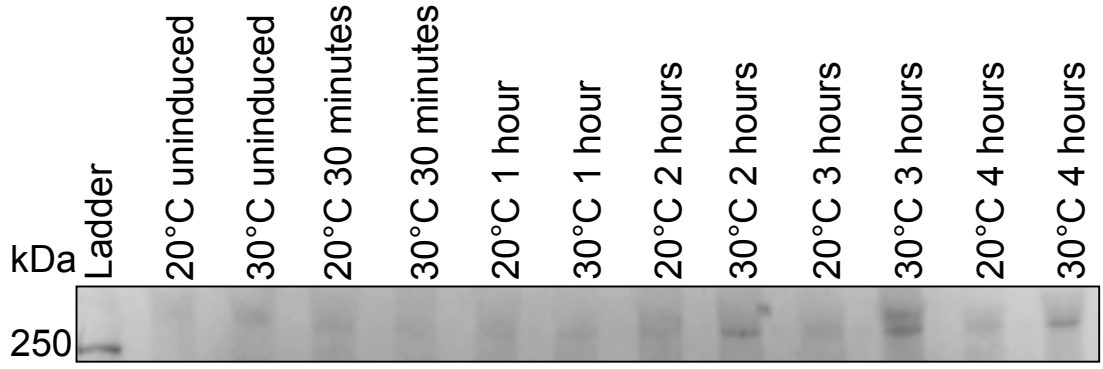

Figure 3.5. Expression time course of DXD-AAA LifA. A time course was run using Enpresso B media as part of determining the optimal growth conditions for mutant protein production. The cells were grown at either 20 or 30°C after induction with 0.2% (w/v) rhamnose and samples were taken at 30 minutes, 1, 2, 3 and 4 hours post-induction. A pre-induction sample was also taken. Incubation at 30°C for 3 hours produced the most DXD-AAA LifA in the cells grown in Enpresso B media. Two protein species are seen in the optimum sample and the identity of the second species is unknown, although it is possible that it is a degraded or processed form of LifA.

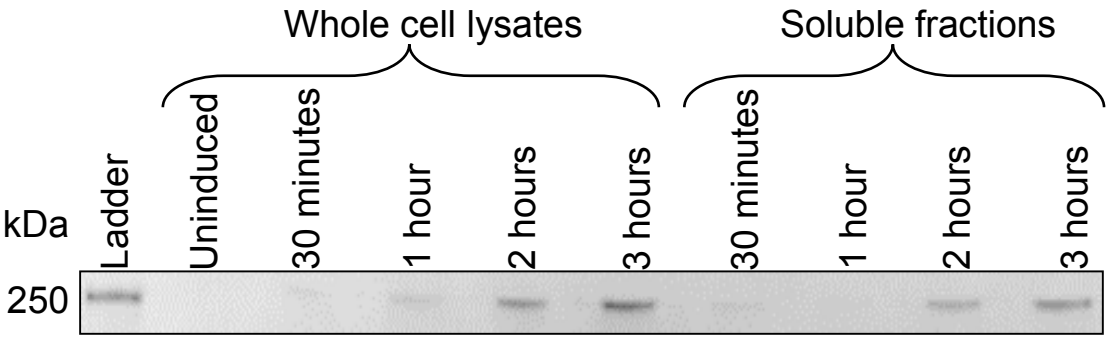

Figure 3.6. Coomassie stain of whole cell lysates and soluble fractions of *E. cloni*® 10G transformed with the pRham-LifA-6xHis DXD-AAA plasmid grown at optimal conditions. The optimal conditions for mutant protein production were found by Liz Blackburn to be LB media at 30°C with 0.2% (w/v) rhamnose for 3 hours, the same as for WT protein production. The protein appears to have a lower molecular weight than expected due to being run on a small Tris-Glycine gel rather than a Tris-Acetate gel.

3.4 DXD-AAA LifA purification

Large-scale production of DXD-AAA LifA was carried out once the optimal conditions for its production were determined and the protein was isolated to a high purity via a five-step process, which was monitored at each step. The DXD-AAA LifA protein was eluted from the IMAC, SEC and ion exchange chromatography columns in a single absorbance peak (Figures 3.7 – 3.9). Ion exchange chromatography was able to separate full-length DXD-AAA LifA from truncated versions of the protein. The DXD-AAA LifA protein was also run through a desalt column before and after the ion exchange to remove excess salt. Although two fractions of high or lower purity were separately handled at each stage (eg. panels A and B of Figures 3.8 and 3.9) only the fractions of highest purity were taken forward for biophysical characterisation. After purification, the DXD-AAA LifA protein was estimated to be >90% pure (Figure 3.10).

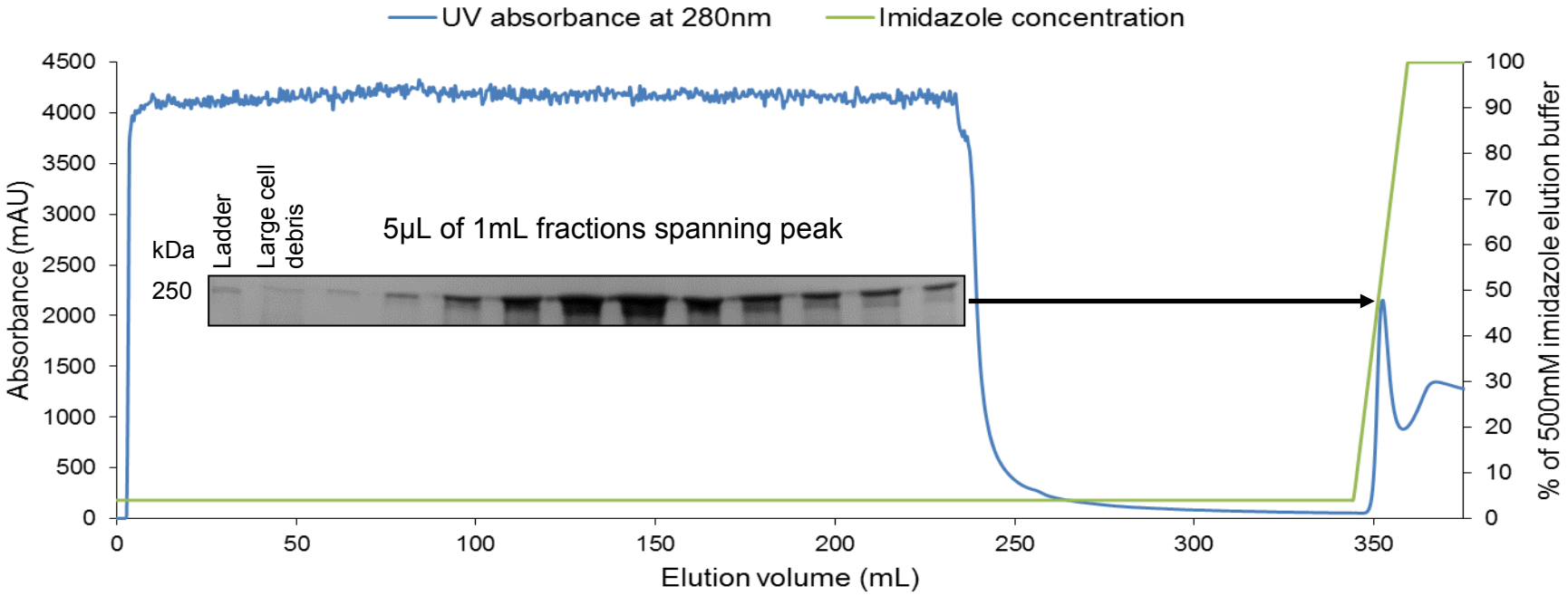

Figure 3.7. Ion metal affinity chromatography (IMAC) purification of DXD-AAA LifA using Ni^{2+}-sepharose. The absorbance of elution buffer at 280nm shows the presence of DXD-AAA LifA where the concentration of imidazole is increased from 20µM to 500µM (marked with an arrow) to elute the protein from the nickel-Sepharose beads. The large absorbance peak between ~0 and 250mL corresponds to large cell debris that do not bind the column. Inset: Coomassie stain of 5µL from 1mL IMAC filtrate fractions showing the DXD-AAA LifA eluted. The protein appears to have a lower molecular weight than expected due to being run on a small Tris-Glycine gel rather than a Tris-Acetate gel.

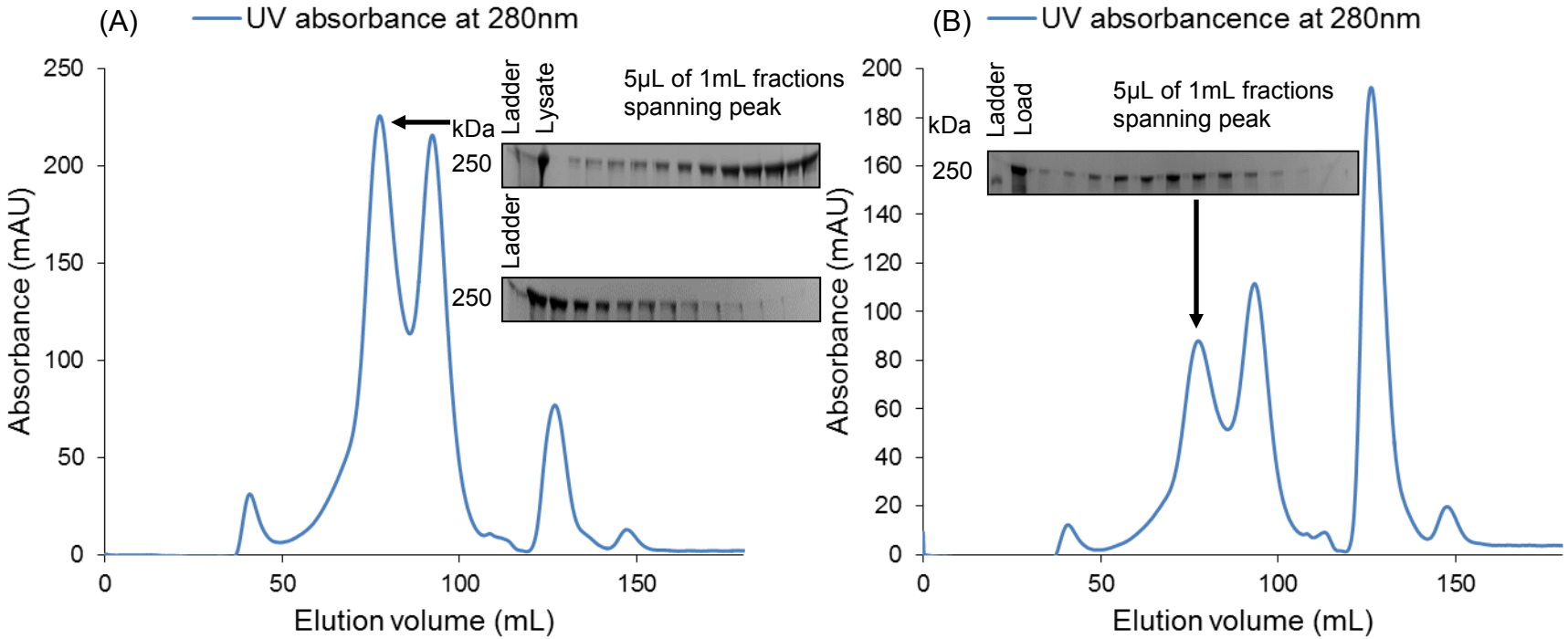

Figure 3.8. Purification of DXD-AAA LifA by size exclusion chromatography (SEC). The absorbance peaks marked with arrows correspond to the presence of DXD-AAA LifA in the filtrates of the Superose 6 SEC columns used to filter (A) the most pure IMAC fractions and (B) the less pure IMAC fractions. Inset: Coomassie stains of 5µL from 1mL SEC filtrate fractions showing the DXD-AAA LifA eluted. The protein appears to have a lower molecular weight than expected due to being run on a small Tris-Glycine gel rather than a Tris-Acetate gel.

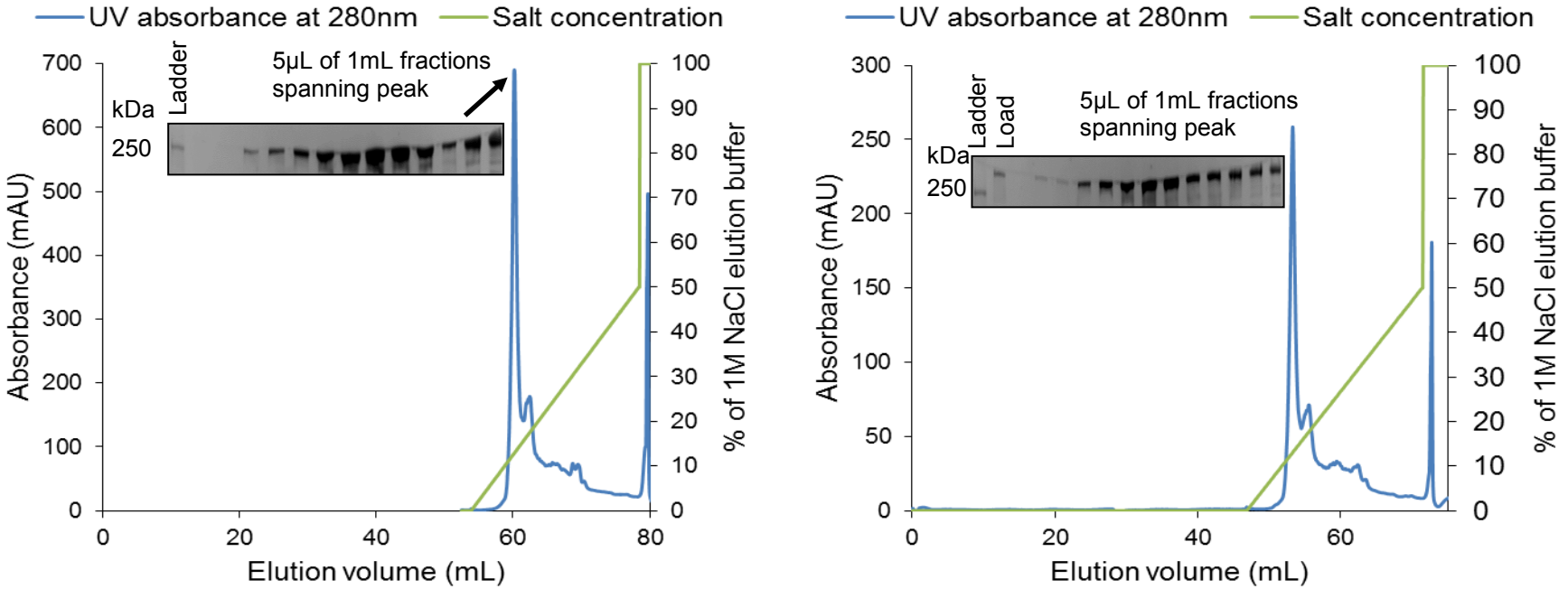

Figure 3.9. Purification of DXD-AAA LifA by ion exchange chromatography. The absorbance peaks marked with arrows correspond to the presence of DXD-AAA LifA in the filtrates of the Mono Q columns used to filter (A) the most pure SEC fractions and (B) the less pure SEC fractions. The most pure and less pure fractions were pooled into separate aliquots after the ion exchange chromatography but only the most pure aliquot was used for further experiments. Inset: Coomassie stains of 5µL from 1mL ion exchange filtrate fractions showing the DXD-AAA LifA eluted. The mutant protein was eluted with 140mM NaCl (12.9% of 1M NaCl elution buffer). The small absorbance peak to the right of the marked peaks corresponds to truncated DXD-AAA LifA. The protein appears to have a lower molecular weight than expected due to being run on a small Tris-Glycine gel rather than a Tris-Acetate gel.

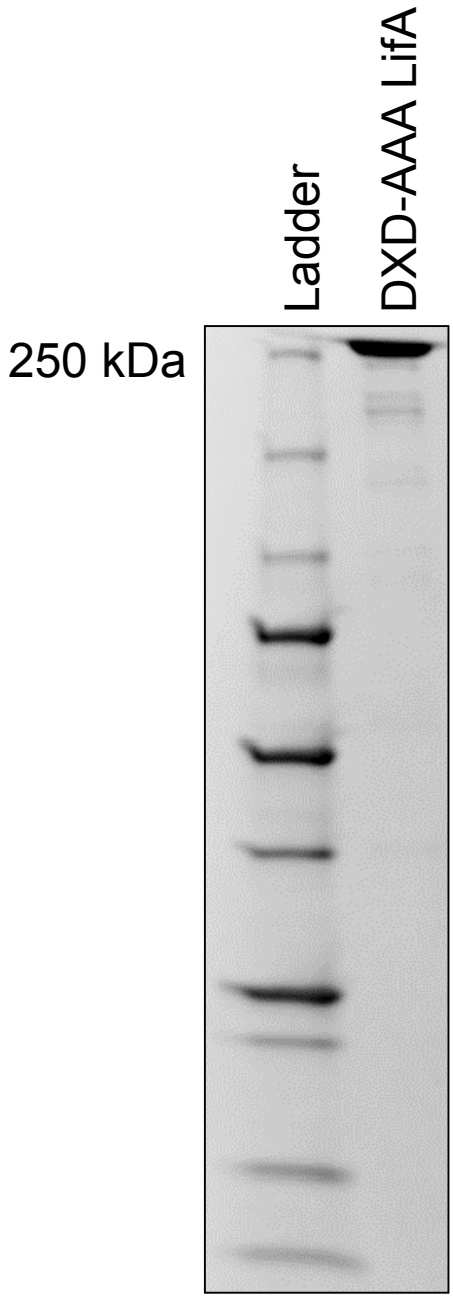

Figure 3.10. Coomassie stain of 1µg DXD-AAA LifA after second desalt. Batches of the most pure DXD-AAA LifA from the ion exchange chromatography were put through another desalt column to remove excess salt that may interfere with the biophysical characterisation of the protein or its sugar binding ability. The estimated purity of the DXD-AAA LifA protein is >90%. The protein appears to have a lower molecular weight than expected due to being run on a small Tris-Glycine gel rather than a Tris-Acetate gel.

3.5 Biophysical characterisation of the purified DXD-AAA LifA

In order to determine whether the DXD-AAA LifA protein was folded and behaved in the same manner as the WT LifA protein, several biophysical measurements were carried out, including dynamic light scattering (DLS), circular dichroism (CD) and thermal shift assays.

3.5.1 DLS shows that DXD-AAA LifA is of a similar size to WT LifA

DLS was used to determine the size and state of the DXD-AAA LifA protein. DLS works by measuring the different intensities of laser scattering caused by the Brownian motion of particles in suspension. This allows protein-specific software supplied with the Zetasizer Auto Plate Sampler to calculate the velocity of the Brownian motion and therefore the size of the particles by using the Stokes-Einstein relationship (Malvern, 2015; Folta-Stogniew, 1999). This allows an approximate size determination and gives some insight into whether the protein is aggregated or multimeric.

Twelve scans of the DXD-AAA LifA protein were performed in triplicate. The size distribution of the protein was measured by the intensity of light scattering and by volume. The distribution by volume provides a more accurate size of the protein and distribution by the intensity of light scattering was used to detect large aggregates, which scatter light at much higher intensity than monomeric protein. Both distribution graphs have one tight peak between 9 and 30nm. The mode hydrodynamic radius of the DXD-AAA LifA protein as measured by intensity and volume is 16.24 and 13.5nm respectively (Figure 3.11). DLS confirmed that DXD-AAA LifA has a hydrodynamic radius of 13.5nm, similar to that of the WT protein (determined by Liz Blackburn). DLS also provided an approximate molecular weight of 358kDa for DXD-AAA LifA based on its size but this is less accurate than measuring the molecular weight by size exclusion chromatography-multi-angled laser light scattering.

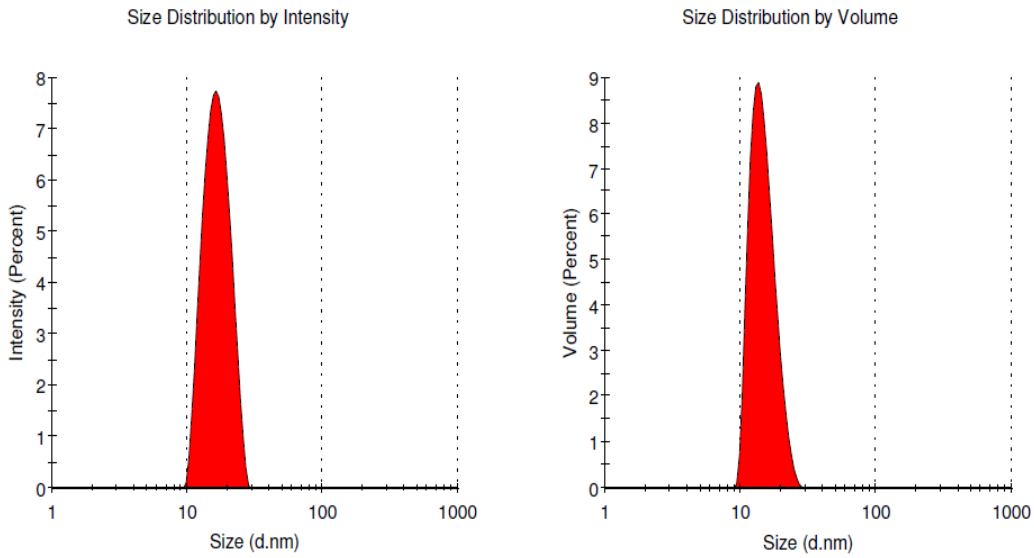

Intensity Distribution Results

	%Int	Mean (d.n...	Mode (d.n...	StD (d.nm...	%Pd	MW (kDa)*
Peak 1:	100.0	16.73	16.24	3.571	21.3	485

Mass Distribution Results

	%Mass	Mean (d.n...	Mode (d.n...	StD (d.nm...	%Pd	MW (kDa)*
Peak 1:	100.0	14.69	13.50	3.069	20.9	358

Figure 3.11. The size distribution of DXD-AAA LifA by intensity and by volume, measured by dynamic light scattering (DLS). DXD-AAA LifA at a concentration of 1.1µM was measured by DLS to determine the size of the mutant protein and ensure that any loss of function was not caused by the protein forming large aggregates. The size distribution by volume provides a more accurate size of the protein than the distribution by intensity, which is primarily used to detect large aggregates that scatter light at a higher intensity than monomeric protein. DLS is also capable of providing an approximate molecular weight for the protein. The peak shift of the volume graph is possibly caused by random aggregation that is picked up by the intensity measurements but not by the volume measurements. The protein was scanned 12 times and the measurements were averaged. This was repeated in triplicate. DLS confirmed that the mutant protein has a hydrodynamic radius of 13.5nm, similar to that of the WT protein (data not shown). Experimental data collection and analysis was carried out by Liz Blackburn, observed and supported by the candidate.

3.5.2 CD shows that DXD-AAA LifA has a similar secondary structure to WT LifA

CD was used to determine if the DXD-AAA LifA protein had folded correctly on a secondary structure level and to observe whether it deviated significantly from the profile obtained for the WT protein. CD works by detecting the difference in absorption between clockwise and anti-clockwise polarised light. CD signals only arise where the absorption of radiation occurs therefore spectral bands can be assigned to distinct structural features of a molecule. The different secondary structures of a protein can be detected because they give rise to characteristic CD spectra in the far UV (Kelly *et al*, 2005).

The protein also had to be scanned by DLS before being subjected to CD because it was desalted into CD buffer rather than the assay buffer used in other experiments. CD buffer, which contains sodium fluoride rather than the sodium chloride used in assay buffer, had to be used for the CD experiment as chloride ions interfere with CD at short wavelengths. The CD profile confirmed that the DXD-AAA LifA had folded correctly and did not significantly differ from WT LifA (Figure 3.12). The mean residue ellipticity peak and trough on the graph correspond to the number of β-sheets and α-helices present in the protein respectively. The percentage of α-helices and β-sheets in DXD-AAA LifA were 31±3% and 25±4% respectively, compared with 37±3% and 22±3% in WT LifA. The percentage of turns and unstructured amino acids in DXD-AAA LifA were 15±4% and 29±5% respectively, compared with 13±3% and 27±6% in WT LifA. Overall, the DXD-AAA LifA protein was folded and had a very similar structural profile to that of the WT protein.

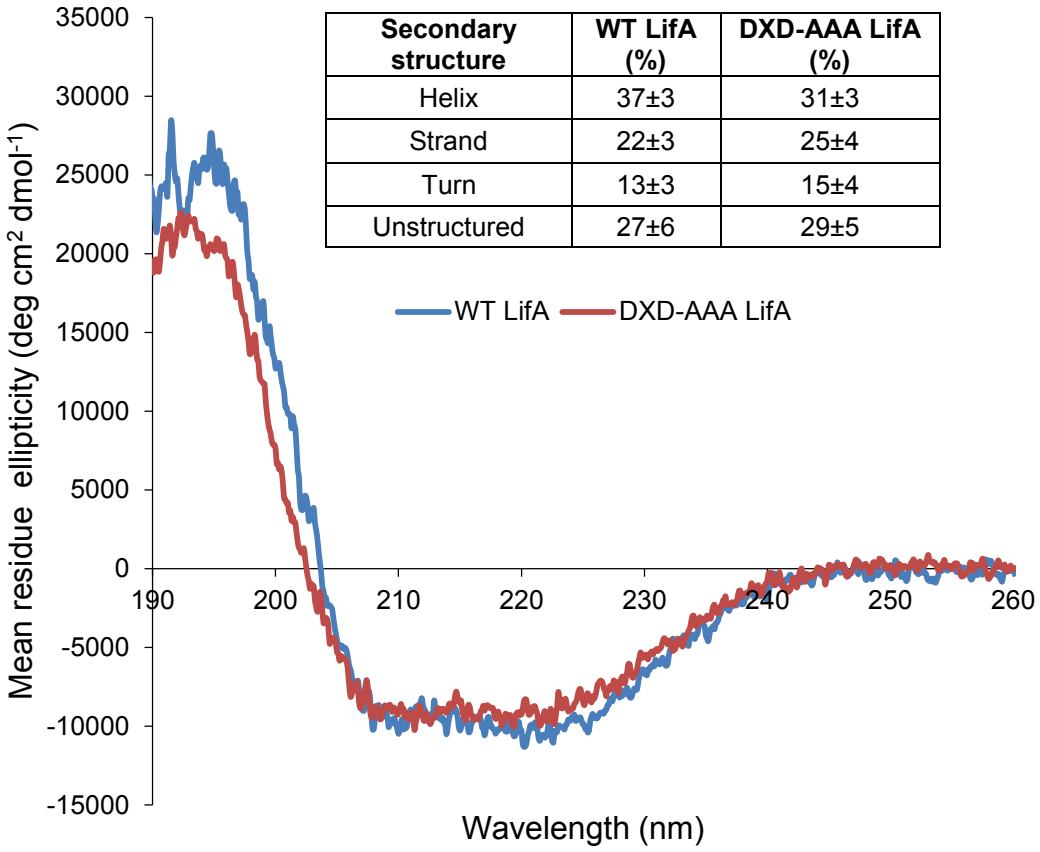

Figure 3.12. Far UV spectrum of DXD-AAA LifA compared to WT LifA. DXD-AAA LifA at a concentration of 0.11µM was measured by CD to compare the secondary structure of the mutant protein with 0.11µM of the WT protein. The mean residue ellipticity peak between 190 and 200nm corresponds to β-sheets and the trough between 200 and 240nm corresponds to α-helices. Each protein was scanned 5 times and the measurements were averaged. The data were analysed using DichroWeb (http://dichroweb.cryst.bbk.ac.uk/html/home.shtml; Lobley *et al*, 2002). The DXD-AAA LifA protein has a similar spectrum to that of the WT protein. WT LifA protein supplied by Liz Blackburn. Experimental data collected and analysis was carried out by Liz Blackburn.

3.5.3 Thermal shift assays show that DXD-AAA LifA has a similar mid-point melting temperature to WT LifA

Thermal shift assays were used to measure the thermal stability of DXD-AAA LifA in comparison to the WT protein. This was carried out by using a fluorescence-based assay using the fluorophore SYPRO orange, which fluoresces weakly in hydrophilic conditions and strongly in hydrophobic conditions, across a range of temperatures. As the temperature increases and the target protein unfolds it reveals hydrophobic amino acid chains that cause the SYPRO orange to increase its fluorescence. The fluorescence intensity is proportional to how much the protein has unfolded (Lo *et al*, 2004; Pantoliano, 2001).

In the first assay, using 0.1μM WT LifA and DXD-AAA LifA, the mid-point melting temperatures (T_m) of the WT LifA and DXD-AAA LifA proteins were 44.2 and 43°C respectively. The second assay included the addition of 0.2μM DXD-AAA LifA to examine whether increasing the concentration of the protein affected the T_m. The T_m for the WT LifA, 0.1μM DXD-AAA LifA and 0.2μM DXD-AAA LifA were 45.5°C, 44.2°C and 44°C respectively (Figure 3.13). Both thermal shift assays that were conducted showed that the DXD-AAA substitution resulted in a decrease of T_m of ~1°C. Increasing the concentration of the DXD-AAA LifA protein did not result in a significantly different T_m. This decrease in T_m was not unexpected due to possible minor structural instability caused by the DXD-AAA substitution.

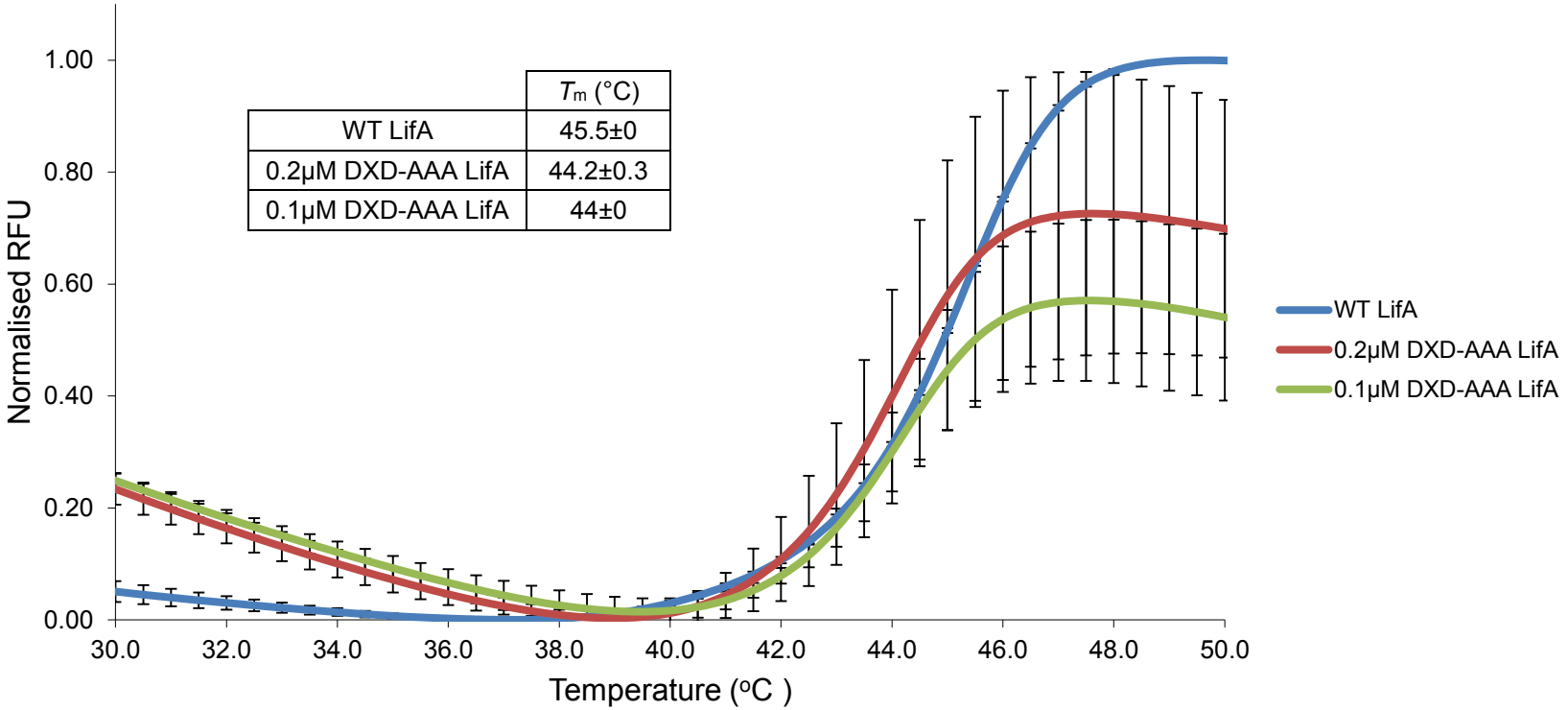

Figure 3.13. Thermal shift assays to evaluate the mid-point melting temperature (T_m) of WT LifA and DXD-AAA LifA. The fluorescence of SYPRO orange dye mixed with WT LifA and DXD-AAA LifA was measured in triplicate over a temperature range of 15 – 70°C to determine the T_m of each protein. WT LifA at a concentration of 0.1μM and DXD-AAA LifA at concentrations of 0.1μM and 0.2μM were compared. Each fluorescence measurement was performed in triplicate. Increasing the concentration of DXD-AAA LifA does not cause any significant change to the T_m. A reproducible decrease of ~1°C in the T_m of the mutant protein is observed.

3.6 Mutation of the DXD motif to AAA abolished sugar binding

LCTs are known glycosyltransferases and contain a conserved DXD motif (Busch *et al*, 1998). *Clostridium novyi* α-toxin is known to bind uridine diphosphate (UDP)-*N*-Acetylglucosamine (GlcNAc; Selzer *et al*, 1996), while others such as *Clostridium difficile* enterotoxin (TcdA) bind UDP-Glucose (Glc) (Just *et al*, 1995). The DXD motif is known to be essential for activity in these molecules and is likely to be important in sugar-binding because it forms bonds with UDP-Glc and a manganese ion in the active site of TcdA (Figure 3.14; Pruitt *et al*, 2012). Recombinant WT LifA has been observed to bind UDP-GlcNAc (Stevens Laboratory, unpublished data) and therefore the dependence of sugar binding on the DXD motif contained within LifA was examined for UDP-GlcNAc and UDP-Glc.

Changes in intrinsic tryptophan (Trp) fluorescence were used to identify the binding of UDP-sugars to WT and DXD-AAA LifA. The fluorescence intensity of Trp residues can indicate whether they are surface-bound or buried within a protein (Eftink and Ghiron, 1976; Price and Nairn, 2009). Intrinsic Trp fluorescence can either decrease via quenching (Price and Nairn, 2009) or increase (Weljie and Vogel, 2000). Fluorescence quenching occurs when an excited Trp residue loses energy by either colliding with molecules in the solvent (collisional quenching) or by forming long-lasting interactions with molecules (static quenching; Price and Nairn, 2009). The exposure of each Trp residue to the quenching molecule determines how easily it is quenched (Eftink and Ghiron, 1976). Intrinsic Trp fluorescence increases when a protein undergoes a conformational change that exposes Trp residues to the solvent, but is stabilised by the binding of another molecule that prevents quenching (Weljie and Vogel, 2000). UDP-GlcNAc should therefore be able to cause a change in the fluorescence of Trp residues in the glycosyltransferase active site if it is able to bind to the purified LifA proteins.

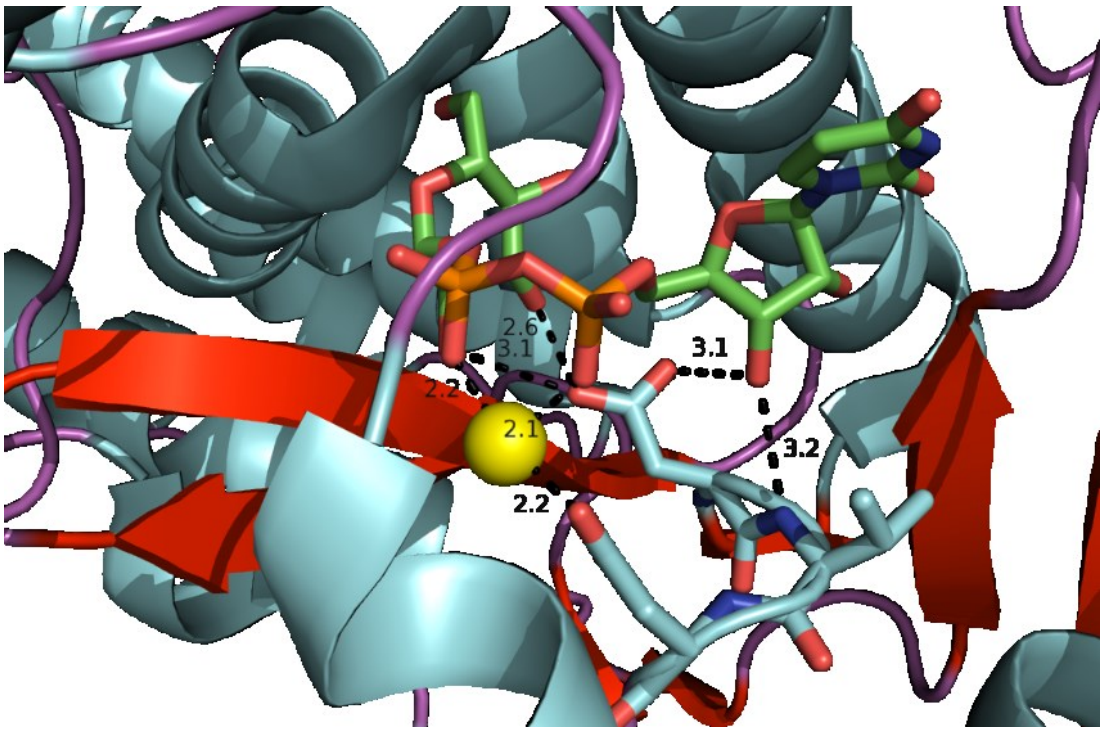

Figure 3.14. Schematic of UDP-Glc binding in the active site of the large clostridial toxin (LCT) TcdA. The putative glycosyltransferase domain of LifA is homologous to LCTs. The glycosyltransferase domain of TcdA also contains a DXD motif with a DVD amino acid sequence rather than the DTD in LifA. This amino acid sequence forms both metal bonds with a manganese ion (yellow sphere) and hydrogen bonds with UDP-Glc (shown in black with bond lengths in Angstroms). It was hypothesised that the DTD sequence in LifA may form bonds with UDP-GlcNAc and an unknown metal ion, making it important for sugar-binding. Therefore the sequence is an ideal target for substitution in order to study whether LifA may act as a glycosyltransferase. UDP-Glc is the green and orange stick model, and the DXD motif is the blue and red stick model. The structure of TcdA was determined by Pruitt *et al* (2012). The schematic was constructed using the 3SRZ.pdb file and Ligand Explorer (both http://www.rcsb.org/pdb/explore/explore.do?structureId=3SRZ), and PyMOL v1.7.6 (http://pymol.org/).

The data were produced by the candidate, with the exception of WT LifA and UDP-GlcNAc (carried out by Liz Blackburn), and analysed using the law of mass

action and the Stern-Volmer relationship (data analysis was carried out by Liz Blackburn). The addition of increasing concentrations of UDP-GlcNAc to WT LifA causes the intrinsic Trp fluorescence to increase before decreasing after the concentration of UDP-GlcNAc is increased beyond ~250μM (Figure 3.15A), indicating that WT LifA binds UDP-GlcNAc. An increase in UDP-GlcNAc concentration causes an increase in sugar-binding. The addition of UDP-Glc to WT LifA or either UDP-sugar to DXD-AAA LifA results in a gradual decrease in fluorescence, indicating that no sugar-binding is occurring, since collisional quenching causes the fluorescence to decrease over time. The binding of UDP-GlcNAc to WT LifA is seen as a curve on the Stern-Volmer plot (Figure 3.15B/C), whereas the lack of binding of UDP-Glc and WT LifA as well as both UDP-sugars with DXD-AAA LifA is evident as straight lines. The Stern-Volmer plot displays the fluorescence of the solution in the absence of UDP-GlcNAc divided by the fluorescence in the presence of UDP-GlcNAc, against the concentration of UDP-GlcNAc added to the solution. In the absence of the DXD motif, UDP-GlcNAc binding by LifA is abolished indicating dependence on this motif.

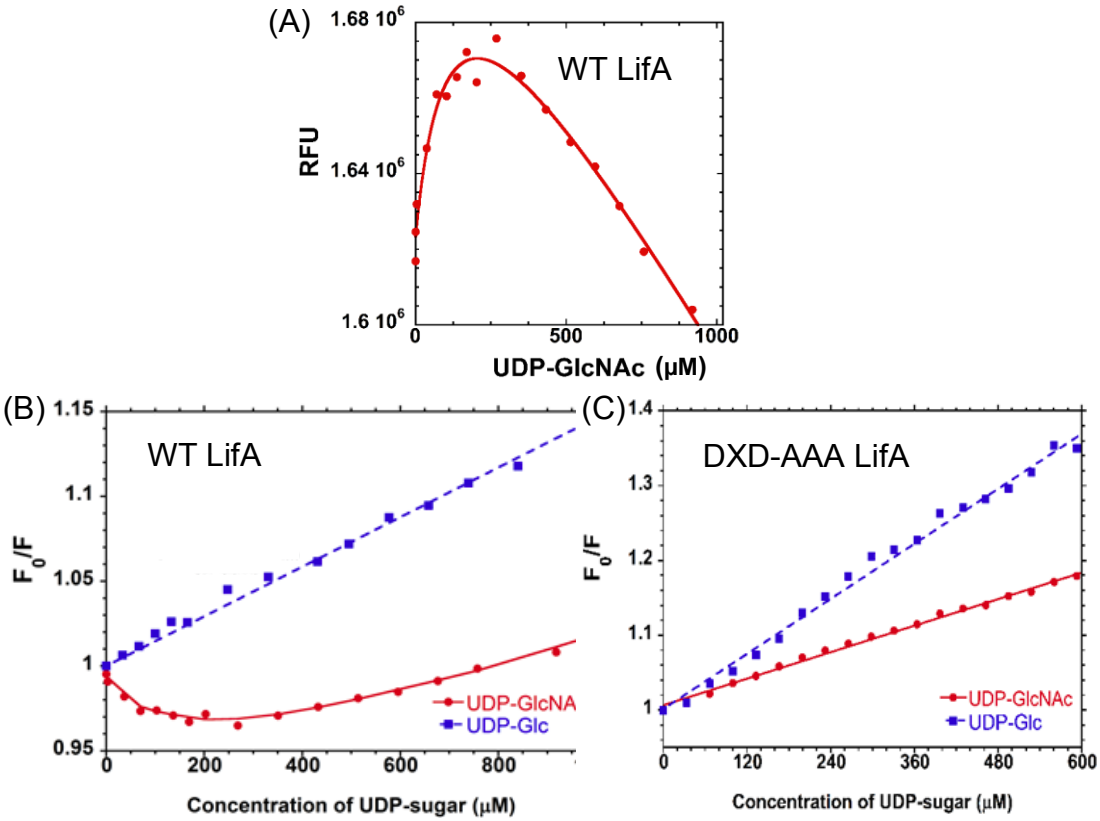

Figure 3.15. Sugar binding to WT LifA and DXD-AAA LifA. UDP-GlcNAc and UDP-Glc were titrated against 0.05μM WT LifA and DXD-AAA LifA and the intrinsic Trp fluorescence was measured in triplicate at 340nm. F_0 and F denote the fluorescence of the solution in the absence and presence of UDP-sugar respectively. (A) Example of raw data of the intrinsic Trp fluorescence of WT LifA against increasing concentrations of UDP-GlcNAc. (B) Stern-Volmer plot of the intrinsic Trp fluorescence of WT LifA against increasing concentrations of UDP-GlcNAc and UDP-Glc. (C) Stern-Volmer plot of the intrinsic Trp fluorescence of DXD-AAA LifA against increasing concentrations of UDP-GlcNac and UDP-Glc. There is a marked loss of UDP-GlcNAc binding to the DXD-AAA LifA protein. Experiments examining WT LifA with UDP-GlcNac were carried out by Liz Blackburn. Experimental data was analysed by Liz Blackburn.

3.7 T cell proliferation assays

It has been observed that cell lysates containing LifA inhibit the mitogen-stimulated proliferation of peripheral blood lymphocytes (Klapproth *et al*, 1995; Klapproth *et al*, 1996; Malstrom and James, 1998; Klapproth *et al*, 2000; Stevens *et al*, 2002). In addition, our laboratory recently showed that purified recombinant WT LifA also inhibits mitogen-stimulated proliferation of bovine T cells. As a result, this is an ideal system to test whether the DXD motif is essential for the biological activity of LifA against T cells.

Peripheral blood T lymphocytes from 3 independent donors were used to test the activity of purified DXD-AAA LifA against ConA-stimulated T cells in comparison to the WT LifA protein using a colourimetric plate-based assay. The assay measures the conversion of an MTS tertrazolium compound into a coloured formazan product by metabolically active cells, the absorbance of which can be detected at around 490nm. The quantity of formazan produced is directly proportional to the metabolic activity of dividing cells in the culture (Promega, 2012).

Titration of WT LifA produces a sigmoid curve, with higher concentrations of LifA causing an increase in inhibition (Figure 3.16). The ratio of proliferation of cell treated with LifA+ConA/ConA alone decreases sharply from 0.98±0.11 at 0.001ng/mL of WT LifA to 0.41±0.04 at 0.1ng/mL, then the curve levels out and decreases to a ratio of 0.3±0.07 at 100ng/mL. DXD-AAA LifA produces a curve that sees the ratio of LifA+ConA/ConA alone gradually decrease from 1.01±0.09 at 0.1ng/mL to 0.49±0.15 at 10µg/mL. It requires an ~100,000 fold increase in concentration for the DXD-AAA LifA protein to have the same inhibitory effect as that of the WT protein. The effective dose at which 50% of lymphocyte proliferation is inhibited (ED_{50}) was 0.014±0.006 for WT LifA and 304.1±16.9ng/mL for DXD-AAA LifA (P value < 0.05). The buffer that the DXD-AAA LifA was dissolved in did not have any effect on the assay. The addition of ConA resulted in an average 3-fold increase of T cell proliferation above the negative control across the 3 experimental repeats.

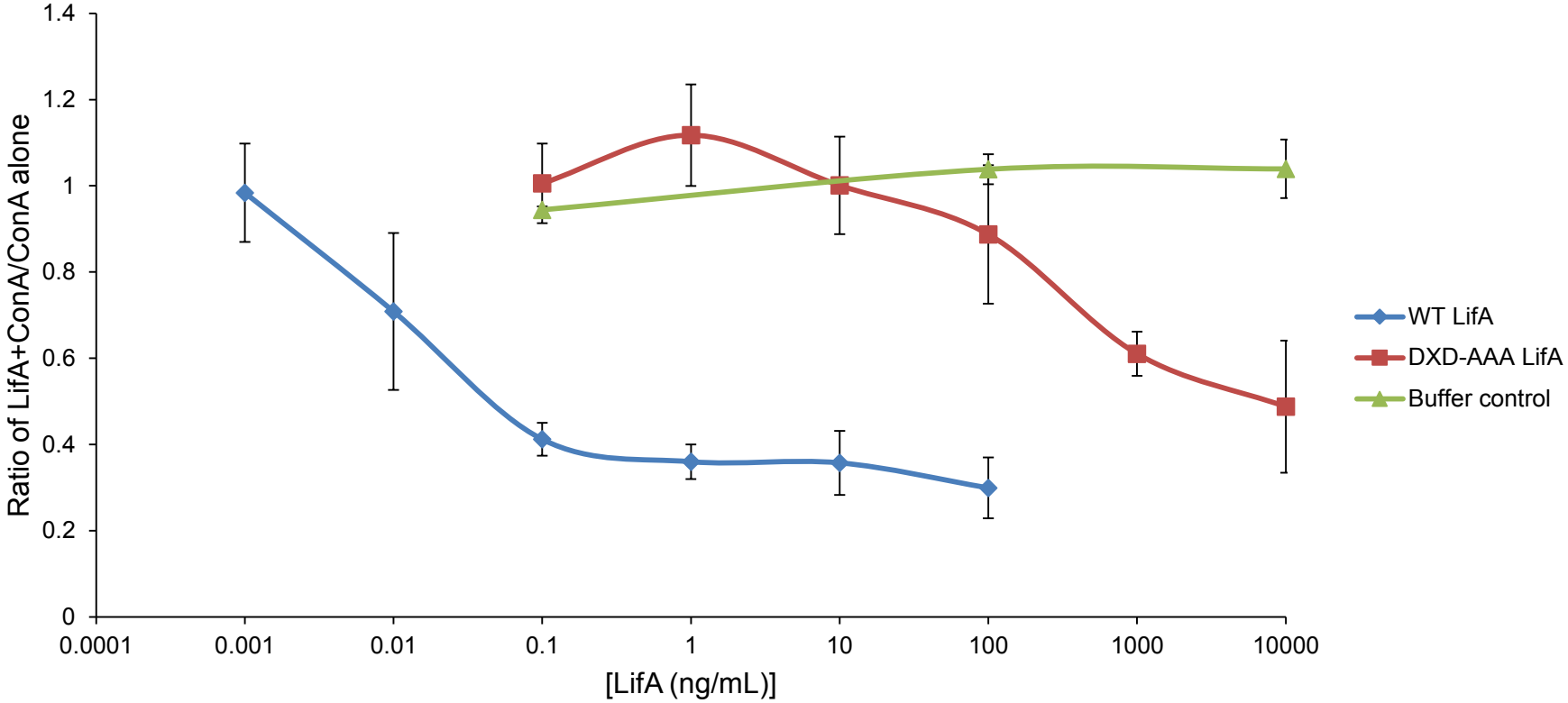

Figure 3.16. Concentration titration of recombinant WT LifA and DXD-AAA LifA against ConA-stimulated peripheral bovine T lymphocytes. An absolute number of 200,000 cells were seeded into the wells of a 96 well plate. Titrations were carried out in triplicate and the results are the average obtained from 3 independent experiments using 3 donors. Error bars indicate the standard deviation of the average ratios from across the 3 experiments. Data were normalised against cells with ConA alone to give a ratio index of proliferation.

3.8 Cytotoxicity assays

The LCTs are well known to have a cytotoxic effect on enterocytes (Triadafilopoulos *et al*, 1987), however, there is no formal evidence that LifA has a direct cytotoxic effect on mammalian cells. As a result, cytotoxicity assays were performed using recombinant WT LifA. As the two main cell types affected by LifA, the adherent HeLa cell line was used as a model for epithelial cells and the suspension Jurkat cell line was used as a model for T cells.

Release of the intracellular protein lactate dehydrogenase (LDH) can be used as a marker of cytotoxicity. Here, a fluorometric plate-based assay was used to measure LDH release (Promega, 2009). The mechanism of LDH detection can be seen in Figure 3.17.

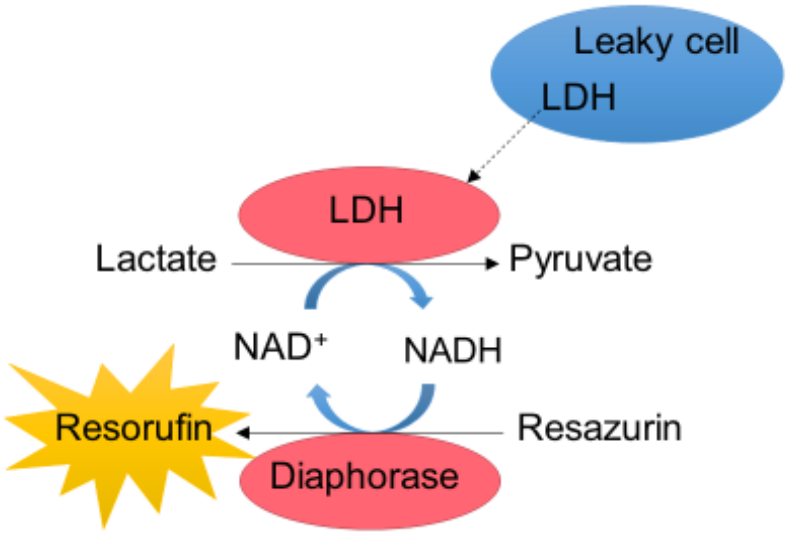

Figure 3.17. Mechanism of fluorescence caused by LDH release. Cells with a compromised membrane activity release LDH. This drives the conversion of NAD^+ to NADH in the conversion of lactate to pyruvate, which is coupled to a reaction that converts resazurin to the fluorescent product resorufin in the CytoTox-ONE substrate mix. The generation of fluorescent resorufin is proportional to the quantity of LDH released (adapted from Promega, 2009).

At both 24 and 48 hours of incubation of cells with LifA, no sign of cytotoxicity was observed. At 24 hours incubation, the percent cytotoxicity observed with the HeLa and Jurkat cell negative controls was 32.6±18.1% and 9.6±3.2% respectively at buffer dilutions equivalent to 10µg/mL LifA. In the presence of LifA at 10µg/mL the percent cytotoxicity was 10.7±2% for the HeLa cells and 31.4±15% for the Jurkat cells. After 48 hours incubation, the percent cytotoxicity observed with the HeLa and Jurkat cell negative controls was 13.9±3.1% and 24.7±13.4% respectively at buffer dilutions equivalent to 10µg/mL LifA. In the presence of LifA at 10µg/mL the percent cytotoxicity was 12.3±4.2% for the HeLa cells and 18.8±10.3% for the Jurkat cells. (Figure 3.18). In addition, a concentration-dependent titration of the protein had no significant effect on LDH release. The results are an average of 3 experimental repeats carried out in triplicate. Regardless of the concentration, the percent cytotoxicity of LifA did not significantly increase above that of the negative control for the HeLa or Jurkat cells at 24 or 48 hours post-addition.

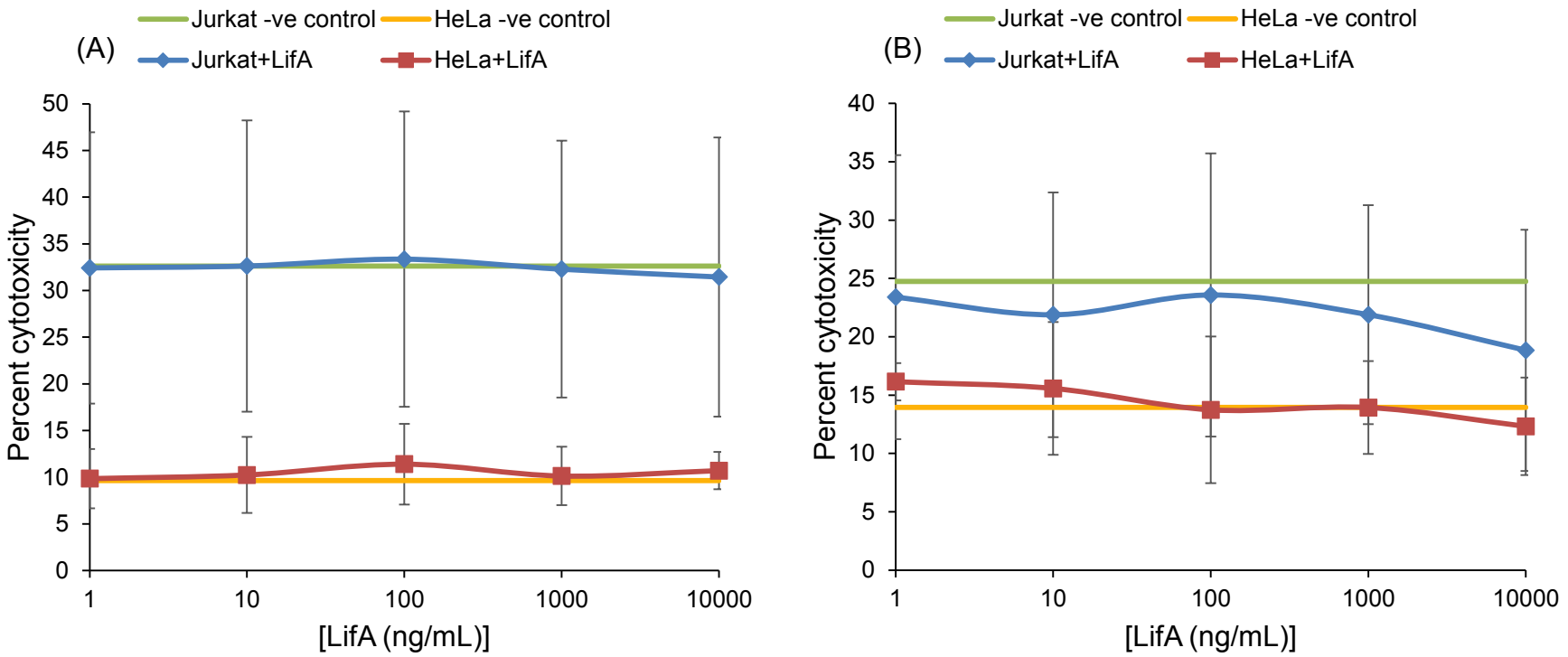

Figure 3.18. Cytotoxicity of WT LifA against HeLa and Jurkat cells. An absolute number of 25,000 cells of each cell type were seeded into the wells of a 96 well opaque sided plate. After incubation with the protein, the percent cytotoxicity of cells at each protein concentration, as well as negative controls, were calculated in comparison to a positive control of maximum possible cell lysis. (A) Cytotoxicity at 24 hours. (B) Cytotoxicity at 48 hours. Titrations were carried out in triplicate and the results are an average of 3 independent experiments. Error bars indicate the standard deviation of the average percent cytotoxicity from across the 3 experiments.

Chapter 4: Discussion

LifA is a large multifunctional protein produced by EPEC and non-O157 EHEC. Although its ability to act as an adhesin and to inhibit the mitogen-stimulated proliferation of lymphocytes and cytokine expression are well documented, little has been done to identify exactly how it functions in the 20 years since its effects were first recorded by Klapproth *et al* (1995). This has most likely been due the inability to produce stable cloning vectors containing the full-length *lifA* gene (Klapproth *et al*, 2000; Nicholls *et al*, 2000; Janka *et al*, 2002). Recent advances in understanding the mode of action of LifA have allowed for the findings reported in this study.

The mechanism(s) of LifA secretion is poorly understood and must be addressed to better understand how LifA is able to act as both a lymphostatin and an adhesin. In this study, the ability of full-length LifA to be secreted via the LEE-encoded T3SS was investigated. This study has shown for the first time that full-length LifA is a Type III secreted effector protein under *in vitro* conditions in WT *E. coli* O127:H6 E2348/69. Full-length LifA was detected in the culture supernatant of the WT strain under T3S-inducing conditions but not in the Δ*escN* strain that lacks the T3SS ATPase. The LifA species detected on the western blots appeared much fainter than other T3S proteins such as EspD, which suggests that LifA may be secreted in lower quantities than these proteins, however, reactivity is a function of antibody affinity and avidity and may not reflect absolute quantities. The RecA control confirmed that secretion of LifA was not the product of cell lysis. Although this finding suggests that LifA may enter enterocytes via translocation through the T3SS, it does not explain how the protein enters lymphocytes, which *E. coli* may not encounter with the same frequency. LifA does not necessarily need to be secreted directly into host cells since Type III secretion is not contact dependent in *E. coli* (Kenny *et al*, 1997b). Thus, some LifA may be injected into cells and some may be secreted into the extracellular milieu by T3SS needle complexes not in contact with host cells. Overall, this study advances our understanding of the secretion of LifA as very little was known about the secretion mechanism(s) of LifA until Deng *et al* (2012) reported that it appeared to be secreted via the T3SS by SILAC analysis, which mapped peptides across the protein. These authors confirmed

that the N-terminal 50 – 100 amino acids were necessary and sufficient to direct secretion of a TEM-1 β-lactamase reporter. This amino acid sequence was chosen because as little as 20 amino acids from the N-terminus of various Type III secreted proteins are required to mediate translocation of these proteins through the T3SS (Charpentier and Oswald, 2004). Deng *et al* (2012) also used a hypersecreting EPEC E2348/69 strain in their experiments and suggested that LifA may only be detectable under hypersecreting conditions. This study has proven that a hypersecreting strain is not necessary to detect LifA and that it can in fact be detected in WT bacteria using our LifA-specific antiserum.

A possible improvement to this experiment would be to use DMEM as a culture medium to induce Type III secretion, as performed by Deng *et al* (2012), rather than MEM to improve the yield of LifA that is secreted. Nicholls *et al* (2000) tested the effects of different media on the expression of a LifA-PhoA fusion and found that Todd-Hewitt broth was the most effective liquid medium for increasing the expression of LifA in EHEC O111:H- E45035N. To achieve optimal LifA secretion, time courses could be run under different T3S-inducing conditions to find which media allows the bacteria to secrete the maximum quantity of LifA before lysing.

Although LifA was not detected in the culture supernatant of the Δ*escN* strain, this does not mean that undetectable quantities of LifA are not being secreted via other mechanisms. There is evidence to suggest that LifA is not strictly dependent on Type III secretion for activity. For instance, cell lysates containing LifA, including laboratory-adapted strains lacking a T3SS, and purified LifA protein have been observed to inhibit the mitogen-stimulated proliferation of T lymphocytes (Klapproth *et al*, 1995; Klapproth *et al*, 1996; Klapproth *et al*, 2000; Stevens *et al*, 2002). A future question to be addressed is how LifA enters target cells when not injected directly as above. It may be that LifA can be both translocated into cells and enter through receptor-mediated endocytosis or other uptake pathways. It is difficult to postulate the exact mechanism of cell entry of LifA considering that its target protein(s) remains unknown. In order to investigate how LifA is taken up by host cells, specific inhibitors that target different endocytic pathways could be used to examine their impact on LifA activity. For instance, bafilomycin could be used to

study the potential requirement for endosome acidification for the escape of LifA from entry vesicles, as is the case for LCTs (Schirmer and Aktories, 2004). In order to understand the mechanism(s) of activity of LifA it is critical to identify its host cell binding partners. Putative protein-protein interactions could be identified by far-western blotting and/or immuno-precipitation studies using cell lysates treated with recombinant LifA. Affinity chromatography, whereby recombinant LifA could be bound to a column via the 6xHis tag, could also be used to isolate binding partners. Putative binding partners could then be identified using mass spectrometry. The yeast two-hybrid system may also be useful for examining the interactions between purified suspected binding partners and LifA.

Western blotting for LifA detected protein species present in the supernatant of WT EPEC and Δ*escN* strains that the Δ*lifA* strain lacked. It is possible that these correspond to shortened versions LifA that are secreted by other mechanisms. The identification of these protein species was outwith the scope of this study but discerning their identity could be grounds for future study. N-terminal sequencing could be used in conjunction with bioinformatic approaches to identify a Sec- or Tat-peptide signal sequence indicative of Type II secretion (Filloux, 2010; von Heijne, 1990; Voulhoux *et al*, 2001).

While this study has detected LifA secretion under T3S-inducing *in vitro* conditions, future research could seek to determine whether LifA production and/or translocation could be detected in the gut of infected animals using reporter fusions (as was carried out by Geddes *et al* (2007) for *Salmonella* Type III secreted proteins) or LifA antiserum. Another area to address is why LifA mutations have an indirect post-transcriptional effect on the expression and secretion of other T3S proteins, such as EspA and Tir in some strains (Stevens *et al*, 2002). It is possible that it may be involved in the hierarchy of secretion of T3S proteins (Wang *et al*, 2008; Mills *et al*, 2013).

LifA's homology with LCTs, including the catalytic DXD motif, suggests that the protein may act at least in part as a glycosyltransferase. In order to test this hypothesis a mutant variant of the pRham-LifA-6xHis plasmid was successfully created during this study, replacing the DTD amino acid sequence in the DXD motif with an AAA sequence. An AAA sequence was chosen for the substitution because

alanine residues are small, non-polar and unreactive. Similar experiments were performed by Deacon *et al* (2010), in which a DXD-AAA substitution was created in the *lifA* gene on the chromosome of EHEC O26:H- rather than on a plasmid vector as in this study. It was found that the colonisation of cattle by EHEC O26:H- was dependent on LifA but not the DXD motif, however, when the mutation was transferred to the chromosome of EPEC O127:H6 E2348/69, the DXD motif was found to be required for lymphostatin activity, albeit in a relatively insensitive assay reliant on crude bacterial lysates. The latter observation is consistent with the observations made in this study although Deacon *et al* (2010) did not make a connection between the LifA protein's function and its sugar binding ability. It is possible that the DXD motif was not required for the effective colonisation of cattle as other activities of LifA exist, for example in promoting adherence, although no defect in adherence to HeLa cells was observed by Deacon *et al* (2010).

The creation of the pRham-LifA-6xHis DXD-AAA plasmid provides a useful tool alongside the existing pRham-LifA-6xHis plasmid for producing recombinant LifA proteins that can be used to examine both the sugar binding ability and function of LifA as a lymphostatin.

In order to ensure that the purified DXD-AAA LifA protein was as similar to the WT recombinant LifA as possible, the DXD-AAA LifA protein was subjected to three different biophysical characterisation experiments. Dynamic light scattering confirmed that the DXD-AAA LifA protein was monomeric by measuring the hydrodynamic radius of the protein. Circular dichroism (CD) confirmed that the DXD-AAA LifA protein had a similar secondary structure to that of the WT protein. The CD spectrum of DXD-AAA LifA was not an exact copy of the spectrum for WT LifA and in particular the percentage of the secondary structure consisting of α-helices appeared to be slightly reduced. However, the error values for each structural motif in the WT and DXD-AAA LifA proteins overlap and so the differences in percentages are acceptable. Thermal shift assays confirmed that the DXD-AAA LifA protein has a similar T_m to that of the WT protein. A reproducible decrease in the T_m of DXD-AAA LifA of ~1°C was observed, which is not unexpected since changing the active site of the protein may result in the loss of the putative metal ion. Assuming that the metal ion also binds to other amino acids in the

active site as it does in TcdA (Pruitt *et al*, 2013), its loss would result in an overall loss of some structural stability. These experiments were performed to ensure that the results seen in future experiments were genuine and not due to the incorrect synthesis and folding of the DXD-AAA LifA protein.

Previous experiments with LifA have shown that it is capable of binding UDP-GlcNAc but not UDP-Glc (Stevens Laboratory, unpublished data). These particular UDP-sugars were chosen as they are both known to bind LCTs (Schirmer and Aktories, 2004). For the first time, the ability of LifA to bind UDP-GlcNAc has been shown in this study to be dependent on the DXD motif. This was done by comparing the ability of both WT and DXD-AAA LifA to bind UDP-GlcNAc and UDP-Glc. The sugar binding ability of these proteins was examined by measuring changes in the intrinsic tryptophan (Trp) fluorescence of the proteins in the presence of each UDP-sugar. Trp fluorescence quenching is commonly used to identify interactions between proteins and ligands when there are Trp residues at the suspected binding pocket, but becomes less sensitive with more Trp residues (Price and Nairn, 2009). There are seven Trp residues in proximity to the glycosyltransferase binding pocket in LifA, making specific interactions between the protein and the UDP-GlcNAc more difficult to detect. However, the fluorescence of WT LifA instead increases in the presence of UDP-GlcNAc, which is likely to be caused by a conformational change in the protein that is stabilised by UDP-GlcNAc binding (Weljie and Vogel, 2000).

It is possible that sugar binding is dependent on the presence of a metal ion in the active site as seen in TcdA from *C. difficile* (Pruitt *et al*, 2012). However, it has not yet been shown that sugar binding in LifA is dependent on a metal ion. A possible method to identify the putative metal ion would be to subject the glycosyltransferase domain of LifA to X-ray crystallography in a similar manner as to how Pruitt *et al* (2012) determined the structure of TcdA. However, Pruitt *et al* (2012) artificially introduced manganese to TcdA. Since the putative metal ion of LifA could be lost or replaced during the production and purification process or LifA may bind multiple different metal ions, crystallography would have to be performed using different metals to find which ones bind. To date, UDP-GlcNAc binding and thermal stability have not proven sensitive to different exogenous metal ions but it is

possible the recombinant protein acquired metal ions during expression and/or purification. The binding of UDP-GlcNAc to LifA is not actually indicative of sugar transfer and so a sugar hydrolysis assay could be used in future work to determine if UDP-GlcNAc is the natural substrate of LifA. Other UDP-sugars should also be tested for their ability to bind LifA. While most LCTs bind only UDP-Glc, *C. novyi* α-toxin is capable of binding UDP-GlcNAc and UDP-Glc, but to a much lesser extent (Schirmer and Aktories, 2004; Busch *et al*, 2000). It is therefore conceivable that LifA may be capable of binding multiple UDP-sugars. If this is the case we can also then determine whether the binding of these UDP-sugars is DXD dependent.

This study has shown that the DXD motif is important for the function of LifA to inhibit the mitogen-stimulated proliferation of bovine T lymphocytes. The ED_{50} of the DXD-AAA LifA was ~10,000 fold greater than the ED_{50} of the WT LifA protein but activity may not have been abolished altogether. Whether the ability of DXD-AAA LifA to inhibit T cell proliferation at high concentrations reflects residual activity or the presence of co-purified proteins or contaminants requires further study. Indeed, even lysates of *E. coli* lacking LifA become inhibitory to bovine PBMCs if used at high concentrations. There are multiple reasons why mutation of the DXD motif could fail to completely abolish the ability of LifA to inhibit the mitogen-stimulated proliferation of T cells: the DXD-AAA LifA protein could still be able to bind small amounts of UDP-GlcNAc that are not detected by the sugar binding assays; the protein is capable of binding other UDP-sugars; or LifA may not act solely as a glycosyltransferase.

Given that LifA binds UDP-GlcNAc, and that the DXD motif is important for this activity, it is likely that LifA acts as a glycosyltransferase to arrest lymphocyte proliferation. A future goal would be to attempt to identify the target protein(s) of glycosyltransferase activity. This would be challenging, however, due to the abundance of proteins in mammalian cells that are capable of accepting GlcNAc. A possible method for identifying the glycosylation target would be to mix radiolabeled UDP-GlcNAc with purified WT LifA and add this mix to T cell lysates. The size of the T cell proteins that have been glycosylated with radiolabeled GlcNAc could be determined by autoradiography. Western blotting using antibodies against O-GlcNAc is an alternative to autoradiography but the O-GlcNAc proteome of

mammalian cells is likely to be complex and we cannot be certain that GlcNAc is transferred to an O-linkage. Shot-gun quantitative mass spectrometry could also be used to look for proteins that shift in size by the mass of UDP-GlcNAc, accounting for different linkage types and the possible addition of multiple GlcNAc molecules. Once protein binding partners have been identified, recombinant forms could be made and mixed with purified LifA and labelled UDP-GlcNAc to confirm the glycosylastion of putative target proteins. This method was used to identify the glycosyltransferase targets of NleB (Li *et al*, 2013; Pearson *et al*, 2013). NleB serves as potential model for LifA activity as it is a T3S effector protein, it contains a DXD motif and binds UDP-GlcNAc, and it inhibits the expression of pro-inflammatory cytokines without acting as a cytotoxin (Gao *et al*, 2013; Li *et al*, 2013; Pearson *et al*, 2013).

Despite LifA's homology with LCTs, which are known to act as cytotoxins by transferring UDP-sugars onto Rho GTPases (Triadafilopoulos *et al*, 1987; Just *et al*, 1995; Selzer *et al*, 1996), LifA itself has never been observed to act as a cytotoxin against T cells or epithelial cells (Klapproth *et al*, 1995; Stevens *et al*, 2002). These experiments used crude bacterial lysates, however, and so in this study, purified recombinant LifA was examined for its potential cytotoxic effects using a fluorometric LDH release assay. Consistent with the previous experiments, this study has shown that the addition of LifA to either HeLa (epithelial cell model) or Jurkat (T cell model) cells does not cause any obvious direct cytotoxic effects to these cell types. Moreover, no direct cytotoxicity has been observed against bovine T cells during lymphostatin assays, indicating that inhibition of proliferation does not involve killing (Stevens Laboratory, unpublished data). This contrasts with the observations by Babbin *et al* (2009) that suggest that LifA produced by *C. rodentium* targets Rho GTPases in mice. However, the actin cytoskeleton did not collapse in a manner similar to that of LCTs but rather tight junctions and subjacent adherens junctions between host cells were disrupted. Deacon *et al* (2010) attempted to replicate the observation that LifA targets Rho GTPases but did not observe any increase in RhoA activation in cells infected with EPEC O127:H6 strain E2348/69, EHEC O26:H- strain 193 nal^R or LifA null mutants of these strains. It does not seem that LifA necessarily acts as a direct cytotoxin or as a cytotoxin at all. An example of

a non-cytotoxic glycosyltransferase is NleB, a T3S effector of EPEC and EHEC, which binds UDP-GlcNAc and GlcNAcylates an arginine residue on the TRADD death domain host receptor (Li *et al*, 2013; Pearson *et al*, 2013). This disrupts tumour necrosis factor signalling in EPEC-infected cells including NF-κB signalling and apoptosis (Li *et al*, 2013; Pearson *et al*, 2013). It seems plausible that LifA may act in a manner akin to NleB, whereby it targets signalling pathways to inhibit both lymphocyte proliferation and cytokine expression, and experiments are planned to determine if LifA acts on key signal transduction pathways. A possible future experiment would be to use ATP assays rather than LDH release assays. This would allow the quantity of energy actually available in LifA treated cells to be measured and indicate whether the cells are healthy even though they are intact.

It is of interest to examine the localisation of LifA inside and on the surface of both bacterial and mammalian cells. This would give further insight into where the target protein(s) of LifA is located and also how LifA acts as an adhesin. The localisation of LifA in bacterial cells could be analysed by fractionating bacterial whole cell lysates and examining the different cell compartments for LifA using western blotting. Alternatively, fluorescent or confocal microscopy could be used to detect recombinant LifA in or on cells using fluorescently labelled anti-His tag antibodies.

Due the success in this study of substituting the DXD motif with an AAA sequence, other regions could be substituted using QuikChange mutagenesis. This technique could be used to mutate other areas of the glycosyltransferase domain to determine how important they are. Alternatively, this technique could be used to make mutations in the putative cysteine protease domain of LifA in order to determine whether it is necessary for the function of LifA. Mutated LifA proteins could be compared against WT LifA in their ability to inhibit T cell proliferation.

To determine which parts of the LifA protein are required for activity, nested truncations or linker scanning mutagenesis could be used to generate fragments of LifA. These fragments could be mixed in different combinations and used in T cell proliferation assays to determine whether particular combinations of LifA fragments can exhibit activity or whether the protein must be whole in order to function.

The ability of LifA to act as an adhesin has not been the focus of this study but it is still an interesting point to consider for future work. Adhesion assays could be used to examine the ability of LifA to mediate adherence to epithelial cells. *E. coli* lab strains transformed with the pRham-LifA-6xHis plasmid and the E2348/69 Δ*lifA* strain could be compared in their ability to adhere to HeLa cells using light microscopy and viable counts of bound bacterial cells. The Δ*lifA* strain could also be transformed with the pRham-LifA-6xHis plasmid to see if the plasmid can restore adherence. Alternatively, mixing recombinant LifA with lab strains and HeLa cells could be used to see if the bacteria show an increase in adherence. Dominant adhesins such as intimin and BFP may mask a subtle role played by LifA, as previously found in masking the role of EspA (Cleary *et al*, 2004), and so would have to be non-functional to see the effects of LifA as an adhesin.

Future research could also focus on areas that are not directly related to LifA function. The role of the truncated LifA′ and ToxB in EHEC O157:H7 as well as the *Chlamydia* cytotoxins could be investigated for instance. Both LifA′ and ToxB were found to be Type III secreted by Deng *et al* (2012) but LifA′ lacks the DXD motif. Abu-Median *et al* (2006) found that both these proteins did not have lymphostatin-like activity but the assays used were insensitive and relied on crude bacterial lysates. With the ability to make stable plasmid clones of these proteins, LifA homologues could be examined for both lymphostatin-like activity and UDP-sugar binding. This study and previous publications have primarily used mitogens to stimulate the proliferation of lymphocytes in lymphostatin assays, however, it is unlikely that lymphocytes would encounter such chemicals *in vivo*. Re-stimulating the lymphocytes with antigens, as performed by Malstrom and James (1998), would be more reflective of how LifA actually functions during an infection. Another avenue of research would be to investigate whether LifA interferes with the development of adaptive immunity against EPEC and EHEC during infection, for example, by immunisation with a model antigen.

Continued studies of the molecular basis of lymphostatin activity have the potential to reveal novel biology, both in understanding bacterial virulence and the processes underlying lymphocyte activation.

References

Abu-Median, A., van Diemen, P.M., Dziva, F., Vlisidou, I., Wallis, T.S. and Stevens, M.P. (2006). Functional Analysis of Lymphostatin Homologues in Enterohaemorrhagic *Escherichia coli*. *FEMS Microbiology Letters* 258, 43–49.

Acheson, D.W., Moore, D., de Breuker, S. Lincicome, L., Jacewicz, M., Skutelsky, E. and Keusch, G.T. (1996). Translocation of Shiga Toxin Across Polarized Intestinal Cells in Tissue Culture. *Infection and Immunity* 64, 3294–3300.

Agilent Technologies (2015). *QuikChange II XLSite-Directed Mutagenesis Kit Instruction Manual*.

Andrade, A., Pardo J.P., Espinosa, N., Pérez-Hernández, G. and González-Pedrajo, B. (2007). Enzymatic Characterization of the Enteropathogenic *Escherichia coli* Type III Secretion ATPase EscN. *Archives of Biochemistry and Biophysics* 468, 121–127.

Asakura, H., Kawamoto, Y., Haishima, Y., Igimi, S., Yamamoto, S. and Makino, S. (2008). Differential Expression of the Outer Membrane Protein W (OmpW) Stress response in Enterohemorrhagic *Escherichia coli* O157:H7 Corresponds to the Viable but Non-Culturable State. *Research in Microbiology* 159, 709–717.

Babbin, B.A., Sasaki, M, Gerner-Schmidt, K.W., Nusrat, A. and Klapproth, J.A. (2009). The Bacterial Virulence Factor Lymphostatin Compromises Intestinal Epithelial Barrier Function by Modulating Rho GTPases. *The American Journal of Pathology* 174, 1347–1357.

Badea, L., Doughty, S., Nicholls, L., Sloan, J., Robins-Browne, R.M. and Hartland, E.L. (2003). Contribution of Efa1/LifA to the Adherence of Enteropathogenic *Escherichia coli* to Epithelial Cells. *Microbial Pathogenesis* 34, 205–215.

Baruch, K., Gur-Arie, L., Nadler, C., Koby, S., Yerushalmi, G., Ben-Neriah, Y., Yogev, O., Shaulian, E., Guttman, C., Zarivach, R. and Rosenshine, I. (2011). Metalloprotease Type III Effectors that Specifically Cleave JNK and NF-κB. *The EMBO Journal* 30, 221–231.

Belland, R.J., Scidmore, M.A., Crane, D.D., Hogan, D.M., Whitmire, W., McClarty, G. and Caldwell, H.D. (2001). *Chlamydia trachomatis* Cytotoxicity Associated with Complete and Partial Cytotoxin Genes. *Proceedings of the National Academy of Sciences of the United States of America* 98, 13984–13989.

Bentley, R. and Meganathan, R. (1982). Biosynthesis of Vitamin K (Menaquinone) in Bacteria. *Microbiological Reviews* 46, 241–280.

Berger, C.N., Crepin, V.F., Baruch, K., Mousnier, A., Rosenshine, I., Frankel, G. (2012). EspZ of Enteropathogenic and Enterohemorrhagic *Escherichia coli* Regulates Type III Secretion System Protein Translocation. *mBio* 3, 1–12.

Bieber, D., Ramer, S.W., Wu, C., Murray, W.J., Tobe, T., Fernandez, R. and Schoolnik G.K. (1998). Type IV Pili, Transient Bacterial Aggregates, and Virulence of Enteropathogenic *Escherichia coli*. *Science* 280, 2114–2118.

Blasche, S., Mörtl, M., Steuber, H., Siszler, G,. Nisa, S., Schwarz, F., Lavrik, I., Gronewold, T.M.A., Maskos, K., Donnenberg, M.S., Ullman, D., Uetz, P. and Kögl, M. (2013). A Next-Generation Approach to the Characterization of a Non-Model Plant Transcriptome. *PLOS ONE* 8, p.e58937.

Blattner, F., Plunkett III, G., Bloch, C.A., Perna, N.T., Burland, V., Riley, M., Collado-Vides, J., Glasner, J.D, Rode, C.K., Mayhew, G.F., Gregor, J., Davis, N.W., Kirkpatrick, H.A., Goeden, M.A., Rose, D.J., Mua, B. and Shao, Y. (1997). The Complete Genome Sequence of *Escherichia coli* K-12. *Science* 277, 1453–1462.

Brady, M.J., Campellone, K.G., Ghildiya, M. and Leong, J.M. (2007). Enterohaemorrhagic and Enteropathogenic *Escherichia coli* Tir Proteins Trigger a Common Nck-Independent Actin Assembly Pathway. *Cellular Microbiology* 9, 2242–2253.

Brooks, J.T., Sowers, E.G., Wells, J.G., Greene, K.D., Griffin, P.M., Hoekstra, R.M. and Stockbine, N.A. (2005). Non-O157 Shiga Toxin-Producing *Escherichia coli* Infections in the United States, 1983-2002. *The Journal of Infectious Diseases* 192, 1422–1429.

Burland, V., Shao, Y., Perna, N.T., Plunkett, G., Sofia, H.J., and Blattner, F.R. (1998). The Complete DNA Sequence and Analysis of the Large Virulence Plasmid of *Escherichia coli* O157:H7. *Nucleic Acids Research* 26, 4196–4204.

Busch, C., Hofmann, F., Selzer, J., Munro, S., Jeckel, D. and Aktories, K. (1998). A Common Motif of Eukaryotic Glycosyltransferases is Essential for the Enzyme Activity of Large Clostridial Cytotoxins. *The Journal of Biological Chemistry* 273, 19566–19572.

Busch, C., Schömig, K., Hofmann, F. and Aktories, K. (2000). Characterization of the Catalytic Domain of *Clostridium novyi* Alpha-Toxin. *Infection and Immunity* 68, 6378–6383.

Buttner, D. (2012). Protein Export According to Schedule: Architecture, Assembly, and Regulation of Type III Secretion Systems from Plant- and Animal-Pathogenic Bacteria. *Microbiology and Molecular Biology Reviews*, 76, 262–310.

Campellone, K.G. and Leong, J.M. (2005). Nck-Independent Actin Assembly is Mediated by Two Phosphorylated Tyrosines Within Enteropathogenic *Escherichia coli* Tir. *Molecular Microbiology* 56, 416–432.

Carlucci, A.F. and Pramer, D. (1959). Factors Affecting the Survival of Bacteria in Sea Water. *Microbiological Progress Report* 7, 388–392.

Charpentier, X. and Oswald, E. (2004). Identification of the Secretion and Translocation Domain of the Enteropathogenic and Enterohemorrhagic *Escherichia coli* Effector Cif, using TEM-1 β-Lactamase as a New Fluorescence-Based Reporter. *Journal of Bacteriology* 186, 5486–5495.

Clark, A.J. and Margulies, D. (1965). Isolation and Characterization of Recombination-Deficient Mutants of *Escherishia coli* K12. *Proceedings of the National Academy of Sciences of the United States of America* 53, 451–459.

Cleary, J., Lai, L., Shaw, R.K., Straatman-Iwanoska, A., Donnenberg, M.S., Frankel, G. and Knutton, S. (2004). Enteropathogenic *Escherichia coli* (EPEC) Adhesion to Intestinal Epithelial Cells: Role of Bundle-Forming Pili (BFP), EspA Filaments and Intimin. *Microbiology* 150, 527–538.

Costa, T.R.D., Felisberto-Rodrigues, C., Meir, A., Prevost, M.S., Redzej, A., Trokter, M. and Waksman, G. (2015). Secretion Systems in Gram-Negative Bacteria: Structural and Mechanistic Insights. *Nature Reviews Microbiology* 13, 343–359.

Creasey, E.A., Delaha, R.M., Daniell, S.J and Frankel, G. (2003). Yeast Two-Hybrid System Survey of Interactions Between LEE-Encoded Proteins of Enteropathogenic *Escherichia coli*. *Microbiology* 149, 2093–2106.

Crepin, F., Shaw, R., Abe, C.M., Knutton, S. and Frankel, G. (2005). Polarity of Enteropathogenic *Escherichia coli* EspA Filament Assembly and Protein Secretion. *Journal of Bacteriology* 187, 2881–2889.

Croxen, M..A and Finlay, B.B. (2010). Molecular Mechanisms of *Escherichia coli* Pathogenicity. *Nature Reviews Microbiology* 8, 26–38.

Daniell, S.J., Koonis, E., Morris, E., Knutton, S., Booy, F.P. and Frankel, G. (2003). 3D Structure of EspA Filaments from Enteropathogenic *Escherichia coli*. *Molecular Microbiology* 49, 301–308.

Deacon, V., Dziva, F., van Diemen, P.M., Frankel, G. and Stevens, M.P. (2010). Efa-1/LifA Mediates Intestinal Colonization of Calves by Enterohaemorrhagic *Escherichia coli* O26 : H-in a Manner Independent of Glycosyltransferase and Cysteine Protease Motifs or Effects on Type III Secretion. *Microbiology* 156, 2527–2536.

Deibel, C., Dersch, P. and Ebel, F. (2001). Intimin from Shiga Toxin-Producing *Escherichia coli* and its Isolated C-Terminal Domain Exhibit Different Binding Properties for Tir and a Eukaryotic Surface Receptor. *International Journal of Medical Microbiology* 290, 683–691.

Deibel, C., Krämer, S., Chakraborty, T. and Ebel, F. (1998). EspE, a Novel Secreted Protein of Attaching and Effacing Bacteria, is Directly Translocated into Infected Host Cells, Where it Appears as a Tyrosine-Phosphorylated 90 kDa Protein. *Molecular Microbiology* 28, 463–474.

Deng, W., de Hoog, C.L., Yu, H.B, Li, Y., Croxen, M.A., Thomas, N.A., Puente, J.L, Foster, L.J. and Finlay, B.B. (2010). A Comprehensive Proteomic Analysis of the Type III Secretome of *Citrobacter rodentium*. *The Journal of Biological Chemistry* 285, 6790–6800.

Deng, W., Li, Y., Vallance, B.A. and Finlay, B.B. (2001). Locus of Enterocyte Effacement from *Citrobacter rodentium*: Sequence Analysis and Evidence for Horizontal Transfer Among Attaching and Effacing Pathogens. *Infection and Immunity* 69, 6323–6335.

Deng, W., Yu, H.B., de Hoog, C.L., Stoynov, N., Li, Y., Foster, L.J. and Finlay, B.B. (2012). Quantitative Proteomic Analysis of Type III Secretome of Enteropathogenic *Escherichia coli* Reveals an Expanded Effector Repertoire for Attaching/Effacing Bacterial Pathogens. *Molecular & Cellular Proteomics* 11, 692–709.

DeVinney, R., Puente, J.L., Gauther, A., Gossney, D. and Finlay, B.B. (2001). Enterohaemorrhagic and Enteropathogenic *Escherichia coli* use a Different Tir-based Mechanism for Pedestal Formation. *Molecular Microbiology* 41, 1445–1458.

DeVinney, R., Stein, M., Reinscheid, D., Abe, A., Ruschowski, S. and Finlay, B.B. (1999). Enterohemorrhagic *Escherichia coli* O157:H7 Produces Tir, which is Translocated to the Host Cell Membrane but is not Tyrosine Phosphorylated. *Infection and Immunity* 67, 2389–2398.

Donnenberg, M.S., Girón, J.A., Nataro, J.P. and Kaper, J.B. (1992). A Plasmid-Encoded Type IV Fimbrial Gene of Enteropathogenic *Escherichia coli* Associated with Localized Adherence. *Molecular Microbiology* 6, 3427–3437.

Donnenberg, M.S., Lai, L. and Taylor, K.A. (1997). The Locus of Enterocyte Effacement Pathogenicity Island of Enteropathogenic *Escherichia coli* Encodes Secretion Functions and Remnants of Transposons at its Extreme Right End. *Gene* 184, 107–114.

Dziva, F., van Diemen P.M., Stevens, M.P., Smith, A.J. and Wallis T.S. (2004). Identification of *Escherichia coli* O157:H7 Genes Influencing Colonization of the Bovine Gastrointestinal Tract Using Signature-Tagged Mutagenesis. *Microbiology* 150, 3631–3645.

Ebel, F., Podzadel, T., Rohde, M., Kresse, A.U., Krämer, S., Deibel, C., Guzmán, C.A. and Chakraborty, T. (1998). Initial Binding of Shiga Toxin-Producing *Escherichia coli* to Host Cells and Subsequent Induction of Actin Rearrangements Depend on Filamentous EspA-Containing Surface Appendages. *Molecular Microbiology* 30, 147–161.

Edberg, S.C., Rice, E.W., Karlin, R.J. and Allen, M.J. (2000). *Escherichia coli*: the Best Biological Drinking Water Indicator for Public Health Protection. *Journal of Applied Microbiology* 88, 106–116.

Eftink, M.R. and Ghiron, C.A. (1976). Exposure of Tryptophanyl Residues in Proteins. Quantitative Determination by Fluorescence Quenching Studies. *Biochemisty* 15, 672–680.

Elliott, S.J., Wainwright, L.A., McDaniel, T.K., Jarvis, K.G., Deng, Y., Lai, L., McNamara, B.P., Donnenberg, M.S. and Kaper, J.B. (1998). The Complete Sequence of the Locus of Enterocyte Effacement (LEE) from Enteropathogenic *Escherichia coli* E2348/69. *Molecular Microbiology* 28, 1–4.

Endo, Y., Tsurugi, K., Yutsudo, T., Takeda, Y., Ogasawara, T. and Igarashi, K. (1988). Site of Action of a Vero Toxin (VT2) from *Escherichia coli* O157:H7 and of Shiga Toxin on Eukaryotic Ribosomes. *European Journal of Biochemistry* 50, 45–50.

Epps, D.E., Raub, T.J., Caiolfa, V., Chiari, A. and Zamai, M. (1999). Determination of the Affinity of Drugs Toward Serum Albumin by Measurement of the Quenching of the Intrinsic Tryptophan Fluorescence of the Protein. *The Journal of Pharmacy and Pharmacology* 51, 41–48.

Faust, M.A., Aotaky, A.E. and Hargadon, M.T. (1975). Effect of Physical Parameters on the *In Situ* Survival of *Escherichia coli* MC-6 in an Estuarine Environment. *Applied Microbiology* 30, 800–806.

Filloux, A. (2010). Secretion Signal and Protein Targeting in Bacteria: A Biological Puzzle. *Journal of Bacteriology* 192, 3847–3849.

Finlay, B.B., Rosenshine, I., Donnenberg, M.S. and Kaper J.B. (1992). Cytoskeletal Composition of Attaching and Effacing Lesions Associated with Enteropathogenic *Escherichia coli* Adherence to HeLa Cells. *Infection and Immunity* 60, 2541–2543.

Folta-Stogniew, E. and Williams, K.R. (1999). Determination of Molecular Masses of Proteins in Solution: Implementation of an HPLC Size Exclusion Chromatography and Laser Light Scattering Service in a Core Laboratory. *Journal of Biomolecular Techniques* 10, 51–63.

Foubister, V., Rosenshine, I., Donnenberg, M.S. and Finlay, B.B. (1994). The *eaeB* Gene of Enteropathogenic *Escherichia coli* is Necessary for Signal Transduction in Epithelial Cells. *Infection and Immunity* 62, 3038–3040.

Frankel, G., Candy, D.C.A. Everest, P. and Dougan, G. (1994). Characterization of the C-Terminal Domains of Intimin-Like Proteins of Enteropathogenic and Enterohemorrhagic *Escherichia coli*, *Citrobacter freundii*, and *Hafnia alvei*. *Infection and Immunity* 62, 1835–1842.

Frankel, G., Lider, O., Hershkoviz, R., Mould, A.P., Kachalsky, S.G., Candy, D.C.A., Cahalon, L., Humphries, M.J. and Dougan, G. (1996). The Cell-Binding Domain of Intimin from Enteropathogenic *Escherichia coli* Binds to β_1-Integrins. *The Journal of Biological Chemistry* 271, 20359–20364.

Fraser, M.E., Chernaia M.M., Kozlov, Y.V. and James, M.N.G. (1994). Crystal Structure of the Holotoxino from Shigella Dysenteriae at 2.5 Å Resolution. *Nature Structural Biology* 1, 59–64.

Gao, X., Wang, X., Pham, T.H., Feuerbacher, L.A., Lubos, M., Huang, M., Olsen, R., Musheglan, A., Slawson, C. and Hardwidge, P.R. (2013). NleB, a Bacterial Effector with Glycosyltransferase Activity Targets GADPH Function to Inhibit NF-κB Activation. *Cell Host and Microbe* 13, 87–99.

Garmendia, J., Phillips, A.D., Carlier, M., Chong, Y., Schüller, S., Marches, O., Dahan, S., Oswald, E., Shaw, R.K., Knutton, S. and Frankel, G. (2004). TccP is an Enterohaemorrhagic *Escherichia coli* O157:H7 Type III Effector Protein that Couples Tir to the Actin-Cytoskeleton. *Cellular Microbiology* 6, 1167–1183.

Garred, Ø., van Deurs, B. and Sandvig, K. (1995). Furin-Induced Cleavage and Activation of Shiga Toxin. *The Journal of Biological Chemistry* 270, 10817–10821.

Gauthier, A., Robertson, M.L., Lowden, M., Ibarra, J.A., Puente, J.L. and Finlay, B.B. (2005). Transcriptional Inhibitor of Virulence Factors in Enteropathogenic *Escherichia coli*. *Antimicrobial Agents and Chemotherapy* 49, 4101–4109.

Geddes, K., Cruz III, F. and Heffron, F., (2007). Analysis of Cells Targeted by *Salmonella* Type III Secretion *in vivo*. *PLOS Pathogens* 3, 2017–2028.

Gerba, C.P. and McLeod, J.S. (1976). Effects of Sediments on the Survival of *Escherichia coli* in Marine Waters. *Applied and Environmental Microbiology* 32, 114–120.

Gerlach, R.G., Jäckel, D., Geymeier, N. and Hensel, M. (2007). *Salmonella* Pathogenicity Island 4-Mediated Adhesion is Coregulated with Invasion Genes in *Salmonella enterica*. *Infection and Immunity* 75, 4697–4709.

Girón, J.A., Ho, A.S.Y and Schoolnik, G.K. (1991). An Inducible Bundle-Forming Pilus of Enteropathogenic *Escherichia coli*. *Science* 254, 710–713.

Gobert, A.P., Vareille, M., Glasser, A., Hindré, T., de Sablet, T. and Martin, C. (2007). Shiga Toxin Produced by Enterohemorrhagic *Escherichia coli* Inhibits PI3K/NF-κB Signaling Pathway in Globotriaosylceramide-3-Negative Human Intestinal Epithelial Cells. *Journal of Immunology* 178, 8168–8174.

Gomes, T.A.T., Vieira, M.A.M., Wachsmuth, I.K., Blake, P.A. and Trabulsi, L.R. (1989). Serotype-Specific Prevalence of *Escherichia coli* Strains with EPEC Adherence Factor Genes in Infants with and without Diarrhea in São Paulo, Brazil. *The Journal of Infectious Diseases* 160, 131–135.

Goosney, D.L., DeVinney, R. and Finlay, B.B. (2001). Recruitment of Cytoskeletal and Signaling Proteins to Enteropathogenic and Enterohemorrhagic *Escherichia coli* Pedestals. *Infection and Immunity* 69, 3315–3322.

Gruenheid, S., DeVinney, R., Bladt, F., Goosney, D., Gelkop, S., Gish, G.D., Pawson, T. and Finlay, B.B. (2001). Enteropathogenic *E. coli* Tir Binds Nck to Initiate Actin Pedestal Formation in Host Cells. *Nature Cell Biology* 3, 856–859.

Hacker, J., Blum-Oehler, G., Mühldorfer, I. and Tschäpe, H. (1997). Pathogenicity Islands of Virulent Bacteria: Structure, Function and Impact on Microbial Evolution. *Molecular Microbiology* 23, 1089–1097.

Hauf, N. and Chakraborty, T. (2003). Suppression of NF-κB Activation and Proinflammatory Cytokine Expression by Shiga Toxin-Producing *Escherichia coli*. *Journal of Immunology* 170, 2074–2082.

Hayashi, T., Makino, K., Ohnishi, M., Kurowaka, K., Ishii, K., Yokoyama, K., Han, C., Ohtsubo, E., Nakayama, K., Murata, T., Tanaka, M., Tobe, T., Iida, T., Takami, H., Honda, T., Sasakawa, C., Ogasawara, N., Yasunaga, T., Kuhara, S., Shiba, T., Hattori, M. and Shinagawa, H. (2001). Complete Genome Sequence of Enterohemorrhagic *Escherichia coli* O157:H7 and Genomic Comparison with a laboratory strain K-12. *DNA Research : an International Journal for Rapid Publication of Reports on Genes and Genomes* 8, 11–22.

von Heijne, G. (1990). The Signal Peptide. *Journal of Membrane Biology* 115, 195–201.

Hemrajani, C., Berger, C.N., Robinson, K.S., Marchès, O., Mousnier, A. and Frankel, G. (2010). NleH Effectors Interact with Bax Inhibitor-1 to Block Apoptosis During Enteropathogenic *Escherichia coli* Infection. *Proceedings of the National Academy of Sciences of the United States of America* 107, 3129–3134.

Ho, N.K., Henry, A.C., Johnson-Henry, K. and Sherman, P.M. (2013). Pathogenicity, Host Responses and Implications for Management of Enterohemorrhagic *Escherichia coli* O157:H7 Infection. *Canadian Journal of Gastroenterology* 27, 281–5.

Hoey, D.E.E., Sharp, L., Currie, C., Lingwood, C.A., Gally, D.L. and Smith D.G.E. (2003). Verotoxin 1 Binding to Intestinal Crypt Epithelial Cells Results in Localization to Lysosomes and Abrogation of Toxicity. *Cellular Microbiology* 5, 85–97.

Holmes, A., Mühlen, S., Roe, A.J. and Dean, P. (2010). The EspF Effector, a Bacterial Pathogen's Swiss Army Knife. *Infection and Immunity* 78, 4445–4453.

Hudault, S., Guignot, J. and Servin, A.L. (2001). *Escherichia coli* Strains Colonising the Gastrointestinal Tract Protect Germfree Mice Against *Salmonella typhimurium* Infection. *Gut*, 49, 47–55.

Hyland, R.M., Sun, J., Griener, T.P., Mulvey, G.L., Klassen, J.S., Donnenberg, M.S. and Armstrong, G.D. (2008). The Bundlin Pilin of Enteropathogenic *Escherichia coli* is an *N*-Acetyllactosamine-Specific Lectin. *Cellular Microbiology* 10, 177–187.

Iguchi, A., Thomson, N.R., Ogura, Y., Saunders, D., Ooka, T., Henderson, I.R., Harris, D., Asadulghani, M., Kurokawa, K., Dean, P., Kenny, B., Quail, M.A., Thurston, S., Dougan, Hayashi, T., Parkhill, J. and Frankel, G. (2009). Complete Genome Sequence and Comparative Genome Analysis of Enteropathogenic *Escherichia coli* O127:H6 Strain E2348/69. *Journal of Bacteriology* 91, 347–354.

Iizumi, Y., Sagara, H., Kabe, Y., Azuma, M., Kume, K., Ogawa, M., Nagai, T., Gillespe, P.G., Sasakawa, C. and Handa, H. (2007). The Enteropathogenic *E. coli* Effector EspB Facilitates Microvillus Effacing and Antiphagocytosis by Inhibiting Myosin Function. *Cell Host and Microbe* 2, 383–392.

Jacewicz, M., Clausen, H., Nudelman, E., Donohue-Rolfe, A. Keusch, G.T. (1986). Pathogenesis of Shigella Diarrhea. XI. Isolation of a Shigella Toxin-Binding Glycolipid from Rabbit Jejunum and HeLa Cells and its Identification as Globotriaosylceramide. *The Journal of Experimental Medicine* 163, 1391–1404.

Janka, A., Bielaszewska, M., Dobrindt, U. and Karch, H. (2002). Identification and Distribution of the Enterohemorrhagic *Escherichia coli* Factor for Adherence (*efa1*) Gene in Sorbitol-Fermenting *Escherichia coli* O157: H-. *International Journal of Medical Microbiology : IJMM* 292, 207–214.

Jarvis, K.G., Girón, J.A., Jerse, A.E., McDaniel, T.K., Donnenberg, M.S. and Kaper, J.B. (1995). Enteropathogenic *Escherichia coli* Contains a Putative Type III Secretion System Necessary for the Export of Proteins Involved in Attaching and Effacing Lesion Formation. *Proceedings of the National Academy of Sciences of the United States of America* 92, 7996–8000.

Jerse, A.E., Yu, J., Tall, B.D. and Kaper, J.B. (1990). A Genetic Locus of Enteropathogenic *Escherichia coli* Necessary for the Production of Attaching and Effacing Lesions on Tissue Culture Cells. *Proceedings of the National Academy of Sciences of the United States of America* 87, 7839–7843.

Jiménez, L., Muñiz, I., Toranzos, G.A. and Hazen, T.C. (1990). Survival and Activity of *Salmonella typhimurium* and *Escherichia coli* in Tropical Freshwater. *Journal of Bacteriology* 67, 23–349.

Johannes, L. and Römer, W. (2010). Shiga Toxins – From Cell Biology to Biomedical Applications. *Nature Reviews Microbiology* 8, 105–116.

Johansen, B.K., Wasteson, Y., Granum, P.E. and Brynestad, S. (2001). Mosaic Structure of Shiga-Toxin-2-Encoding Phages Isolated from *Escherichia coli* O157:H7 Indicates Frequent Gene Exchange Between Lambdoid Phage Genomes. *Microbiology* 147, 1929–1936.

Just, I., Wilm, M., Selzer, J., Rex, G., von Eichel-Streibert, C., Mann, M. and Aktories, K. (1995). The Enterotoxin from *Clostridium difficile* (ToxA) Monoglucosylates the Rho Proteins. *The Journal of Biological Chemistry* 270, 13932–13936.

Kelly, S.M., Jess, T.J. and Price, N.C. (2005). How to Study Proteins by Circular Dichroism. *Biochimica et Biophysica Acta - Proteins and Proteomics*, 1751, 119–139.

Kenny, B. (1999). Phosphorylation of Tyrosine 474 of the Enteropathogenic *Escherichia coli* (EPEC) Tir Receptor Molecule is Essential for Actin Nucleating Activity and is Preceded by Additional Host Modifications. *Molecular Microbiology* 31, 1229–1241.

Kenny, B., Abe, A., Stein, M. and Finlay, B.B. (1997b). Enteropathogenic *Escherichia coli* Protein Secretion is Induced in Response to Conditions Similar to Those in the Gastrointestinal Tract. *Infection and Immunity* 65, pp.2606–2612.

Kenny, B., DeVinney, R., Stein, M., Reinscheid, D.J., Frey, E.A. Finlay, B.B. (1997a). Enteropathogenic *E. coli* (EPEC) Transfers its Receptor for Intimate Adherence into Mammalian Cells. *Cell* 91, 511–520.

Klapproth, J.A. (2010). The Role of Lymphostatin/EHEC Factor for Adherence-1 in the Pathogenesis of Gram Negative Infection. *Toxins* 2, 954–962.

Klapproth, J., Donnenberg, M.S., Abraham, J.M. and James, S.P. (1996). Products of Enteropathogenic *E. coli* Inhibit Lymphokine Production by Gastrointestinal Lymphocytes. *The American Journal of Physiology* 271, 841–848.

Klapproth, J., Donnenberg, M.S, Abraham, J.M., Mobley, H.L.T. and James, S.P. (1995). Products of Enteropathogenic *Escherichia coli* Inhibit Lymphocyte Activation and Lymphokine Production. *Infection and Immunity* 63, 2248–2254.

Klapproth, J.A. Saskia, M. Sherman, M. Babbin, B. Donnenberg, M.S. Fernandes, P.J. Scaletsky, I.C.A. Kalman, D. Nusrat, A Williams, I., 2005. *Citrobacter rodentium lifA/efa1* is Essential for Colonic Colonization and Crypt Cell Hyperplasia *In Vivo*. *Infection and Immunity* 73 pp.1441–1451.

Klapproth, J.A., Scaletsky, I.C., McNamara, B., Lai, L., Malstrom, C., James, S.P. and Donnenberg, M.S. (2000). A Large Toxin from Pathogenic *Escherichia coli* Strains That Inhibits Lymphocyte Activation. *Infection and Immunity* 68, 2148–2155.

Knutton, S., Rosenhine, I., Pallen, M.J., Nisan, I., Neves, B.C., Bain, C., Wolff, C., Dougan, G. and Frankel, G. (1998). A Novel EspA-Associated Surface Organelle of Enteropathogenic *Escherichia coli* Involved in Protein Translocation into Epithelial Cells. *The EMBO Journal* 17, .2166–2176.

Knutton, S., Shaw, R.K., Anantha, R.P., Donnenberg, M.S. and Zorgani, A.A. (1999). The Ype IV Bundle-Forming Pilus of Enteropathogenic *Escherichia coli* Undergoes Dramatic Alterations in Structure Associated with Bacterial Adherence, Aggregation and Dispersal. *Molecular Microbiology* 33, 499–509.

Kresse, A.U., Beltrametti, F., Müller, A., Ebel, F. and Guzmán, C.A. (2000). Characterization of SepL of Enterohemorrhagic *Escherichia coli*. *Journal of Bacteriology* 182, 6490–6498.

Kresse, A.U., Rohde, M. and Guzmán, C.A. (1999). The EspD Protein of Enterohemorrhagic *Escherichia coli* is Required for the Formation of Bacterial Surface Appendages and is Incorporated in the Cytoplasmic Membranes of Target Cells. *Infection and Immunity* 67, 4834–4842.

Lai, L., Wainwright, L.A., Stone, K.D. and Donnenberg, M.S. (1997). A Third Secreted Protein that is Encoded by the Enteropathogenic *Escherichia coli* Pathogenicity Island is Required for Transduction of Signals and for Attaching and Effacing Activities in Host Cells. *Infection and Immunity* 65, 2211–2217.

Law, H.T., Chua, M., Moon, K., Foster, L.J. and Guttman, J.A. (2015). Mass Spectrometry-Based Proteomics Identification of Enteropathogenic *Escherichia coli* Pedestal Constituents. *Journal of Proteome Research* 14, 2520–2527.

Lea, N., Lord, J.M. and Roberts, L.M. (1999). Proteolytic Cleavage of the A Subunit is Essential for Maximal Cytotoxicity of *Escherichia coli* O157:H7 Shiga-Like Toxin-1. *Microbiology* 145, 999–1004.

Leimbach, A., Hacker, J. and Dobrindt, U. (2013). *E. coli* as an All-Rounder: The Thin Line Between Commensalism and Pathogenicity. *Current Topics in Microbiology and Immunology vol. 358: Between Pathogenicity and Commensalism*, pp.3 - 33. Springer Heildelberg, New York.

Levine, M.M. and Edelman, R. (1984). Enteropathogenic *Escherichia coli* of Classic Serotypes Associated with Infant Diarrhea: Epidemiology and Pathogenesis. *Epidemiological Reviews* 6, 31–51.

Levine, M.M., Bergquist, E.J., Nalin, D.R., Waterman, D.H., Hornick, R.B., Young, C.R. and Sotman, S. (1978). *Escherichia coli* Strains that Cause Diarrhoea but do not Produce Heat-Labile or Heat-Stable Enterotoxins and are Non-Invasive. *The Lancet* 1, 1119–1122.

Levine, M.M., Nataro, J.P., Karch, H., Baldini, M.M., Kaper, J.B., Black, R.E., Clements, M.L. and O'Brien, A.D. (1985). The Diarrheal Response of Humans to Some Classic Serotypes of Enteropathogenic *Escherichia coli* is Dependent on a Plasmid Encoding an Enteroadhesiveness Factor. *The Journal of Infectious Diseases*, 152, 550–559.

Li, L., Mendis, N., Trigui, H., Oliver, J.D. and Faucher, S.P. (2014). The Importance of the Viable but Non-Culturable State in Human Bacterial Pathogens. *Frontiers in Microbiology* 5, 1–20.

Li, S., Zhang, L., Yoa, Q., Li, L., Dong, N., Rong, J., Gao, W., Ding, X., Sun, L., Chen, X., Chen, S. and Shao, F. (2013). Pathogen Blocks Host Death Receptor Signalling by Arginine GlcNAcylation of Death Domains. *Nature* 501, 242–246.

Lindberg, A., Brown, J.E, Strömberg, N., Westling-Ryd, M., Schultz J.E. and Karlsson, K. (1987). Identification of the Carbohydrate Receptor for Shiga Toxin Produced by *Shigella dysenteriae* Type 1. *The Journal of Biological Chemistry* 262, 1779–85.

Lo, M.C., Aulabaugh, A., Jin, G., Cowling, R., Bard, J., Malamas, M. and Ellestad, G. (2004). Evaluation of Fluorescence-Based Thermal Shift Assays for Hit Identification in Drug Discovery. *Analytical Biochemistry* 332, 153–159.

Lobley, A., Whitmore, L. and Wallace, B.A. (2002). DICHROWEB: an Interactive Website for the Analysis of Protein Secondary Structure from Circular Dichroism Spectra. *Bioinformatics* 18, 211–212.

Madden, T. (2002). The BLAST Sequence Analysis Tool. *The NCBI Handbook [Internet]*. Bethesda (MD): National Center for Biotechnology Information (US). URL: http://www.ncbi.nlm.nih.gov/books/NBK21097/

Makino, K., Ishii, K., Yasunaga, T., Hattori, M., Yokoyama, K., Yutsudo, C.H., Kubota, Y. Yamaichi, Y., Iida, T., Yamamoto, K., Honda, T., Han, C., Ohtsubo, E., Kasamatsu, M., Hayashi, T., Kuhara, S. and Shinagawa, H. (1998). Complete Nucleotide Sequences of 93-kb and 3.3-kb Plasmids of an Enterohemorrhagic *Escherichia coli* O157:H7 Derived from Sakai Outbreak. *DNA Research : an International Journal for Rapid Publication of Reports on Genes and Genomes* 5, 1–9.

Mallard, F., Antony, C., Tenza, D., Salamero, J., Goud, B. and Johannes, L. (1998). Direct Pathway from Early/Recycling Endosomes to the Golgi Apparatus Revealed Through the Study of Shiga Toxin B-Fragment Transport. *Journal of Cell Biology* 143, 973–990.

Malstrom, C. and James, S. (199)8. Inhibition of Murine Splenic and Mucosal Lymphocyte Function by Enteric Bacterial Products. *Infection and Immunity* 66, 3120–3127.

Malvern (2015). Dynamic Light Scattering. URL: http://www.malvern.com/en/products/technology/dynamic-light-scattering/

Malyukova, I., Murray, K.F., Zhu, C., Boedeker, E., Kane, A., Patterson, K., Peterson, J.R., Donowitz, M. and Kovbasnjuk, O. (2009). Macropinocytosis in Shiga Toxin 1 Uptake by Human Intestinal Epithelial Cells and Transcellular Transcytosis. *American Journal of Physiology Gastrointestinal and Liver Physiology*, 21205, 78–92.

Manjarrez-Hernandez, H.A., Baldwin, T.J., Aitken, A., Knutton, S. and Williams, P.H. (1992). Intestinal Epithelial Cell Protein Phophorylation in Enteropathogenic *Escherichia coli* Diarrhoea. *The Lancet* 339, 521–523.

Maslon, M.M., Hrstka, R., Vojtesek, B. and Hupp, T.R. (2010). A Divergent Substrate-Binding Loop within the Pro-Oncogenic Protein Anterior Gradient-2 Forms a Docking Site for Reptin. *Journal of Molecular Biology* 404, 418–438.

McDaniel, T.K., Jarvis, K.G., Donnenberg, M.S. and Kaper, J.B. (1995). A Genetic Locus of Enterocyte Effacement Conserved Among Diverse Enterobacterial Pathogens. *Proceedings of the National Academy of Sciences of the United States of America* 92, 1664–1668.

McNeilly, T.N., Mitchell, M.C., Rosser, T., McAteer, S., Low, J.C., Smith, D.G.E., Huntley, J.F., Mahajan, A. and Gally, D. (2010). Immunization of Cattle with a Combination of Purified Intimin-531, EspA and Tir Significantly Reduces Shedding of *Escherichia coli* O157:H7 Following Oral Challenge. *Vaccine* 28, 1422–1428.

Mellies, J.L. and Lorenzen, E. (2014). Enterohemorrhagic *Escherichia coli* Virulence Gene Regulation. *Microbiology Spectrum* 2.

Mellies, J.L., Barron, A.M.S. and Carmona, A.M. (2007). Enteropathogenic and Enterohemorrhagic *Escherichia coli* Virulence Gene Regulation. *Infection and Immunity* 75, 4199–4210.

Mellmann, A., Bielaszewska, M., Köck, R., Friedrich, A.W., Fruth, A., Middendorf, B., Harmsen, D., Schmidt, M.A. and Karch, H. (2008). Analysis of Collection of Hemolytic Uremic Syndrome-Associated Enterohemorrhagic *Escherichia coli*. *Emerging Infectious Diseases* 14, 1287–1290.

Menge, C., Wieler, L.H., Schlapp, T. and Baljer, G. (1999). Shiga Toxin 1 from *Escherichia coli* Blocks Activation and Proliferation of Bovine Lymphocyte Subpopulations *in vitro*. *Infection and Immunity* 67, 2209–2217.

Mills, E., Baruch, K., Aviv, G., Nitzan, M. and Rosenshine I. (2013). Dynamics of the Type III Secretion System Activity of Enteropathogenic *Escherichia coli*. *mBio* 4, 1–9.

Morgan, E., Bowen, A.J., Carnell, S.C., Wallis, T.S. and Stevens, M.P. (2007). SiiE is Secreted by the *Salmonella enterica* Serovar Typhimurium Pathogenicity Island 4-Encoded Secretion System and Contributes to Intestinal Colonization in Cattle. *Infection and Immunity* 75, 1524–1533.

Nadler, C., Baruch, K., Kobi, S., Mills, E., Haviv, G., Farago, M., Alkalay, I., Bartfeld, S., Meyer, T.F., Ben-Neriah, Y. and Rosenshine, I. (2010). The Type III Secretion Effector NleE Inhibits NF-κB Activation. *PLOS Pathogens* 6, 1–11.

Nataro, J.P. and Kaper, J.B. (1998). Diarrheagenic *Escherichia coli*. *Clinical Microbiology Reviews* 11, 142–201.

Nataro, J.P., Maher, K.O., Mackie, P. and Kaper, J.B. (1987). Characterization of Plasmids Encoding the Adherence Factor of Enteropathogenic *Escherichia coli*. *Infection and Immunity* 55, 2370–2377.

Naylor, S.W., Roe, A.J., Nart, P., Spears, K., Smith, D.G.E., Low, J.C. and Gally, D.L. (2005). *Escherichia coli* O157:H7 Forms Attaching and Effacing Lesions at the Terminal Rectum of Cattle and Colonization Requires the LEE4 operon. *Microbiology* 151, 2773–2781.

Neely, M.N. and Friedman, D.I. (1998). Functional and Genetic Analysis of Regulatory Regions of Coliphage H-19B: Location of Shiga-Like toxin and Lysis Genes Suggest a Role for Phage Functions in Toxin Release. *Molecular Microbiology* 28, 1255–1267.

Nicholls, L., Grant, T.H. and Robins-Browne, R.M. (2000). Identification of a Novel Genetic Locus that is Required for *in vitro* Adhesion of a Clinical Isolate of Enterohaemorrhagic *Escherichia coli* to Epithelial Eells. *Molecular Microbiology* 35, 275–288.

O'Brien, A.D., Newland, J.W., Miller, S.F., Holmes, R.K., Smith, H.W. and Formal, S.B. (1983). Shiga-Like Toxin-Converting Phage from *Escherichia coli* Strains That Cause Hemorrhagic Colitis or Infantile Diarrhea. *Science* 226, 694–696.

Ochoa, T.J. and Contreras, C.A. (2011). Enteropathogenic *E. coli* (EPEC) Infection in Children. *Current Opinion in Infectious Dis*ease 24, 478–483.

O'Connell, C.B., Creasey, E.A., Knutton, S., Elliot, S., Crowther, L.J., Luo, W., Albert, M.J., Kaper, J.B., Frankel, G. and Donnenberg, M.S. (2004). SepL, a Protein Required for Enteropathogenic *Escherichia coli* Type III Translocation, Interacts with Secretion Component SepD. *Molecular Microbiology* 52, 1613–1625.

Ogura, Y., Ooka, T., Iguchi, A., Toh, H., Asadulghani, M., Oshima, K., Kodama, T., Abe, H., Nakayama, K., Kurokawa, K., Tobe, T., Hattori, M. and Hayashi, T. (2009). Comparative Genomics Reveal the Mechanism of the Parallel Evolution of O157 and Non-O157 Enterohemorrhagic *Escherichia coli*. *Proceedings of the National Academy of Sciences of the United States of America* 106, 17939–17944.

Pacheco, A.R. and Sperandio, V. (2012). Shiga Toxin in Enterohemorrhagic *E. coli*: Regulation and Novel Anti-Virulence Strategies. *Frontiers in Cellular and Infection Microbiology* 2, 1–12.

Pantoliano, M.W. Petrella, E.C. Kwasnoski, J.D. Lobanov, V.S. Myslik, J. Graf, E. Carver, T Asel, E. Springer, B.A. Lane, P. and Salemme, F.R. 2001. High-Density Miniaturized Thermal Shift Assays as a General Strategy for Drug Discovery. *Journal of Biomolecular Screening* 6, 429–440.

Pearson, J.S., Glogha, C., Ong, S.Y., Kennedy, C.L., Kelly, M., Robinson, K.S., Lung, T.W.F., Mansel, A., Riedmaler, P., Oates, C.V.L., Zaid, A., Mühlen, S., Crepin, V.F., Marches, O., Ang, C., Williamson, N.A., O'Reilly, L.A., Bankovaki, A., Nachbur, U., Infusini, G., Webb, A.I., Silke, J., Strasser, A., Frankel, G. and Hartland, E.L. (2013). A Type III Effector Antagonizes Death Receptor Signalling During Bacterial Gut Infection. *Nature* 501, pp.247–51.

Pearson, J.S., Riedmaier, P., Marchès, O., Frankel, G. and Hartland, E.L. (2011). A Type III Effector Protease NleC from Enteropathogenic *Escherichia coli* Targets NF-κB for Degradation. *Molecular Microbiology* 80, 219–230.

Perna, N.T., Plunkett III, G., Burland, V., Mau, B., Glasner, J.D., Rose, D.J., Mayhew, G.F., Evans, P.S., Gregor, J., Kirkpatrick, H.A., Pósfai, G., Hackett, J., Klink, S., Boutin, A., Shao, Y., Miller, L., Grotbeck, E.J., Davis, N.W., Lim, A., Dimalanta, E.T., Potamousis, K.D., Apodaca, J., Anantharaman, T.S., Lin, J., Yen, G., Schwartz, D.C., Welch, R.A. and Blattner F.R (2001). Genome Sequence of Enterohaemorrhagic *Escherichia coli* O157: H7. *Nature* 409, 529–533.

Pierard, D., Huyghens, L. and Lauwers, S. (1991). Diarrhoea Associated with *Escherichia coli* Producing Porcine Oedema Disease Verotoxin. *The Lancet* 338, 762.

Price, N.C. and Nairn, J. (2009). Spectroscopic Methods to Study Secondary and Tertiary Structure. *Exploring Proteins*, pp.358 - 365. Oxford University Press Inc., New York.

Promega (2009). *CytoTox-ONE™ Homogenous Membrane Integrity Assay Technical Bulletin*.

Promega (2012). *CellTitre 96® AQ_{ueous} One Solution Cell Proliferation Assay Technical Bulletin*.

Pruimboom-Brees, I.M., Morgan, T.W., Ackermann, M.R., Nystrom, E.D., Samuel, J.E., Cornick, N.A. and Moon, H.W. (2000). Cattle Lack Vascular Receptors for *Escherichia coli* O157:H7 Shiga Toxins. *Proceedings of the National Academy of Sciences of the United States of America* 97, 10325–10329.

Pruitt, R.N., Chumbler, N.M., Rutherford, S.A., Farrow, M.A., Friedman, D.B, Spiller, B. and Lacy, D.B. (2012). Structural Determinants of *Clostridium difficile* Toxin A Glucosyltransferase Activity. *The Journal of Biological Chemistry* 287, 8013–8020.

Puente, J.L., Bieber, D., Ramer, S.W., Murray, W. and Schoolnik, G.K. (1996). The Bundle-Forming Pili of Enteropathogenic *Escherichia coli*: Transcriptional Regulation by Environmental signals. *Molecular Microbiology* 20, 87–100.

Rasko, D.A., Moreira, C.G., Li, D.R., Reading, N.C., Ritchie, J.M., Waldor, M.K., William, N., Taussig, R., Wei, S., Roth, M., Hughes, D.T., Huntley, J.F., Fina, M.W., Falck, J.R. and Sperandio, V. (2008). Targeting QseC Signaling and Virulence for Antibiotic Development. *Science* 321, 1078–1080.

Reineke, J., Tenzer, S., Rupnik, M., Koschinski, A., Hasselmayer, O., Schrattenholz, A., Schild, H. and von Eichel-Streiber, C. (2007). Autocatalytic Cleavage of *Clostridium difficile* Toxin B. *Nature* 446, 415–419.

Reissbrodt, R., Rienaecker, I., Romanova, J.M., Freestone, P.P.E., Haigh, R.D., Lyte, M., Tschäpe, H. and Williams, P.H. (2002). Resuscitation of *Salmonella enterica* Serovar Typhimurium and Enterohemorrhagic *Escherichia coli* from the Viable but Nonculturable State by Heat-Stable Enterobacterial Autoinducer. *Applied and Environmental Microbiology* 68, 4788–4794.

Rivera, S.C., Hazen, T.C. and Toranzos, G.A. (1988). Isolation of Fecal Coliform from Pristine Sites in a Tropical Rain Forest. *Applied and Environmental Microbiology* 54, 513–517.

Römer, W., Berland, L., Chambon, V., Gaus, K., Windschiegl, B., Tenza, D., Aly, M.R.E., Fraisier, V., Florent, J., Perrais, D., Lamaze, C., Raposo, G., Steinem, C., Sens, P., Bassereau, P. and Johannes, L. (2007). Shiga Toxin Induces Tubular Membrane Invaginations for its Uptake into Cells. *Nature* 450, 670–675.

Rosenshine, I., Donnenberg, M.S., Kaper, J.B. and Finlay, B.B. (1992). Signal Transduction Between Enteropathogenic *Escherichia coli* (EPEC) and Epithelial Cells: EPEC Induces Tyrosine Phosphorylation of Host Cell Proteins to Initiate Cytoskeletal Rearrangement and Bacterial Uptake. *The EMBO Journal* 11, 3551–3560.

Rosenshine, I., Ruschkowski, S. and Finlay, B.B. (1996). Expression of Attaching/Effacing Activity by Enteropathogenic *Escherichia coli* Depends on Growth Phase, Temperature, and Protein Synthesis upon Contact with Epithelial Cells. *Infection and Immunity* 64, 966–973.

Rosqvist, R., Magnusson, K.E. and Wolf-Watz, H. (1994). Target Cell Contact Triggers Expression and Polarized Transfer of *Yersinia* YopE Cytotoxin into Mammalian Cells. *The EMBO Journal* 13, 964–972.

Saldaña, Z., Erdem, A.L., Schüller, S., Okeke, I.N., Lucas, M., Sivananthan, A., Phillips, A.D., Kaper, J.B., Puente, J.L. and Girón, J.A. (2009). The *Escherichia coli* Common Pilus and the Bundle-Forming Pilus Act in Concert During the Formation of Localized Adherence by Enteropathogenic *E. coli*. *Journal of Bacteriology* 191, 3451–3461.

Sandvig, K., Garred, Ø., Prydz, K., Kozlov, J.V., Hansen, S.T. and van Deurs, B. (1992). Retrograde Transport of Endocytosed Shiga Toxin to the Endoplasmic Reticulum. *Nature* 358, 510–512.

Sandvig, K., Olsnes, S., Brown, J.E., Peterson, O.W. and van Deurs, B. (1989). Endocytosis from Coated Pits of Shiga Toxin: A Glycolipid-Binding Protein from *Shigella dysenteriae* 1. *Journal of Cell Biology* 108, 1331–1343.

Sanger, J.M., Chang, R., Ashton, F., Kaper, J.B. and Sanger, J.W. (1996). Novel Form of Actin-Based Motility Transports Bacteria on the Surface of Infected Cells. *Cell Motilily and the Cytoskeleton* 34, 279–287.

Savageau, M.A. (1983). *Esherichia coli* Habitats, Cell Types, and Molecular Mechanisms of Gene Control. *The American Naturalist*, 122, 732–744.

Savkovic, S.D., Koutsouris, A. and Hecht, G.. (1997). Activation of NF-κB in Intestinal Epithelial Cells by Enteropathogenic *Escherichia coli*. *The American Journal of Physiology* 273, 1160–1167.

Schirmer, J. & Aktories, K. (2004). Large Clostridial Cytotoxins: Cellular Biology of Rho/Ras-Glucosylating toxins. *Biochimica et Biophysica Acta - General Subjects* 1673, 66–74.

Schüller, S., Frankel, G. and Phillips, A.D. (2004). Interaction of Shiga Toxin from *Escherichia coli* with Human Intestinal Epithelial Cell Lines and Explants: Stx2 Induces Epithelial Damage in Organ Culture. *Cellular Microbiology* 6, 289–301.

Selzer, J., Hofmann, Rex, G., Wilm, M., Mann, M., Just, I. and Aktories (1996). *Clostridium novyi* α-Toxin-Catalyzed Incorporation of GlcNAc into Rho Subfamily Proteins. *The Journal of Biological Chemistry* 271, 25173–25177.

Shao, F., Meritt, P.M., Bao, Z., Innes, R.W. and Dixon, J.E. (2002). A *Yersinia* Effector and a *Pseudomonas* Avirulence Protein Define a Family of Cysteine Proteases Functioning in Bacterial Pathogenesis. *Cell* 109, 575–588.

Shaw, R.K., Cleary, J., Murphy, M.S., Frankel, G. and Knutton, S. (2005). Interaction of Enteropathogenic *Escherichia coli* with Human Intestinal Mucosa: Role of Effector Proteins in Brush Border Remodeling and Formation of Attaching and Effacing Lesions. *Infection and Immunity* 73, 1243–1251.

Sinclair, J.F. and O'Brien, A.D. (2002). Cell Surface-Localized Nucleolin is a Eukaryotic Receptor for the Adhesin Intimin-γ of Enterohemorrhagic *Escherichia coli* O157:H7. *The Journal of Biological Chemistry* 277, 2876–2885.

Sinclair, J.F. and O'Brien, A.D. (2004). Intimin Types α, β, and γ Bind to Nucleolin with Equivalent Affinity but Lower Avidity than to the Translocated Intimin Receptor. *The Journal of Biological Chemistry* 279, 33751–33758.

Sohel, I., Puente, J.L., Ramer, S.W., Bieber, D., Wu, C. and Schoolnik, G.K. (1996). Enteropathogenic *Escherichia coli*: Identification of a Gene Cluster Coding for Bundle-Forming Pilus Morphogenesis. *Journal of Bacteriology* 178, 2613–2628.

Solo-Gabriele, H.M., Wolfert, M.A., Desmarais, T.R. and Palmer, C.J. (2000). Sources of *Escherichia coli* in a Coastal Subtropical Environment. *Applied and Environmental Microbiology* 66, 230–237.

Stein, P.E., Boodhoo, A., Tyrrell, G.J., Brunton, J.L. and Read, R.J. (1992). Crystal Structure of the Cell-Binding B Oligomer of Verotoxin-1 from *E. coli*. *Nature*, 355, 748–750.

Stevens, M.P. & Frankel, G.M. (2014). The Locus of Enterocyte Effacement and Associated Virulence Factors of Enterohemorrhagic Escherichia coli. *Microbiology Spectrum* 2.

Stevens, M.P., Roe, A.J., Vlisidou, I., van Diemen, P.M., La Ragione, R.M., Best, A., Woodward, M.J., Gally, D.I. and Wallis, T.S. (2004). Mutation of *toxB* and a Truncated Version of the *efa-1* Gene in *Escherichia coli* O157: H7 Influences the Expression and Secretion of Locus of Enterocyte Effacement-Encoded Proteins but not Intestinal Colonization in Calves. *Infection and Immunity* 72, 5402–5411.

Stevens, M.P., van Diemen, P.M., Frankel, G., Phillips, A.D. and Wallis, T.S. (2002). Efa1 Influences Colonization of the Bovine Intestine by Shiga Toxin-Producing *Escherichia coli* serotypes O5 and O111. *Infection and Immunity* 70, 5158–5166.

Stone, K.D., Zhang, H., Carlson, L.K. and Donnenberg, M.S. (1996). A Cluster of Fourteen Genes from Enteropathogenic *Escherichia coli* is Sufficient for the Biogenesis of a Type IV Pilus. *Molecular Microbiology* 20, 325–337.

Strom, M.S. and Lory, S. (1993). Structure-Function and Biogenesis of the Type IV Pili. *Annual Review of Microbiology* 47, 565–596.

Tam, P.J. and Lingwood, C.A. (2007). Membrane-Cytosolic Translocation of Verotoxin A_1 Subunit in Target Cells. *Microbiology* 153, 2700–2710.

Tatsuno, I., Horie, M., Abe, H., Miki, T., Makino, K., Shinagawa, H., Tagucji, H., Kamiya, S., Hayashi, T. and Sasakawa, C. (2001). Gene on pO157 of Enterohemorrhagic *Escherichia coli* O157:H7 is Required for Full Epithelial Cell Adherence Phenotype. *Infection and Immunity* 69, 6660–6669.

Taylor, J. (1970). Infectious Infantile Enteritis, Yesterday and Today. *Section of Epidemiology & Preventive Medicine* 63, 1297–1301.

Taylor, K.A., O'Connell, C.B., Luther, P.W. and Donnenberg, M.S. (1998). The EspB Protein of Enteropathogenic *Escherichia coli* is Targeted to the Cytoplasm of Infected HeLa Cells. *Infection and Immunity* 66, 5501–5507.

Temple, K.L., Camper, A.K. and McFeters, G.A. (1980). Survival of Two Enterobacteria in Feces Buried in Soil Under Field Conditions. *Applied and Environmental Microbiology* 40, 794–797.

Thanabalasuriar, A., Koutsouris, A., Weflen, A., Mimee, M., Hecht, G. and Gruenheid, S. (2011). The Bacterial Virulence Factor NleA is Required for the Disruption of Intestinal Tight Junxtions by Enteropathogenic *E. coli*. *Cell*, 12, 31–41.

Tobe, T., Schoolnik, G.K., Sohel, I., Bustamante, V.H. and Puente, J.L. (1996). Cloning and Characterization of *bfpTVW*, Genes Required for the Transcriptional Activation of *bfpA* in Enteropathogenic *Escherichia coli*. *Molecular Microbiology* 21, 963–975.

Toshima, H., Yoshimura, A., Arikawa, K., Hidaka, A., Ogasawara, J., Hase, A., Masaki, H. and Nishikawa, Y. (2007). Enhancement of Shiga Toxin Production in Enterohemorrhagic *Escherichia coli* Serotype O157:H7 by DNase Colicins. *Applied and Environmental Microbiology* 73, 7582–7588.

Tozzoli, R., Caprioli, A. and Morabito, S. (2005). Detection of *toxB*, a Plasmid Virulence Gene of Escherichia coli O157, in Enterohemorrhagic and Enteropathogenic *E. coli*. *Journal of Clinical Microbiology* 43, 4052–4056.

Trabulsi, L.R., Keller, R. and Gomes, T.A.T. (2002). Typical and Atypical Enteropathogenic *Escherichia coli*. *Emerging Infectious Diseases* 8, 508–513.

Tree, J.J., Wang, D., McInally, C., Mahajan, A., Layton, A., Houghton, I., Elofsson, M., Stevens, M.P., Gally, D.L. and Roe, A.J. (2009). Characterization of the Effects of Salicylidene Acylhydrazide Compounds on Type III Secretion in *Escherichia coli* O157:H7. *Infection and Immunity* 77, 4209–4220.

Triadafilopoulos, G., Pothoulakis, C., O'Brien, M.J. and LaMont, J.T. (1987). Differential Effects of *Clostridium difficile* toxins A and B on Rabbit Ileum. *Gastroenterology* 93, 273–279.

Veenendaal, A.K.J., Sundin, C. and Blocker, A.J. (2009). Small-Molecule Type III Secretion System Inhibitors Block Assembly of the *Shigella* Type III Secreton. *Journal of Bacteriology* 191, 563–570.

Vlisidou, I., Dziva, F., la Ragione, R.M., Best, A., Garmendia, J., Hawes, P., Monaghan, P., Cawthraw, S.A., Frankel, G., Woodward, M.J. and Stevens, M.P. (2006). Role of Intimin-Tir Interactions and the Tir-Cytoskeleton Coupling Protein in the Colonization of Calves and Lambs by *Eschenchia coli* O157:H7. *Infection and Immunity* 74, 758–764.

Voulhoux, R., Ball, G., Ize, B., Vasil, M.L., Lazdunski, A., Wu, L. and Filloux, A. (2001). Involvement of the Twin-Arginine Translocation System in Protein Secretion via the Type II Pathway. *The EMBO Journal* 20, pp.6735–6741.

Wachter, C., Beinke, C., Mattes, M. and Schmidt, M.A. (1999). Insertion of EspD into Epithelial Target Cell Membranes by Infecting Enteropathogenic *Escherichia coli*. *Molecular Microbiology* 31, 1695–1707.

Wang, D., Roe, A.J., McAteer, S., Shipston, M.J. and Gally, D.L. (2008). Hierarchal Type III Secretion of Translocators and Effectors from *Escherichia coli* O157:H7 Requires the Carboxy Terminus of SepL that Binds to Tir. *Molecular Microbiology* 69, 1499–1512.

Warawa, J., Finlay, B.B. and Kenny, B. (1999). Type III Secretion-Dependent Hemolytic Activity of Enteropathogenic *Escherichia coli*. *Infection and Immunity* 67, 5538–5540.

Weljie, A.M. and Vogel, H.J. (2000). Tryptophan Fluorescence of Calmodulin Binding Domain Peptides Interacting with Calmodulin Containing Unnatural Methionine Analogues. *Protein Engineering* 13, 59–66.

Winfield, M.D. and Groisman, E.A. (2003). Role of Nonhost Environments in the Lifestyles of *Salmonella* and *Escherichia coli*. *Applied and Environmental Microbiology* 69, 3687–3694.

Wolff, C., Nisan, I., Hanski, E., Frankel, G. and Rosenshine, I. (1998). Protein Translocation into host Epithelial Cells by Infecting Enteropathogenic *Escherichia coli*. *Molecular Microbiology* 28, 143–155.

Wu, B., Skarina, T., Yee, A., Jobin, M., DiLeo, R., Semesi, A., Fares, C., Lemak, A., Coombes, B.K., Arrowsmith, C.H., Singer, A.U. and Savchenko, A. (2010). NleG Type 3 Effectors from Enterohaemorrhagic *Escherichia coli* are U-Box E3 Ubiquitin Ligases. *PLOS Pathogens* 6, 1–17.

Xie, G., Bonner, C.A. and Jensen, R.A. (2002). Dynamic Diversity of the Tryptophan Pathway in Chlamydiae: Reductive Evolution and a Novel Operon for Tryptophan Recapture. *Genome Biology* 3, 1–17.

Yu, J. and Kaper, J.B. (1992). Cloning and Characterization of the *eae* Gene of Enterohaemorrhagic *Escherichia coli* O157:H7. *Molecular Microbiology* 6, 411–417.

Zhang, H. and Donnenberg, M.S. (1996). DsbA is Required for Stability of the Type IV Pilin of Enteropathogenic *Escherichia coli*. *Molecular Microbiology* 21, 787–797.

Zhang, H., Lory, S. and Donnenberg, M.S. (1994). A Plasmid-Encoded Prepilin Peptidase Gene from Enteropathogenic *Escherichia coli*. *Journal of Bacteriology* 176, 6885–6891.

Zhang, X., McDaniel, A.D., Wolf, L.E., Keusch, G.T., Waldor, M.K. and Acheson, D.W.K. (2000). Quinolone Antibiotics Induce Shiga Toxin-Encoding Bacteriophages, Toxin Production, and Death in Mice. *The Journal of Infectious Diseases* 181, 664–670.

Appendix 1: Composition of buffers and reagents

TRIS buffer was composed of 50mL distilled water (dH_2O) with 1.5M TRIS base buffer and made up to pH 8.8 using NaOH and HCl.

To make 300mL of NZY^+ broth, 2g of NZ amine, 1g of yeast extract and 1g of NaCl was dissolved in dH_2O and made up to pH 7.5 using NaOH and HCl. The media was autoclaved then 2.5mL of sterile 1M MgCl and 1M $MgSO_4$ was added along with 0.4% (w/v) glucose.

IMAC buffer A was composed of 500mL dH_2O with 20mM NaH_2PO_4, 300mM NaCl, 5% (v/v) glycerol and 0.1% (v/v) Tween 20. It was made up to pH 7.8 using NaOH and HCl and 1mM fresh DTT was added before use. It was kept on ice or at 6°C when not in use.

IMAC buffer B was composed of 200mL dH_2O with 20mM NaH_2PO_4, 5% (v/v) glycerol, 0.1% (v/v) Tween 20 and 500mM imidazole. It was made up to pH 7.8 using NaOH and HCl and 1mM fresh DTT was added before use. It was kept on ice or at 6°C when not in use.

The low salt buffer used for SEC was composed of 200mL dH_2O with 10mM NaH_2PO_4, 50mM NaCl, 5% (v/v) glycerol and 0.025% (v/v) Tween 20. It was made up to pH 7.8 using NaOH and HCl and 1mM fresh DTT was added before use. It was kept on ice or at 6°C when not in use.

The low salt buffer used for ion exchange chromatography was composed of 200mL dH_2O with 10mM NaH_2PO_4, 1mM NaCl, 5% (v/v) glycerol and 0.025% (v/v) Tween 20. It was made up to pH 7.8 using NaOH and HCl and 1mM fresh DTT was added before use. It was kept on ice or at 6°C when not in use.

Assay buffer was composed of 200mL of dH_2O with 15mM NaH_2PO_4, 150mM NaCl and 5% (v/v) glycerol. It was made up to pH 7.8 using NaOH and HCl and 1mM fresh DTT was added before use. It was kept on ice or at 6°C when not in use.

CD buffer was composed of 200mL of dH_2O with 15mM NaH_2PO_4, 150mM NaF and 5% (v/v) glycerol. It was made up to pH 7.6 using NaOH and HCl and 1mM fresh DTT was added before use. It was kept on ice or at 6°C when not in use.

Red blood cell lysis buffer was composed of 1L dH_2O with 100mM $KHCO_3$, 1.5mM NH_4Cl and 10mM EDTA. It was made up to pH 8 using NaOH and HCl split into 10 x 100mL aliquots and autoclaved.

WT LifA buffer is the buffer that WT LifA was in after being filtered through the desalt column. It contains 15mM NaH_2PO_4, 180mM NaCl, 1mM DTT, 10% (v/v) glycerol and 0.05% Tween 20 in dH_2O.

DXD-AAA LifA buffer is the buffer that DXD-AAA LifA was in after being filtered through the desalt column. It contains 10mM NaH_2PO_4, 180mM NaCl, 1mM DTT, 20% (v/v) glycerol and 0.025% Tween 20 in dH_2O.

Appendix 2: Nucleotide sequence of the DXD-AAA *lifA* gene

The substituted DXD motif-encoding codons are highlighted in yellow.

ATGAGACTGCCAGAGAAAGTTCTTTTTCCTCCTGTCACTAGTGGCCTGTC
AGGGCAGGAAAAACAAAAAAAACCGAAGAGCATTACCGGATTTCAGGA
AAATTATCAACGCAATATCAGGCCAATCAAAACAGCATCAGAAGCCCGA
CTACGCTTCTTTGATAAAATGGTTTCGAAAGAAAACTCTCTGGAAGATGT
TGTTTCTTTAGGTGAAATGATTCAGAAGGAAATTTATGGGCATGAACAAA
GAACATTTTCACCAGTTCATCATACAGGTAACTGGAAATCATCATTGTTA
CACAACGCGCTCCTTGGTCTGGCAAATGTTTATAATGGCTTACGGGAAAC
AGAATACCCTAACACTTTCAACAGAGATGGTATAAAAAGTACTAACTCTT
TTAGAGATAACTTATTGACAAAAACAAGAACTCCCAGAGATAATTTTGA
GGAAGGAATAAAACATCCTGAACATGCAACAATACCATATGACAACGAC
AATGAAAGTAATAAATTGCTAAAAGCAGGAAAGATAGCTGGTAACAATA
ACGAGCTGTTGATGGAAATAAAAAAGGAATCCCAAAGCGACCATCAAAT
CCCCCTGTCAGATAAGTTCCTGAAAAGGAAAAAACGATCTCCTGTAGCTG
AAGATAAAGTTCAAAACTCGTTAACACCAGAAAATTTTGTTCAGAAAATT
TCACTTAGTGATGAGCTTAAAACAAAATATGCAAATGAAATTATAGAGA
TAAAAAGAATAATGGGAGAATACAATCTTTTACCGGATAAAAACAGTCG
TAATGGTCTAAAACTTCTACAGAAGCAAGCTGATTTACTAAAAATAATCA
TGGAGGATACCTCCGTTACAGAAAATACCTTTAAAAACATAGAGATAGC
TATAACAGATATAAAAAGGGAGTACTATTCGCATACAGTTGATATTGAG
AAAAATATTCATGCCATATGGGTTGCGGGTTCCCCACCTGAAAGCATTTC
GGACTATATTAAGACTTTTCTCAAAACCTACAAAGAGTTTACTTACTATC
TTTGGGTTGATGAAAAAGCATTTGGAGCCGCGAAATTTACCAGTGTCTTA
AAACAAATTGCATTTGATTTAGCATGCAGAACTATACAGCAGAATACTCC
ACAAAAAAATATTGATTTTATTAATCTATATAATGAAATAAGGAAGAAAT
ACAACAACAACCCATCGGGACAACAAGAGTACTTAAACAAACTCAGAGA
GCTTTATGCTACTTATCAAAAAATATCCACCCCTCTGAAACACATGTTTA
ATTCATTTTTTTTAGAAAACATGATTAAACTTCAGGATAATTTCTTCAACT
ATTGCATTGTCAAAGGTGTTACAGAGATTAATGATGAGTTACGAATAAAC
TACCTTAAAAATGTAATAAAACTGTCAGACGATGACATTGGTAATTACCA
GAAAACAATTAACGACAATAAAGATAGAGTAAAAAAACTAATTCTTGAT
TTACAGAAACAATTTGGTGAAAACCGCATTTCAATTAAAGATGTTAACTC
TTTAACCTCTCTTTCAAAATCAGAAAATAATCACAATTATCAAACTGAAA
TGTTGCTTCGATGGAACTATCCTGCCGCCTCAGACCTGCTCAGGATGTAT
ATCCTTAAAGAGCATGGTGGTATTTATACAGCGGCCGCGATGATGCCTGC
ATACTCTAAACAAGTAATTTTTAAAATTATGATGCAGACAAACGGAGATA
ATCGTTTCTTGGAAGATTTGAAACTACGTCGTGCAATATCTGATGGTGTA
TTAAGATATGTTAATAACCAAAATATTGATGAAGTTAACTATAATGAAAT
CAGTGATGCAGATAAAAACATTATCAAGAAGATATTAACAGAAATATCT
AAAATGCCAGAAGATAGTATTTTTACTAAGATCAATACAAGGATTCCTCG
AGACACAATGCCCATCCTTCGTCGTTATCACCTATGGCCTGATGGATGGA
ATATTCGTGGGCTCAATGGATTCATGCTATCACATAAAGGTAGTGAAGTG
ATTGATGCTGTTATCGCAGGCCAGAATCAGGCTTACAGGGAACTAAGAA

GAATAAGAGATAATATTCATAGTGAAATATACTTCAAACAAACTGATGA
ATTGTCCTCACTTCCAGATACAGACAAAATTGGAGGGATTCTGGTAAAAA
AATACCTTTCAGGAAGTCTTTTTTCAAAATTCAGACAAGATACTATTATC
CCGGAGGCATTGAGCACCCTCCAGATATCAGGTCCTGACTTGATTCAAAG
AAAGATGTTGCAATTTTTCAGGAGTAGAGGGGTGTTAGGTGAAGAGTTC
ATTAATGAAAGAAAACTGAGTGATAAAGCTTATATTGGTGTCTACAAAA
CAACTGGCACAGGGAAATATGACTGGTTAACCCCTGAATCGATCGGCGTT
AATGATGTCACGCCCGCAGATGAAAGTACCTGGTGTATAGGAAAAGGCC
GGTGTGTTGATGACTTCCTGTTCAAAGATGTTTCAACACTAAAAACAGAA
AATCTTCCAGAATTATTCTTAACAAAAATAGATACTGATACGTTTTTCTCT
CAGTGGTCAACCAAAACCAAGAAAGATCTGCAAAAAAAAATACAAGACC
TTACTGTACGTTATAATGAGCTAATTGACTCGTCGACTATCGACTTTAAA
AATCTATATGAAATAGATCAAATGCTCCATATGATTATGCTAGAGATGAA
TGATGATATAGCCAAAAGGTCATTGTTTTCATTGCAAGTTCAAATAGCCG
AAAAAATTCGGAGGATGACCATTCCTGTAGACAATATAATTAACATCTAT
CCTGATCTACATAAAAAAAATGACAATGATCTGAGTATGTCCATAAAAG
GCTTTCTTGCGAGTAATCCACATACAAAAATAAATATTCTTTATAGCAAT
AAGACTGAGCATAATATTTTTATAAAGGATTTATTCTCCTTCGCAGTTATG
GAAAATGAGTTAAGAGACATTATCAATAACATGAGCAAAGATAAGACTC
CTGAAAACTGGGAAGGGAGGGTAATGTTACAAAGATATCTCGAATTAAA
AATGAAAGATCATCTTAGTTTGCAATCTTCTCAGGAAGCAAATGAGTTTC
TTGAAATATCTACTTTTATTTATGAGAATGATTTCTTGAGAGAAAAGATT
GAAGCAGTAAAAAACAAAATGAATTCTCACGAACTTTATTTTGAAAAAA
TAAAAAAAGAACAAAACACATGGCAGGATCTGTCCACAAAAGAACAAA
AATTACAGCTTATTAAAGCATTGAAAGAAATTTCAGGAAATACAGAGAA
GGACTCTCATTACGATAGACTTCTTGATGCTTTTTTTAAAAAACATAATG
AAAATATTCATAATAAAATACAAAGAATAAAAGACGAGTTCAAGGAATA
CTCCCGTGTAGCCATTCATAATATAGATAAAGTTATATTTAAAGGGCAAA
CACTGGATCGTCTTTATCATGAAGGATATGTATTTTCTGATATCAATACCT
TGTCTCGTTATACACTACACGGACTAGGAATAACTGGTGTACATACTGAA
GAAAACCTGCTACCAGCTCCTTCATCGTCCTTAATTAATATATTGAAAGA
ACATTATAATGAAGATGAAATTAGTGCGAAATTACCACTAGCATATGATT
ACATTTTAAATAAAAAAGAATCAAGCTCTATTCCTGTTGAAATTTTGAAC
AAACTTTCAGAGTTACCACCACATGAACTACTCACACCTGTTCTTGGCCA
GAGTGTTAATCCTCTGGGCATGGGCTACTCATCCGATAATGGAAAAATCA
CAGAGCAAGTAATAGTCAGTGGAGCTGATGGATTTGATAATCCCATATCT
GGACTTATATATACCTATCTTGAAGATCTATATAACATCCATGTAAGGAT
GCGAGAAGGTACACTAAATTCACAGAATCTTCGTCAGCTTCTGGAAAACT
CTGTTTCTTCATGCTTTTTGACTGAGCAAAGTATTAATAAATTACTTAGTG
AGGCAGAAAAAAGGCCTTATCAGTCTTTAACAGAAATACATCAGCATCT
CACAGGATTACCAACTATTGCCGATGCAACCCTTTCATTACTTTCTGTTGG
ATTACCTGGTACGGGAAAACTATTGCGCAGGGAGCAGGACTATGGGCGT
CCACCAGTTACAGCAATTCAGGATTCCACATTTGTACTCCCTTATAATTTC
AAAGGTATTGGTTTTAACGATAACATTATATCCTCTGCACCTGTAGCCTC
CTCATTACATTTTATCGCTGAACATGCGAAATATACTTTATTGTCATGGCC
TGAGTTTTATCGTCATCATGCACAGCGATGGTTCGAAATGGCTAAAGGAT
ATGGAAGCCAGAATATTGATTTTCACCCTCAGTCTCTATTGGTAACCCAA
GAAGGACGCTGTATGGGATTAGCCTTACTTTATTTACAGACTGAAGATAC

TGCTCATTATAGCATTCTCCAGGAAAACCTAATGACTGTGAGTGCACTTC
ATCAGACCAGTAATCGCGATAAGTTGCCACTGTCCAAAGATGATAATTCC
TTAATGACAAGAACTTATAGTCTGATTGAAATGCTACAGTATCAGGGAAA
CAAATATATTACCAACGAATCGCTACTACATAAGACCGCATGGAACCAA
GAAAGAATAACTTTATTATTCAATGAAAAAGGAGTTAAGCGAGCCCTGA
TAAGCACGCCTAATCATACTCTGGTTCTGCAACAACTGGAGGATATTTAC
CGGCTCACTGATCCAAATTTTGGGCATGCAGATTTCCTTTCACCTATAGAT
GCTCTGAAGTTTATTGAGGCTATGATACAATTAACTCCAACACTTCAGGA
ATATTATGGCCTATTAAACAAAGACATTAATAAACATATACAAGTACATT
ATGCCGAATCAGATATGGTCTGGAATAAGCTTCTGCCAGAAAATGATGCT
GGACTGAGCACCAGAATTCAGCACACCACCACCGACCGTCTGGCGAATC
TGGCTGAACCAGTCGCTGTTGCAGGTATCTCCCTGCCAGTAAAAACACTT
TATGATATCGGAGCCACCCTTGACGGTCGGCGCATCACCTCTCCTCCAAC
ATCGGAGCAAATCCCTTCTCTGCGTCTCAACGGTGATGTTCTGAATGATT
ATCTGTCCCGCACAGTTCTGACTCCAGAACAGGCTGATAACATAAGAAA
AATACTGCACACTCAGGGAATACGCAGCGGTACCCGTCCCATAGATCCG
GAGATGATTCGTGGGACGCAGGATGACCTAGTTTCGTCACAGACTCGTCT
GCAAAGGCAAGCAACACGGGTTAAACAGCAACTCGCCGGTGTACTTGAT
ACTCTGCAACAGCACTTCCAGAACATTCCACGTTCATCCGGTCGTCATCT
TTCTGTAGAGAATATTGAGCTGGCTGATATCGGAAGTGGGCGTTTCAACC
TTCAAATTCGAGATGGAGAAACATTGCATACCACTTCTGTGGAAGTACCG
GAAGTTGTGTCCCGTTTTCAGAAACTTTCTACCATGCTTTCAGCCCTGCCT
GCCAGTGGAATCATGGATTTCGACCTCGGCATGAGTGTGGTCGGAGTCGT
CCAGTATGCCCGCCTGCTACAGCAGGGGCACGAAGACAGTACCCTAGCC
AAGATAAATCTAGCTATGGATATCAAGCAACTTTCCGAAGCAACTCTCGG
CAGCATGATTCAGATTGCCGGGAATAAGTTTCTCAATACAGAAGGAATCC
AGGGGTTCAGACTGGAAAGCGCCGTCGCTGAAGGTATGCGCTCAGTAGC
AACCCGTACCGGAGGCACAATGGGGAAAGCCCTTTCTGCCAGTGCCCGT
GTTCTTGAACTGCCTGTACTGGAAACAGTTCTGGGGACATGGAACCTGTA
CAACAGCGTCATTCAGCTCCAGCAAGCTACATCTTATTCTGAGACAATGG
CTGCCCGGGTACAGATTGCGTTTGATTCCATTTCTCTGGGATTAACTGCCG
CTTCGGTAGCTTTCCCGCCACTAATTATTGCCACTGGCCCCATTGCGGCTA
TTGGTATGGGAGCTTCCAGTATTGCACGTAATGTGGCACGGAAAGAAGA
ACGGCATACACAATGGCTGGAATATAAAAAATTCCTGACTGATGGCAGT
AAACACATTGTTGTGGCCTCTCCGGAAAGAGGTCTGCTGGATTTCTCCGG
AAACAAAGTTTTTGGAAAAATGGTGCTGGATCTGCGTCAGTCTCCTCCTC
TCTTGCATGGAGAAAGCTCTTTTAACGCTGACCGCAAAATCGGTCATCGT
CCGGATCTGGGGGACTGGCAAATTCGTGAGAAGGTGGGGTATGCCAACA
GTATCAGTCCCTACTCTTCTCTGGCGCACGGTTACGCCAACAGTAAATGG
CCACGAACAATACCGAAAATTCCCTCGGGAGAATATGACACCATAATTCT
GGGCTACGGTCACCAGTATCAGGCCAATACGGAAATAGAATATCTGTCT
AACTGGATTGTATGGCGGGAAGCCGTACCAGACAGTACTTCCCGCCACA
AACGTCCTCCTCTGGAGGTTCTTAATAGTCAGTGTACTGTGATAGCTGGA
GAGCGTAAAACCACAGTACTTCCCCTGAGAGTGCTCAGCGATCTGACACC
GGAATGCACAGAACAGGCTATATCGTTAAAAGATTATAAATTCATACTG
AGAGGGGGAAGCGGTGGGCTGGCTGTTCAGGTCGGTGGCGCGGGATATT
ATGATATTGATGCAAATCTTGTGGCAAAAGAAAATACGCTCTCTTTTCGC
GGGCTACCGGAAGAGTTTCCGCTCACCTTTGATTTATCAAAACAAACACA

GTCGGTCATGCTGAAAACACCAGACGATGAGGTGCCGGTAATGACCATT
ACCCAGAAGGGAATAAACACCCTGGTAGGTACAGCCGCCGGTAAAGACC
GACTAATCGGTAACGATAAGGACAATACCTTCCATACAAGCTCTGGCGG
CGGTACAGTCATCTCCGGAGGCGGGAATAACCGCTATATTATCCCCCGGG
ATTTAAAAACGCCGTTGACACTGACGCTGTCCAGTAACTCAGTCTCTCAC
GAAATCTTTCTGCCAGAAACAACCCTAGCTGAATTAAAACCTGTCGCCTT
TGAGCTGAGTTTGATTTACTGGGCCGGGAACAACATAAATGTTCAACCAG
AGGATGAAGCAAAACTGAACCACTTTGCCGGAAACTTCAGGGTGCATAC
CCGTGATGGCATGACTCTGGAGGCGGTTTCCCGGGAAAATGGTATTCAAC
TGGCGATTTCATTATGTGATGTTCAACGCTGGCAGGCTGTTTATCCGGAA
GAAAATAACAGACCGGATGCCATACTGGACAGGCTGCATGATATGGGCT
GGAGTCTGACACCAGAAGTCCGGTTCCAAGGAGGAGAAACACAAGTCAG
CTATGATCCCCTGACTCGTCAGCTCGTTTACCAGCTTCAGGCGCGTTACTC
TGAATTCCAGTTGGCCGGTAGTCGCCACCATACCACGGCTGTAACCGGAA
CTCCGGGAAGCCGATACATTATCATGAAGCCAGTTACAACACAGATATTA
CCGACACAAATCATACTGGCTGGTGATAATGACCATCCGGAAACGATTG
ATTTACTGGAAGCTAGTCCTGTTCTGGTTGAAGGGAAAAAAGACAAAAA
CAGCGTGATATTAACGATTGCTACGATTCAGTATTCCCTTCAACTGACAA
TATCCGGGATCGAAGAATCGCTGCCCGAGACAACCCGTGTGGCAATTCA
GCCTCAGGATACCCGTTTACTGGGTGACGTACTCCGGATCTTACCAGATA
ATGGTAACTGGGTGGGGATTTTCCGGAGTGGTCATACACCAACGGTAAA
CCGGCTGGAAAATTTGATGGCACTGAATCAGGTAATGACGTTCCTGCCCC
GGGTATCCGGAAGTGCAGAGCAGGTATTATGCCTCGAAAACCTAGGTGG
CGTAAGGAAAAAAGTGGAGGGGGAGTTACTGTCAGGGAAGCTGAAAGG
TGCGTGGAAAGCCGAAGGTGAACCTACTGTTCCGGTAAATATCTCAGATC
TAAGTATCCCACCCTATTCACGTCTGTATCTGATTTTTGAAGGGAAAAAT
AATGTGTTGCTACGCAGTAAAGTACATGCAGCTCCGTTGAAAATAACATC
CGCAGGAGAGATGCAGTTATCTGAAAGGCAGTGGCAACAGCAGGAACAT
ATTATTGTCAAGCCCGACAACGAAGCCCCCTCATTAATACTCAGTGAATT
TCGTCGTTTCACTATTTCATCGGATAAAACATTTTCTTTAAAACTGATGTG
CCATCAGGGTATGGTCCGCATCGACCGCAGATCATTATCGGTCAGATTGT
TCTATCTGCGTGAACAGCCAGGTATCGGCAGTTTACGTCTGACGTTCAGA
GATTTTTTCACAGAAGTGATGGATACAACGGACAGGGAAATTCTGGAGA
AAGAGCTGAGACCAATTCTGATAGGAGATACACACCGCTTTATCAACGCT
GCATACAAAAATCATCTGAATATCCAGTTAGGAGATGGCGTTCTGAATCT
GGCAGACATTGTTGCGGAATACGCCCGTATTCAAAAGGAAGAAACATCA
AAAATATTGTATCAATATCAAGGTGCCATGAAAAAAAAAACAGATGGAC
CATCTGTGGTAGAAGATGCCATTATGACCACTACTGTCACAACAGATTCA
GGTGAACTATTCCCTACCTTCCACCCGTGGTATACAGATGATTTATCAGG
GCGTTATAAGAGCGTACCTATGGCAAGAAAAGCAGATACTTTGTATCACC
TGACACCAAAAGGTGATCTACAGATAATATATCAGGTAGCTACAAAAAT
GGTGAATCAGGCGATGATTGTATCCCTGCCAAACTACCGACACGAGTGG
GAAAAATATAATTTAAGCATCTTATCCGAAATCCCTCAGAACAATAATAC
TGTTGTACATTCAATCCTCAGGGTTAATGGCCCCACAATGCAGGTGCGCA
CAATTGACTACAGAGGAACGGATGAAAACAATCCCATAGTATCTTTTTCA
GATACAACCTTCATCAATGGTGAACAGATGTTGAGTTATGACTCGCATTC
ATCAGGGCGAGTCTATTCCAGAGAAGAATATATGATGTGGGAATTGCAG
CAACGGGTATCAGAAGCTTCCAGTGCCCGGACACAGGATTACTGGCTGA

TGGATGCAGCGGTAAGAAACGGAGAATGGAAGATCACACCAGAATTATT
ACGTCACACACCGGGATATATCCGGAGTACGGTATCGAAATGGTCCAGA
GGATGGCTGAAAACCGGCACAATACTCCAGACTCCAGAAGACAGAAATA
CGGATGTATACCTGACTACCATACAGAACAATGTATTTAGTCGTCAGGGG
GGCGGCTACCAAGTGTATTATCGGATTGATGGAATGGCTGGTGCGGATAT
AGCGGATAATGCACCAGGGGAAACCCGCTGCACCCTCAGGCCCGGAACA
TGTTTTGAAGTGACAAGTGTGGATGAAAGGCATTATGAGTGGAATATCAT
TTATGTCACGCTGAAAACCTGTGGCTGGAGCCGAAATGGCCAAAGCAAA
ACGCCGAATGGTGACAACCTTTTTAACCATCATCACCACCATCACTAATA
GAGCGGCCGCCACCGCTGAGCAATAACTAGCATAACCCCTTGGGGCCTCT
AAACGGGTCTTGAGGGGTTTTTTGCTGAAAGGAGGAACTATATCCGGGTA
ACGAATTCAAGCTTGATATCATTCAGGACGAGCCTCAGACTCCAGCGTAA
CTGGACTGCAATCAACTCACTGGCTCACCTTCACGGGTGGGCCTTTCTTC
GGTAGAAAATCAAAGGATCTTCTTGAGATCCTTTTTTTCTGCGCGTAATCT
GCTGCTTGCAAACAAAAAAACCACCGCTACCAGCGGTGGTTTGTTTGCCG
GATCAAGAGCTACCAACTCTTTTTCCGAGGTAACTGGCTTCAGCAGAGCG
CAGATACCAAATACTGTTCTTCTAGTGTAGCCGTAGTTAGGCCACCACTT
CAAGAACTCTGTAGCACCGCCTACATACCTCGCTCTGCTAATCCTGTTAC
CAGTGGCTGCTGCCAGTGGCGATAAGTCGTGTCTTACCGGGTTGGACTCA
AGACGATAGTTACCGGATAAGGCGCAGCGGTCGGGCTGAACGGGGGGTT
CGTGCACACAGCCCAGCTTGGAGCGAACGACCTACACCGGAACTGGAGA
TCCCTACAGCCGTGAGCTTATGAGAAAAGCGCCCACGCCTTCCCCGAAAG
GGGAGAAAAGGCGGGACAGGGTATCCCGGTAAAGCGGGCAGGGGTCCG
GAAACAAGGAAAAGCGGCCACGAGGGGAGCTTTCCCAGGGGGGGAAAA
CCGCCCTGGGTTATCCTTTTATTAGTTCCCTGGTCCGGGGTTTTCCGCCCA
CCCTCCTTGAACTTTGGAGCCATCCGGTTTTTTTTGGGG

Appendix 3: Relevant published papers

The following published paper incorporates work from this thesis. This paper is included with the author's permission. It was published in The Journal of Biological Chemistry, January 2016. The paper can also be found at: http://www.jbc.org/content/early/2016/01/20/jbc.M115.709600.full.pdf+html?sid=14b9bc92-1284-4a90-a991-b79e370db717.